DYNAMIC BEHAVIOUR OF BATTER PILES AND PILE GROUPS

Ph.D. THESIS

by

BHARATHI M.

DEPARTMENT OF EARTHQUAKE ENGINEERING
INDIAN INSTITUTE OF TECHNOLOGY ROORKEE
ROORKEE - 247667 (INDIA)
JUNE, 2019

DYNAMIC BEHAVIOUR OF BATTER PILES AND PILE GROUPS

A THESIS

Submitted in partial fulfilment of the requirements for the award of the degree

of

DOCTOR OF PHILOSOPHY

in

EARTHQUAKE ENGINEERING

by

BHARATHI M.

DEPARTMENT OF EARTHQUAKE ENGINEERING
INDIAN INSTITUTE OF TECHNOLOGY ROORKEE
ROORKEE - 247667 (INDIA)
JUNE, 2019

INDIAN INSTITUTE OF TECHNOLOGY ROORKEE
ROORKEE

CANDIDATE'S DECLARATION

I hereby certify that the work which is being presented in the thesis entitled "**DYNAMIC BEHAVIOUR OF BATTER PILES AND PILE GROUPS**" in partial fulfilment of the requirements for the award of the Degree of Doctor of Philosophy and submitted in the Department of Earthquake Engineering of the Indian Institute of Technology Roorkee, Roorkee is an authentic record of my own work carried out during a period from July, 2013 to June, 2019 under the supervision of Dr. R.N. Dubey, Associate Professor, Department of Earthquake Engineering, Indian Institute of Technology Roorkee, Roorkee.

The matter presented in this thesis has not been submitted by me for the award of any other degree of this or any other Institution.

(BHARATHI M.)

This is to certify that the above statement made by the candidate is correct to the best of my knowledge.

(R.N. Dubey)
Supervisor

Date: June 28, 2019

தொட்டனைத் தூறும் மணற்கேணி மாந்தர்க்குக்
கற்றனைத் தூறும் அறிவு

திருக்குறள் (396) - கி.மு. முதல் நூற்றாண்டு

As a sandy fount yields more water every time you dig, so does knowledge grow, the more you read, the deeper

Thirukkural (396) – *first century B.C.*

This thesis is dedicated to my parents
Mohanasundaram P. *and* ***Vijaya G.***

ABSTRACT

Batter piles (also known as inclined or raker piles) are often used for supporting bridges, offshore structures, transmission line towers, etc., where the horizontal load per pile may exceed the capacity of vertical pile. During the past seismic events, batter piles have shown both beneficial and detrimental effects. Several researchers have discussed and debated on the virtues and drawbacks of batter piles which further helped in understanding their response in a better manner. A number of documents are available on the seismic performance of batter pile groups based on controlled tests on scaled laboratory models. The primary objective of the present study is to examine the dynamic behaviour of bored cast in-situ batter piles and pile groups in the field conditions. In this thesis, extensive field investigations along with finite element (FE) models are discussed in detail to understand the dynamic response of batter piles and pile groups. This research comprises four major components: (a) dynamic pile load tests on single vertical and batter piles; (b) dynamic pile load tests on vertical and batter pile groups; (c) 3D finite element analysis of single piles and pile groups and (d) measurement of dynamic pile load test induced vibration in adjacent building and its finite element analysis.

In the initial phase, the behaviour of bored cast in-situ reinforced concrete (RC) six single piles: (a) single vertical pile (B0); (b) vertical pile with an under-ream bulb (B0U1); (c) 10° batter pile (B10); (d) 10° batter pile with an under-ream bulb (B10U1); (e) 20° batter pile (B20); and (f) 20° batter pile with an under-ream bulb (B20U1), subjected to lateral and vertical dynamic loading is examined experimentally. All these six piles are subjected to dynamic load generated by an oscillator motor assembly firmly mounted on top of the pile cap. In each direction, the piles are subjected to six different intensity of force levels (varied in the form of eccentricity of the oscillating mass). In addition, four different RC pile groups consisting of: (a) three vertical piles (3VG); (b) three 20° batter piles (3BG); (c) four vertical piles (4VG); and (d) four 20° batter piles (4BG), are also constructed by bored cast in-situ method and tested for five different intensity of force levels. Further, the effect of lateral loading direction on the dynamic responses of these piles and pile groups is also explored. The dynamic response of piles and pile groups is recorded in real time using piezoelectric accelerometers placed at appropriated location on the pile cap. From the recorded dynamic response, the variation in resonant frequency, peak displacement, induced strain etc., is obtained and discussed in detail.

Numerical investigations are also performed to evaluate the behaviour of batter piles and pile groups subjected to dynamic loading using 3D FE models. Appropriate loading and dynamic boundary conditions, element sizes and lateral extents of the model are used to develop 3D FE

models. The material properties of both soil and pile are considered similar to the experimental investigation test site. The effect of loading direction, intensity of exciting force level, material nonlinearity etc., are explored in detail. In addition, an attempt is also made to understand the bending moment profiles of batter piles through a hybrid modelling approach. The developed 3D FE models reasonably replicate the experimental findings. Thus, the model developed could also be used for other parametric studies which are not experimentally feasible. The effect of pile-soil modulus ratios (E_p/E_s) on the dynamic response of batter piles is also examined using 3D FE model.

When dynamic tests are conducted on pile groups, the vibrations propagated through the soil mass to the adjacent structure. These vibrations are measured at the source and at different floor levels (including ground floor and roof) of the adjacent building, in the form of acceleration and velocity time histories. The response obtained through the experiment is also compared with 2D FE analyses of the integrated building-pile group-soil system. The estimated vibration responses in terms of peak ground acceleration (PGA), peak ground velocity (PGV), pseudo-spectral acceleration (PSA) and predominant frequencies (f) are compared with the permissible limits recommended in the relevant standards and codes of practice.

ACKNOWLEDGMENT

I would like to express my sincere gratitude to my advisor **Prof. R.N. Dubey**, Department of Earthquake Engineering, Indian Institute of Technology Roorkee for his continuous support and guidance to complete this research work. His immense patience and faith in me have helped me to stay motivated during my entire Ph.D. journey. I am also grateful for all his priceless advice on both research as well as on my career.

I would like to thank **Prof. Yogendra Singh,** for all his valuable recommendations throughout the research work. Thoughtful suggestions by **Prof. M.N. Viladkar** at various stages has been very helpful in shaping this research work. Suggestions by **Prof. R.S. Jakka** was also really useful. All support received from **Prof. M.L. Sharma** as the past Head of Earthquake Engineering Department is duly acknowledged. My special thanks are due to **Prof. B.K. Maheshwari,** for all his extended support in accessing the facilities of Soil Dynamics Lab whenever required. I am also thankful to all other faculty members at the Department of Earthquake Engineering for their invaluable suggestions, whenever needed.

The advice and suggestions provided by **Prof. Sanjay K. Shukla,** Associate Professor, Civil and Environmental Engineering, Edith Cowan University, Australia, have been very helpful. His constructive criticism and appreciations have highly motivated me in carrying out this work.

I would like to thank **Prof. Swami Saran** (retd.) and **Prof. Shyamal Mukerjee** (retd.), IIT Roorkee for their continuous encouragement and blessings since my Masters. My sincere thanks are due to **Shri. N.P. Aterkar,** Director, Soilex Consultant Private Ltd. for sharing his invaluable experience at various stages especially while constructing the experimental setups.

Special thanks are due to **Dr. K. Babu Kannan** and **Dr. K. Ramadevi**, my undergraduate mentors from Kumaraguru College of Technology, Coimbatore, TamilNadu for their valuable advice and encouragement without which this could not have been possible.

I wish to extend my warm thanks to all my fellow students, seniors and juniors, who provided candid help, meaningful suggestions and persistent encouragement. Thank you all for being with me, in all my ups and downs, with all your support whenever I needed.

My thanks and appreciations are due to all the technical and non-technical staffs especially **Shri. Subodh Jain**, **Shri. Rishi Chand** and **Shri. Prem Chand** at the Department of Earthquake Engineering for all their support.

Finally, I would like to deeply thank my father, **Shri Mohanasundaram P.**, mother, **Smt. Vijaya G.** for their unconditional and endless love, support and encouragement throughout in absence of which I could never have reached to this position. I would also like to express my indebtedness for their immense faith in me. It would be unfair if I do not name my younger sister **Ms. Monica M.**, who has carried all the responsibilities of our family in my absence with immense maturity in spite of difficulties. My special thanks to dear friend **Dr. Dhiraj Raj** and his family for their love, encouragement and motivation which has also been a strong moral support throughout.

I sincerely acknowledge the financial support for this research work received from **Ministry of Human Resource Development**, Government of India.

Finally, my salutations to the Almighty for providing the faith, inspiration, patience, guidance and strength to carry out this work.

Dated: June 28, 2019 **(Bharathi M.)**

CONTENTS

LIST OF FIGURES

LIST OF TABLES

NOTATIONS

Symbol	Explanation
δ_{stat}	Static displacement
$\overline{T}$	Typical period of vibration
Δt	Time step
μ	Magnification factor
A_θ	Rotational amplitude
d	Diameter of pile
d_x	Lateral displacement in X direction
d_{x1}	Displacement corresponding to accelerometer A1
d_{x2}	Displacement corresponding to accelerometer A2
d_{x3}	Displacement corresponding to accelerometer A3
d_x'	Peak displacement amplitude in X direction
d_y'	Peak vertical displacement
d_z	Lateral displacement in Z direction
d_z'	Peak displacement amplitude in Z direction
E_c	Young's modulus of concrete
e	Eccentricity of the oscillator
E_p	Young's modulus of pile
E_s	Young's modulus of soil
f	Operating frequency
F_b	Building factor
F_d	Dynamic force
F_g	Foundation factor
F_m	Material factor
f_{ndx}	Damped natural frequency of the system in X direction
f_{ndz}	Damped natural frequency of the system in Z direction
f_{nx}	Undamped natural frequency in X direction
f_{nz}	Undamped natural frequency in Z direction
f_s	Frictional resistance
f_x	Frequency in X direction
f_x'	Resonant frequency in X direction
f_y'	Resonant frequency in Y direction
f_z	Frequency in Z direction
f_z'	Resonant frequency in Z direction
G	Specific gravity of soil
g	Acceleration due to gravity
h	Element size
$K_{\theta x}$	Rotational stiffness of the soil-pile system in X direction
$K_{\theta z}$	Rotational stiffness of the soil-pile system in Z direction

Symbol	Explanation
l	Length of pile
L_e	Effective length of pile
m_0	Eccentric mass
M_d	Exciting moment
M_w	Moment magnitude
M_x	Bending moment in X direction
M_z	Bending moment in Z direction
p	Soil pressure per unit length of pile
q_c	Tip resistance
r	Crank radius
S	Spacing between the piles
u	Pore water pressure
V	Maximum allowable PPV value for transient vibration
V_0	Vertical component of uncorrected vibration velocity at the base of the building
V_s	Shear wave velocity of soil
w_L	Liquid limit
w_P	Plastic limit
y	Pile deflection
α_{rd}	Mass proportional Rayleigh damping coefficient
β	Batter angle
β_{rd}	Stiffness proportional Rayleigh damping coefficient
γ_c	Density of concrete
γ_s	Density of soil
ε_x	Shear strain in X direction
ε_y	Axial strain
ε_z	Shear strain in Z direction
ν_c	Poison's ratio of concrete
ν_s	Poison's ratio of soil
ξ	Damping ratio of material
ξ_x	Damping ratios of the soil-pile system in X direction
ξ_z	Damping ratios of the soil-pile system in Z direction
ω	Operating frequency

ABBREVIATIONS

Abbreviation	Explanation
3BG	Pile group with three 20° batter piles
3D	3 Dimensional
3VG	Pile group with three vertical piles
4BG	Pile group with four 20° batter piles
4VG	Pile group with four vertical piles
B0	Single vertial pile
B0U1	Vertical pile with an under-ream bulb
B10	10° Batter pile
B10U1	10° Batter pile with an under-ream bulb
B20	20° Batter pile
B20U1	20° Batter pile with an under-ream bulb
B22	3-node quadratic beam element in a plane
B33	2-node beam element with cubic interpolation in space
BH	Borehole
C3D4	4-node tetrahedral element
C3D8R	8-node brick element with reduced integration
CIN3D8	8-node linear one-way infinite brick element
CPE8R	8-node biquadratic plane strain quadrilateral element with reduced integration
CPT	Cone Penetration Test
DC	Direct Current
DEQ	Department of Earthquake Engineering
DMRC	Delhi Metro Rail Corporation
FE	Finite Element
FEA	Finite Element Analysis
FFT	Fast Fourier Transform
GL	Ground Level
HHT	Hilbert-Hughes-Taylor
HP	Horse Power
HS	Hardened Steel
IITR	Indian Institute of Technology Roorkee
PGA	Peak Ground Acceleration
PGV	Peak Ground Velocity

Abbreviation	Explanation
PPV	Peak Particle Velocity
PSA	Pseudo-Spectral Acceleration
RC	Reinforced Concrete
SDOF	Single Degree of Freedom
SPT	Standard Penetration Test
TMT	Thermo-Mechanically Treated
UDL	Uniformly distributed load
WT	Water Table

Chapter 1

INTRODUCTION

1.1 INTRODUCTION

Pile foundations are widely used in relatively weak soil deposits to support various structures subjected to static lateral load and bending moment apart from static vertical loads. In addition, the structures along with its foundation systems are often exposed to additional dynamic loads from various sources. Hence, pile foundations experience comparatively higher bending moment in addition to low and high strain rate reversals at each cycle, leading to passive pressure mobilization of soil-mass in the surrounding. This phenomenon may result in the collapse of the integrated soil-pile system along with structural failure of the pile itself. The increasing growth of industries and technology advancement necessitates the use of a large range of machines that generate the dynamic loads. Moreover, the structures (e.g. offshore structures, towers, and industrial plants) along with their foundation systems, are often exposed to additional dynamic loads. The dynamic behaviour of pile foundations has been an important topic of research during the past several decades. In practice, a combination of vertical and batter piles (also known as inclined or raker piles) is used for supporting bridges, offshore structures, transmission line towers, etc., to handle huge overturning moments due to wind and wave action as well as to sustain large impacts from ships. These batter piles are often used where the horizontal load per pile may exceed the capacity of vertical pile.

1.2 PERFORMANCE OF BATTER PILES IN THE PAST

The observations on the seismic performance of batter piles in the past has been reported as case histories. A few of them were emphasizing on the satisfactory behaviour while the others provided evidence for the detrimental behaviour of batter pile supported structures. A brief note on important findings from these case histories are highlighted below.

During the 1989 Loma Prieta earthquake [M_w 7.0] the Public Container Wharf at 7th Street Terminal Complex experienced the most severe damage. The square pre-stressed concrete batter piles failed in tension especially at its connection with the deck (Fig. 1.1). Liquefaction,

settlements and lateral soil spreading were other important factor contributing to damage of batter piles. The concrete wharf supported by batter piles at the Matson terminal experienced additional damage of vertical piles at the back row. The damages observed at the APL terminal and Howard terminal were mainly due to the inadequate detailing of the connections and connection of pile to pile cap (Mitchell et al. 1991).

At San Francisco, batter piles supporting the Ferry Plaza pier experienced tensile failure at the connection of the deck with even some piles punching the slab during the 1989 Loma Prieta earthquake [M_w 7.0] (Mitchell et al. 1991). Similar damage was also observed at piers 27 and 29 as shown in Fig. 1.2.

During the 1991 Costa Rica earthquake, [M_w 7.5] large rotations led the collapse of the deck of Rio Vizcaya bridge (Fig. 1.3). Batter piles at the front experienced more damage in flexure and shear (as shown in Fig. 1.4) when compared to rear vertical piles at the Rio Banano bridge (Priestley et al. 1991).

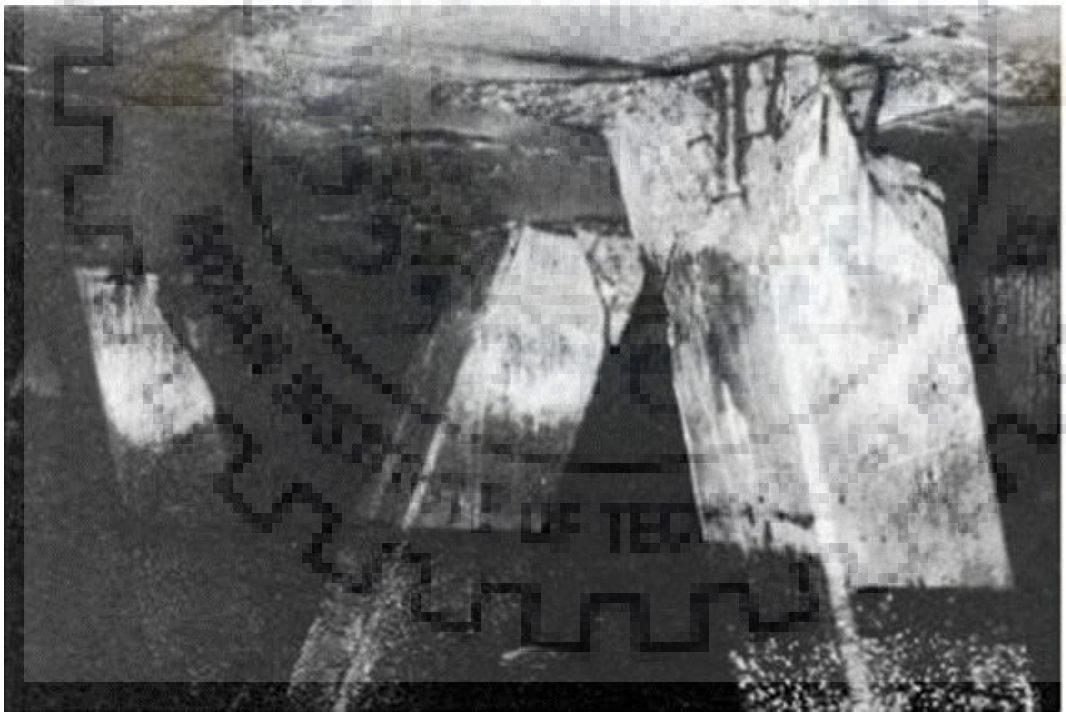

Fig. 1.1 Damaged batter piles at port of Oakland 7th street terminal (SEAOC 1991)

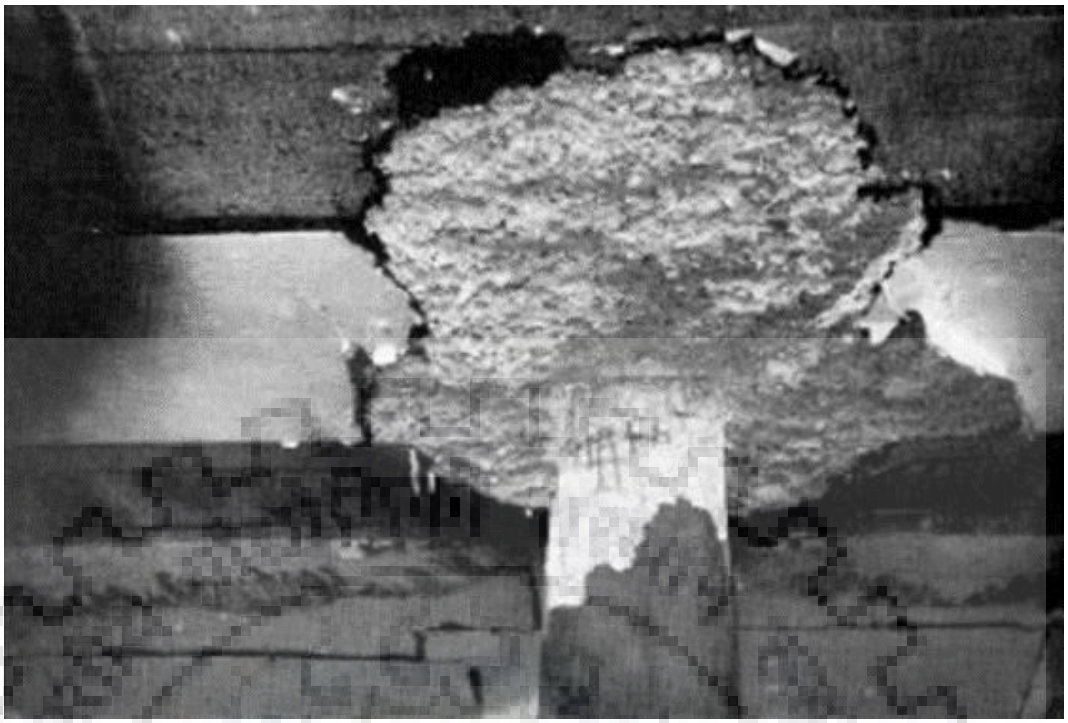

Fig. 1.2 Damaged batter piles at port of San Francisco at piers 27 and 29 (SEAOC 1991)

Fig. 1.3 Failure of Rio Vizcaya bridge (Priestley et al. 1991)

Fig. 1.4 Damage to front batter pile of Rio Banano bridge (Priestley et al. 1991)

On the contrary, Berrill et al. (1997) and Berrill et al. (2001) revealed evidence in support of batter piles. The pier of Landing Road bridge withstood approximately 2 m lateral movement due to liquefaction of sandy layer. However, the presence of batter piles provided additional lateral stiffness to the pile groups supporting the bridge during 1987 Edgecumbe earthquake [M_w 6.3]. Another case study in support of batter piles for its seismic performance by Kastranta et al. (1998) claimed the quay walls of Maya Wharf supported on batter piles withstood severe seismic shaking with only 20 cm displacement during 1995 Kobe earthquake [M_w 6.9]. Whereas an adjacent wall supported on vertical piles experienced a displacement of about 3 m and was completely devastated during the earthquake. The hollow RC batter piles supporting the berths of Kandla Port performed satisfactorily during the 2001 Bhuj earthquake [M_w 7.7] (Bhattacharya et al. 2009).

Due to a series of poor seismic performance of batter piles many codes suggested to avoid these batter piles. For instance, according to the French seismic code "*Inclined piles should not be used to resist seismic loads*" (AFPS 1990). The Euro code (EC8 2003) dealing with geotechnics and foundations, is less restrictive on use of batter piles, states "*It is recommended that no inclined piles be used for transmitting lateral loads to the soil. If, in any case, such piles*

are used, they must be designed to carry safely axial as well as bending loading". A monograph on Seismic Design of Port and Harbour Facilities published by the American Society of Civil Engineers Technical Council on Lifeline Earthquake Engineering advised that "*The use of batter piles at ports is typically not encouraged because of their poor seismic performance during past earthquakes*" (Werner 1998). Gazetas and Mylonakis (1998) provided evidences in support of better seismic performance of batter piles when subjected to lateral loading. AASHTO (2014) further recommended to consider increased foundation stiffness for batter piles used in seismic prone areas while designing the pile foundations.

However researchers discussed and debated on the virtues and drawbacks of batter piles which further helped in understanding their response in a better manner. The beneficial and detrimental effect of batter piles were not justified due to the limited available literature on full scale field tests. Since no research was conducted to understand the dynamic behaviour of cast in-situ batter piles, this thesis aims to study the dynamic behaviour of bored cast in-situ reinforced concrete (RC) batter piles and pile groups in field conditions. In this thesis, extensive field investigations along with finite element (FE) models are discussed in detail to understand the dynamic response of batter piles and pile groups. This research comprises four major components: (a) dynamic pile load tests on single vertical and batter piles; (b) dynamic pile load tests on vertical and batter pile groups; (c) 3D finite element analysis of single piles and pile groups and (d) experimental measurement and finite element analysis of dynamic pile load test induced vibration in adjacent building.

1.3 OBJECTIVES OF THE STUDY

The primary aim of the study presented in this thesis is to understand the dynamic behaviour of cast in-situ RC batter piles and pile groups. The present study has been conducted with the following specific objectives:

i. To investigate the behaviour of bored cast in-situ RC single vertical and batter piles subjected to dynamic loading.
ii. To estimate the effect of an under-reamed bulb in bored cast in-situ RC single vertical and batter piles subjected to dynamic loading.
iii. To examine the dynamic behaviour of bored cast in-situ RC vertical and batter pile groups experimentally in field conditions.
iv. To evaluate the dynamic performance of batter piles and pile groups through 3D FE simulations.

1.4 METHODOLOGY AND SCOPE OF THE STUDY

Initially, to estimate the dynamic behaviour of batter piles and pile groups a set of six single piles and four pile groups were constructed by bored cast in-situ method at the test site in the Department of Earthquake Engineering, IIT Roorkee. Dynamic pile load tests has been conducted on these piles and pile groups with the help of an oscillator motor assembly firmly mounted on the top of the pile cap. The effect of intensity of exciting force level and loading direction have also been studied.

A series of 3D FE analysis have also been performed to understand the dynamic behaviour of batter piles and pile groups. The material properties of both soil, piles and pile groups were kept similar to those observed in the previous experimental investigation. Dynamic load was applied in the form of sine sweep at appropriate location in the developed 3D FE model. The influence of intensity of exciting force level and loading direction on the dynamic response has been explored in detail. A comparison of the simulated dynamic behaviour with the experimentally obtained results has also been presented. In addition an attempt has also been made to understand the variation of displacement and bending moment along the length of the pile from the 3D FE models.

When dynamic tests were conducted on pile groups, the vibrations propagated through the soil mass to the adjacent structure. To assess these vibrations induced in an adjacent building accelerometers and seismometers were placed on different floor levels of the building and the vibration were measured simultaneously during pile load tests. In addition, a 2D FE coupled building pile group soil system has also been developed. The results obtained from the study are compared to permissible limits of vibrations prescribed in various standards and guidelines.

1.5 ORGANIZATION OF THE THESIS

This thesis has been organized in six chapters as follows:

Chapter 1 presents a brief introduction of the research topic, performance of batter piles in the past, objectives, methodology and scope of the present study, organization and novelty of the thesis.

Chapter 2 presents a comprehensive literature review of case histories, controlled laboratory experiments, analytical formulations and numerical studies on the static and dynamic behaviour of batter piles.

Chapter 3 presents the dynamic behaviour of six single piles and four pile groups through experimental investigations conducted in the field. An extensive experimental work has been performed on all the piles and pile groups subjected to increasing intensity of exciting force level in ascending order. The influence of intensity of force level, loading direction on the dynamic behaviour of batter piles and pile groups has been explored.

Chapter 4 presents a numerical study on evaluation of the behaviour of batter piles and pile groups subjected to dynamic loading. 3D Finite Element Analysis (FEA) have been performed for this purpose. The computed dynamic behavior have also been compared with their respective experimental results obtained in the previous chapter.

Chapter 5 presents the effect of vibrations induced in an adjacent building from dynamic pile load tests. The vibrations induced were measured experimentally and in addition 2D FEA has also been carried out on coupled building pile group soil system. The vibrations induced in the building has been checked for permissible limits by standards.

Chapter 6 summarizes the observations and conclusions of the present work along with a few recommendations for future work.

1.6 NOVELTY OF THE THESIS

The novelty of the thesis principally lies in the following points:

i. It's the first time that the batter piles and pile groups subjected to dynamic loads generated from a mechanical oscillator motor assembly has been examined through field investigations.
ii. It's also the first time the presence of an under-reamed bulb in a batter pile is evaluated for its dynamic response through field investigations.
iii. It's also the first time that the dynamic pile load test induced vibration in an adjacent building is measured.

Chapter 2

LITERATURE REVIEW

2.1 INTRODUCTION

Batter piles or raked piles have been used since long time in offshore structures, bridges, and towers to resist large lateral loads from winds, water waves, soil pressure and impacts. They carry lateral loads primarily in axial compression and/or tension while vertical piles carry lateral loads in shear and bending. Due to poor performance of batter piles in some earthquakes, they don't have a good reputation for seismic resistance. After a series of poor performance many researchers thought use of batter piles in seismic prone areas may be detrimental and several codes wanted such piles to be avoided. In the past, the seismic/ dynamic behaviour of batter piles or groups were explored through centrifuge tests/ scaled laboratory experiments or analytical/ numerical solutions. In practice, a combination of vertical and batter piles is used in many coastal and offshore structures to handle huge overturning moments due to wind and wave action as well as to sustain large impacts from ships.

In the past numerous analytical models have been developed to understand the dynamic behaviour of piles. Relatively, only a few dynamic load tests on piles have been reported in the literature. Novak and Grigg (1976) conducted the dynamic tests on small-scale single piles and pile groups in the field. A large pile group with 102 closely spaced piles was examined experimentally for vertical, horizontal, and torsional mode of vibrations by El Sharnouby and Novak (1984) and later these experimental results were evaluated by them (Novak and El Sharnouby 1984). Several researchers have investigated the response of vertical piles, under-reamed piles and vertical pile groups through filed experiments, scaled laboratory models, numerical simulation considering soil pile interaction (Kaynia and Kausel 1982; Sen et al. 1985; Hanna and Afram 1986; Han and Novak 1988; Dickin and Leung 1990; Mamoon et al. 1990; Kaynia and Kausel 1991; Dickin and Leung 1992; El-Marsafawi et al. 1992; Han and Vaziri 1992; Naggar and Novak 1994; Veeresh and Rao 1996; Burr et al. 1997; Mylonakis and Gazetas 1999; Naggar and Bentley 2000; Ilamparuthi and Dickin 2001a; Ilamparuthi and Dickin 2001b; Maheshwari et al. 2004; Boominathan and Ayothiraman 2005; Cairo et al. 2005; Maheshwari et al. 2005; Peter et al. 2006; Boominathan and Ayothiraman 2006a; Boominathan and Ayothiraman 2006b; Boominathan and Ayothiraman 2007; Adhikari and Bhattacharya 2008;

Allotey and El Naggar 2008; Banerjee 2009; Emani and Maheshwari 2009; Juneja 2009; Manna and Baidya 2009; Mroueh and Shahrour 2009; Xu et al. 2009; Yang et al. 2009; Manna and Baidya 2010a; Manna and Baidya 2010b; Honda et al. 2011; Hokmabadi et al. 2012; Manna and Baidya 2012; Niroumand et al. 2012; Phanikanth and Choudhury 2012; Qian et al. 2012; Ayothiraman and Boominathan 2013; Banerjee and Lee 2013; Bhowmik et al. 2013; Chandrasekaran et al. 2013; Nazir and Nasr 2013; Phanikanth and Choudhury 2013; Phanikanth et al. 2013; Wu et al. 2013; Alielahi et al. 2014; Banerjee and Shirole 2014; Farokhi et al. 2014; Fatahi et al. 2014; Qian et al. 2014; Qin and Guo 2014; Shadlou and Bhattacharya 2014; Bhardwaj and Singh 2015; Boominathan et al. 2015; Harris and Madabhushi 2015; Hokmabadi et al. 2015; Nazir et al. 2015; Chatterjee et al. 2015a; Chatterjee et al. 2015b; Ai et al. 2016; Chatterjee and Choudhury 2016; Hokmabadi and Fatahi 2016; Juneja and Mohammed Aslam 2016; Ladhane and Sawant 2016; Zheng et al. 2016; Rathod et al. 2016a; Rathod et al. 2016b; Basack and Nimbalkar 2017; Fattah et al. 2017; Hu et al. 2017; Moayedi and Mosallanezhad 2017; Rathod et al. 2017; Tombari et al. 2017; Basack and Nimbalkar 2018; Juneja and Mohammed-Aslam 2018; Rathod et al. 2018; Xu and Fatahi 2018; Bhattacharya et al. 2019; Moayedi and Rezaei 2019; Nimbalkar et al. 2019; Rathod et al. 2019; Yao and Xiao 2019). However, only Mohan et al. (1979) and Rahman and Sengupta (2017) examined the uplift resistance of under-reamed batter piles and pile groups though laboratory and field investigations, respectively.

Feagin (1937) examined the behaviour of laterally loaded batter piles made of timber. Further the research work on lateral behaviour of batter piles was carried over by few researchers (Tschebotarioff 1953; Murthy 1964; Prakash and Subramanyam 1965; Manoliu et al. 1977; Ranjan et al. 1980; Lu 1981). Later on, laterally loaded pile groups in sand was studied through centrifuge experiments (McVay et al. 1996; Pinto et al. 1997). Harn (2004) briefed the concept of displacement based design for a batter pile supported pier structure. Based on their observations batter piles inclined in the opposite direction of loading offered higher lateral resistance than batter piles inclined in the direction of loading. Limited literature is available on the dynamic behavior of batter piles. The following section will discuss briefly on the available literatures on batter piles through field tests, experimental investigation on scaled models and numerical simulation.

Zhang et al. (1998) tested the behaviour of 3 × 3 and 4 × 4 fixed head batter pile groups in loose and medium dense sand subjected to vertical loads were tested 45g using centrifuge. The distribution of axial force in a batter pile is much varied and it depends on position of pile, batter

arrangement and density of soil. Zhang et al. (1999) conducted lateral load tests on single piles, embedded in loose and medium dense dry sand, in centrifuge at 45g. Five different pile inclinations were considered. Based on the test results nonlinear *p-y* curves were also proposed.

Juran et al. (2001) conducted centrifuge tests at 20g on single piles, pile groups and network systems embedded in loose to medium dry sand consisting of inclined micropiles (β = 25°) to investigate their seismic response. The effect of superstructure was considered by applying 50% to 90% of axial load corresponding to static tests at the top of pile cap. In addition, parametric study was conducted by varying the length to diameter ratio of the pile and the spacing between piles in the pile group. The obtained results were used to develop *p-y* curves. Further, the results were also presented in terms of variation in bending moment, displacement and axial forces. The use of batter pile showed reduction in the pile cap displacement and increase in both axial force and bending moment at pile cap connections.

Rajashree and Sitharam (2001) developed a finite element model idealizing the pile as beam elements and the soil was considered in form of springs. The soil non-linearity was considered through hyperbolic and modified hyperbolic relations. The soil-pile interaction accounting for degradation and gap was incorporated in the form of empirical relation in the modified hyperbolic relation. The static and cyclic lateral response of vertical and batter piles (β = 10° and 30°) was studied with the developed model.

Sadek and Shahrour (2004) conducted using three dimensional finite element analysis on group of four micropiles embedded in a homogeneous soil (uniform stiffness) subjected to seismic loading. A group with four vertical piles and other with four inclined piles (β = 20°) was considered. The superstructure consisting of a lumped mass and a column was modelled as single degree of freedom (SDOF) system, whereas the micropiles are modelled using 3D beam elements. The effect of homogenous soil with varying stiffness was also studied. In case of homogenous soil with uniform stiffness, increasing the batter angle induced a reduction of 35% in bending moment at the micropile head.

Wong (2004) examined the seismic behaviour of single micropiles and two groups one with four vertical piles and other with four inclined piles (β = 20°) through 2D FEA considering a bounding surface plasticity model. Ricker wavelet of three different intensities were considered as the seismic input motion. Large lateral stiffness leading to reduction in acceleration was observed at the pile head with inclined micropiles.

Okawa et al. (2005) investigated the dynamic response of two 4 × 2 pile group (one with vertical piles and other with exterior inclined piles (β = 10°) and internal vertical piles) through centrifuge tests at 45g. In addition, seismic performance of real scale steel pile foundation was also analysed numerically. The results were presented in terms of variation in bending moment, axial force and displacement at foundation and superstructure. They also found that the acceleration and displacement at both foundation and superstructure was much higher for vertical pile group configuration. In contrary to the findings of Juran et al. (2001) they observed that the bending moment at the pile head of batter piles were lesser in comparison to vertical piles.

Poulos (2006) computed the axial and lateral response through a FORTRAN program (EMPIG) based on boundary element analysis. Three cases considering the groups subjected to vertical and lateral loading with: (1) no ground movements; (2) vertical ground movement acting on the group; and (3) horizontal ground movements acting on the group, were analyzed. The effect of batter angle (β = 0°, 7.5° and 15°) on group settlement, lateral deflection and rotation, pile loads and moments were examined. In absence of ground movement providing batter piles helped in reducing the settlement, lateral displacement, rotation at pile cap and also pile vertical load and pile head moment. In view of achieving the benefits of batter piles, it was suggested to account for considerable caution especially when a pile was subjected to either lateral or vertical ground movements in addition to applied static loads.

Sadek and Shahrour (2006) examined the influence of pile head connection conditions at when subjected to seismic loading considering both pinned head and fixed head connection. 3D FEA was carried out of both groups vertical and inclined micropiles (β = 20°). The piles were embedded in soil layer with increasing Young's modulus underlain by rigid bedrock. The soil mass was assumed to be linear elastic. The bending moment of inclined pile group with pinned connection experienced about 80% reduction in the maximum bending moment. However, when the inclined micropiles were embedded with its tip resting in a stiff layer the maximum axial force increases by 27 times. Thus, embedding inclined micropiles in stiff layers was not recommend for seismic areas.

Deng et al. (2007) conducted 3-D seismic analysis for a foundation consisting of battered and vertical piles designed for a heavy machine foundation located in a seismically active region considering soil pile group interaction using SASSI2000. The pile group with batter piles (battered at 1H:6V) at the perimeter consisted of 47 steel pipe piles filled with concrete. The batter piles attract 5 to 8 times axial load higher than vertical piles.

Ravazi et al. (2007) investigated the performance a typical pier deck supported on 16 steel pipe piles with and without batter piles using SAP 2000. The nonlinear static pushover was conducted on the pier deck pile group system (ATC 1996; FEMA 2000). The deck was modelled as shell element whereas the piles were modelled as frame element. Soil pile interaction was considered in the form of elasto-plastic nonlinear links which considers the elastic spring stiffness and nonlinear behaviour of soil according to API (2000). It was observed that the batter piles being the stiffest member of the structure attracted huge portion of the exerted load, further leading to failure. However, the piers supported on batter piles had less ductility than pier without batter piles.

Escoffier et al. (2008) and Escoffier (2012) conducted a series of centrifuge tests on two 2 × 1 pile groups one with two vertical piles and another with a vertical and batter pile (β = 25°). Repeated horizontal and impact loading on floating and end bearing pile groups with rigid pile to cap connection was conducted on scaled models.

Gerolymos et al. (2008) examined the seismic behaviour of 2 × 1 vertical pile group, batter pile group (β = 25°) and a group with a vertical and a batter pile (β = 25°) through 3D FE models considering both soil and pile as a linear elastic material. All the developed models were analyzed for a homogenous and non-homogenous soil profile, fixed and hinged pile to cap connection and acceleration time histories corresponding to the 2003 Lefkada, 1995 Aegion and 1995 Kobe earthquake. In addition, the effect of superstructure was also considered by modelling a SDOF system (of different height say a short and a tall slender structure) on top of the pile cap. The response of pile groups was discussed in terms of displacement, bending moment and axial force along the pile whereas the response of the superstructure was discussed in terms of maximum drift of the superstructure. Due to hinge connection between pile and the cap, satisfactory performance of both foundation and tall slender structure supported on batter pile groups was observed.

Zhang et al. (2008) conducted centrifuge tests at 45g on two model pile groups of 4 × 2 configuration founded in loose sand. Among the two groups one consisted of all vertical piles and the other consisted of 4 corner piles (β = 10°) and four vertical piles at the centre. In addition, effect of superstructure was also evaluated. The pile groups were tested for Higashi Kobe Bridge record obtained during the 1995 Hyogo-Ken Nanbu Earthquake. A comparison of experimental results to elastoplastic dynamic FEA was also presented. Inclusion of inclined piles leads to lesser correlation between the sectional and inertial forces.

Giannakou et al. (2010) conducted 3D FE modelling of 2 × 1 vertical and batter (β = 5°, 10°, 15°, 20° and 25°) pile group assuming elastic behaviour of soil, pile and superstructure. The seismic behaviour of the pile groups (with and without the superstructure considered as SDOF system) was examined for three acceleration time histories similar to (Gerolymos et al. 2008) considering a homogenous, non-homogenous and layered (double layered with top stiff and double layered with stiffer bottom) soil profiles. They concluded that the use of batter piles can be either beneficial or detrimental based on the relationship between the shear force and overturning moment.

Padrón et al. (2010) discussed the behaviour of single inclined piles, 2 × 2 and 3 × 3 pile groups with batter piles using a coupled boundary element-finite element analytical solution (Padrón 2009). The soil was modelled as homogenous viscoelastic half space and the piles were considered as elastic compressible Euler Bernoulli beams. Parametric study was conducted considering different configurations, batter angle (β = 10°, 20° and 30°) and varying pile soil modulus ratio (E_p/E_s). The results obtained were discussed in terms of dynamic stiffness and damping functions. Deeper insights on inclined piles, were achieved by using the developed coupled boundary element-finite element analytical solution (Padrón et al. 2012; Medina et al. 2014; Medina et al. 2015; Padrón et al. 2015).

Tazoh et al. (2010) conducted centrifuge tests at 30g on scaled models (1/30) of 2 × 2 vertical and batter pile (β = 10°) foundations. These models were tested for sweep test, sinusoidal motion and El-Centro record. The response of the pile groups were compared in terms of lateral displacement, rotation angle, variation of bending and axial strain and frequency transfer functions. The maximum values of both the bending and axial strains were attained at the pile heads. However, the bending and axial strain in the foundation with batter piles were higher than those in foundation with vertical piles.

Abu-Farsakh et al. (2011) conducted full scale lateral tests on M19 eastbound pier of the I-10 Twin Span Bridge supported on batter pile group foundations and developed *p-y* curves based on the results obtained. Later on, 3D FEA was also carried out by Souri et al. (2015) for the same pier to obtain the displacement, bending moment and soil resistance with depth.

Ghasemzadeh and Alibeikloo (2011) estimated the interaction between the soil mass and piles in a pile group consisting of both vertical and batter piles based on generalized Winkler-type model for pile-soil and pile-soil-pile interaction.

Tamura et al. (2012) conducted centrifuge tests at 40g on a single pile (new pile) and a single pile located at the centre of 2 × 2 pile group (existing piles). The lateral response of these piles were evaluated based on cyclic tests. In addition, 2D FEA was also conducted.

Ghazavi et al. (2013) presented analytical solutions dealing with dynamic pile soil pile interaction in battered pile groups. The pile groups were considered to be embedded in half space medium without any slippage and subjected to inclined harmonic force or seismic excitation. In addition, the effect of a receiver pile in a two-pile group was also evaluated. Parametric study was conducted considering varying properties of pile and soil, pile geometry, distance and batter angles. More pronounced changes in interaction factors were observed with increasing batter angles in two-pile group. However, in vertical direction the interaction decreases with increasing batter angle.

Goit and Saitoh (2013) and Goit and Saitoh (2014) conducted uniaxial shake table tests on single piles (β = 5° and 10°) and 2 × 2 solid cylindrical acrylic pile group (β = 0°, 5° and 10°) installed in a laminar shear box.

Subramanian and Boominathan (2015) carried out finite element analysis on the scaled modes used in their experimental study (Subramanian and Boominathan 2016). The lateral dynamic tests on scaled model pile groups consisting of 2 × 1 aluminium pipe piles of varying inclinations (β = 0°, 10° and 20°) installed on clay with high plasticity were conducted in an elastic half space tank. These model piles were tested for lateral dynamic loads varying in between 20 to 45% of static ultimate lateral capacity of the vertical pile group. In FE model the pile (β = 0°, 10°, 20° and 30°) was modelled using linear elastic material model and it was discretized as beam elements and soil was characterized using modified Drucker-Prager cap model. The dynamic response was discussed in terms of frequency, peak displacement and bending strain.

Dezi et al. (2016) investigated the dynamic response of soil pile foundation system with inclined piles considering soil pile interaction. This study was further extended to a soil pile foundation system consisting of inclined piles supporting a bridge pier by Carbonari et al. (2017).

Li et al. (2016a) conducted centrifuge experiments 1 × 2 pile groups with either vertical or batter piles (β = 15°) subjected to a series of sinusoidal dynamic loads. The effect of input motion was taken care by considering two different frequency content, one matching the frequency of the soil column and the other matching the frequency of the structure. In addition,

the effect of height of centre of gravity was taken into account by considering a tall slender and short superstructure. This study was further extended to earthquake excitation (Li et al. 2016b).

Wang et al. (2017) estimated the horizontal dynamic impedance and interaction factors of fixed head inclined piles embedded in homogenous elastic half space. Parametric study was conducted varying the slenderness ratio, E_p/E_s and batter angles (β = 5°, 10°, 15°, 20°, 25° and 30°) to estimate the coupled horizontal and vertical interaction factors.

Sarkar et al. (2018) evaluated the dynamic performance of 2 × 2 vertical and batter (β = 15°) pile groups through three dimensional finite element codes developed in MATLAB. Parametric study was conducted for two both (a) uniform and (b) triangular variation of soil modulus along depth. The effect of varying soil modulus, spacing between piles and varying excitation frequency were also explored. The seismic behaviour of the developed FE models supporting a portal frame was also examined for 1940 El-Centro Earthquake. The response of pile groups was discussed in terms of dynamic stiffness and kinematic interaction factor, whereas, the response of the portal frame was discussed as variation of roof displacement and base shear.

2.2 SUMMARY

The available literature on dynamic performance of batter piles is limited mainly to the controlled laboratory tests on scaled models and numerical simulations. The beneficial and detrimental effect of batter piles were not justified due to the limited available literature on full scale field tests. Since no research was conducted to understand the dynamic behaviour of cast in-situ batter piles, this thesis aims to study the dynamic behaviour of bored cast in-situ reinforced concrete (RC) batter piles and pile groups in field conditions.

Chapter 3

DYNAMIC RESPONSE OF BATTER PILES AND PILE GROUPS : EXPERIMENTAL INVESTIGATION

3.1 INTRODUCTION

It has been found from the available literature that, so far, the behaviour of batter piles have not been studied: (a) for bored cast in-situ piles; (b) subjected to dynamic loading from a mechanical oscillator; (c) considering the effect of an under-reamed bulb; and (d) effect of lateral loading direction. In this chapter, an attempt is made to address all the above issues and understand the associated failure mechanisms. To this end, six single piles and four pile groups are constructed by bored cast in-situ method at the selected test site and subjected to dynamic loading with the help of a mechanical oscillator. The details of the experimental program along with the results obtained are explained in detail in the following sections.

3.2 EXPERIMENTAL PROGRAM

All the six single piles and four pile groups considered in this study were constructed near the field adjacent to the Soil Dynamics Laboratory of the Department of Earthquake Engineering, Indian Institute of Technology Roorkee, India. All single piles were constructed at test site 1, whereas the pile groups were constructed few metres apart at test site 2. The detailed arrangements of these locations is shown clearly in Fig. 3.1. In the present study, lateral dynamic tests of varying excitation levels have been carried out on three reinforced concrete piles B0U1, B10U1 and B20U1 inclined at angles, β = 0º, 10º, and 20º from the vertical axis, respectively. An oscillator motor assembly has been used to generate dynamic (sinusoidal) load. The responses of these piles have been compared in terms of resonant frequency, peak lateral displacement amplitude at the pile cap, pile head (*i.e.* at the ground level) lateral displacement and shear strain. The effect of batter angle and under-reamed bulb on the rotational stiffness and damping ratio of the soil-pile system has been also discussed in detail.

Fig. 3.1 Location of test sites and arrangement of piles and pile groups (GoogleMaps 2019)

3.2.1 Site Characterization

Variation in soil profile at the test site 1 has been explored with the help of a borehole (BH) created up to a depth of 6.0 m below the ground level. The water table was encountered in the borehole at a depth of 5.5 m and 6.5 m below the ground level at test site 1 and 2 respectively. To conduct laboratory tests, disturbed representative samples from the borehole were obtained from the test location at every half meter interval. Different laboratory tests have been performed to obtain the index properties of the collected soil samples (BIS 1973; BIS 1985a; BIS 1985b). Based on different laboratory test results, the soil profile at the test sites has been divided into three layers as per (BIS 1970) (as shown in Fig. 3.2). Tables 3.1 and 3.2 reports the soil properties of each layer at test sites 1 and 2 respectively. Since the length of all the piles and pile group is 2.5 m, the entire length lies in the topmost layer as depicted in Fig. 3.2. Thus, the dynamic behaviour of the piles and pile groups considered will be significantly governed by the topmost silty sand layer. In addition, Standard penetration test (SPT) and cone penetration test (CPT) were also conducted at the test site 2. The position of all four pile groups along with the SPT and CPT locations are clearly represented in Fig. 3.1. The SPT and CPT profiles at the selected site are presented in Fig. 3.3(a-d).

Table 3.1 Soil properties at test site 1

Property of soil (depth below GL)	**Silty sand, SP-SM (0 to 3.50 m)**	**Silty clay, SC or SP-SC (3.50 to 5.50 m)**	**Silty sand, SP-SM (below 5.50 m)**
Density, γ_s (kN/m^3)	16.20	13.40	15.90
Moisture content (%)	12.00	30.00	50.00
Specific gravity, G	2.68	2.72	2.66
Liquid limit, w_L (%)	-	40.00	-
Plastic limit, w_P (%)	-	25.56	-

Table 3.2 Soil properties at test site 2

Property of soil (depth below GL)	**Silty sand, SP-SM (0 to 4.0 m)**	**Silty clay, SC or SP-SC (4.0 to 6.0 m)**	**Silty sand, SP-SM (below 6.0 m)**
Density, γ_s (kN/m^3)	18.82	19.36	19.22
Moisture content (%)	14.96	25.43	32.00
Specific gravity, G	2.76	2.81	2.64
Liquid limit, w_L (%)	-	39.50	-
Plastic limit, w_P (%)	-	28.89	-

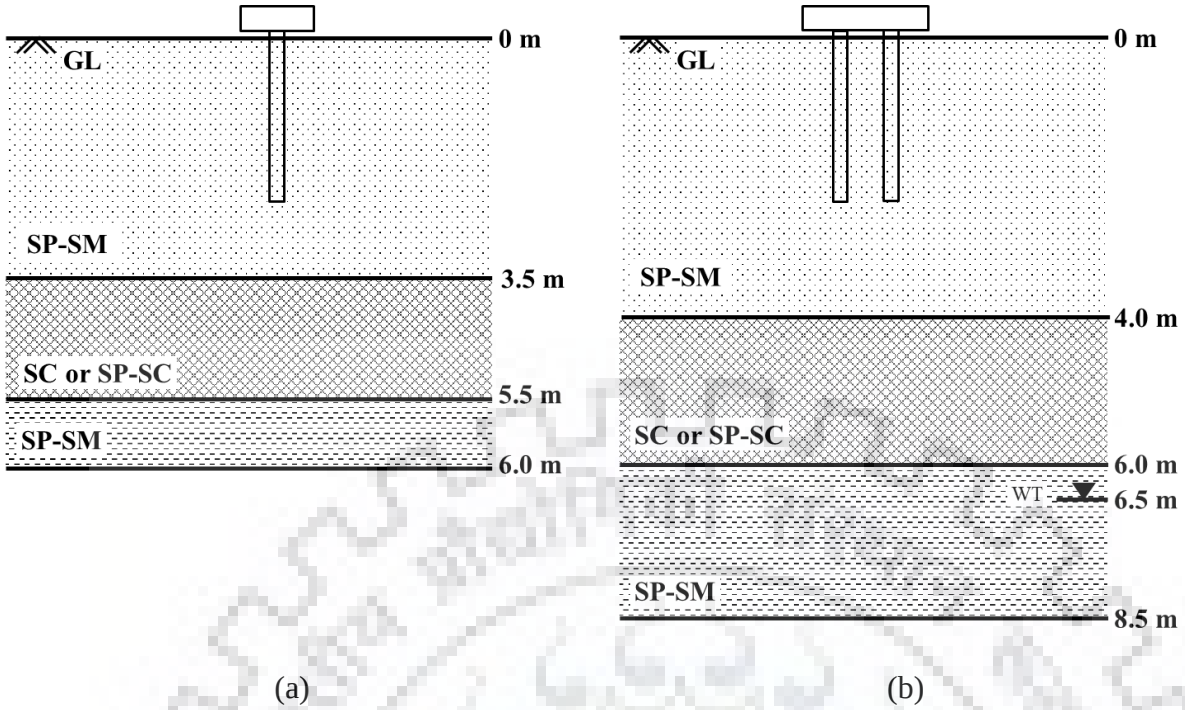

Fig. 3.2 Representative soil profiles at (a) test site 1; and (b) test site 2

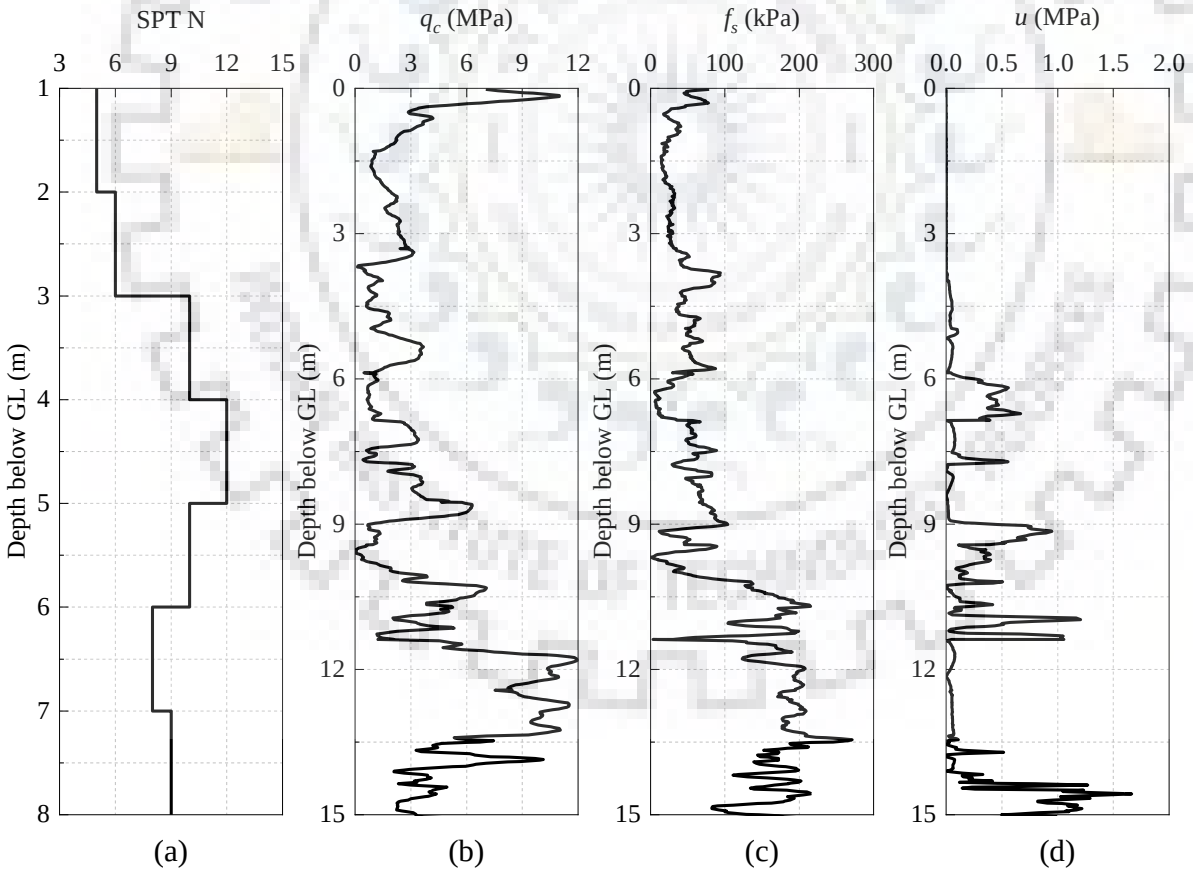

Fig. 3.3 Soil profile at test site 2 (a) SPT N value; (b) tip resistance, q_c; (c) frictional resistance, f_s; and (d) pore water pressure, u

3.2.2 Installation of Piles and Pile Groups with Cap

Six single piles: (a) single vertial pile (B0); (b) vertical pile with an under-ream bulb (B0U1); (c) 10° batter pile (B10); (d) 10° batter pile with an under-ream bulb (B10U1); (e) 20° batter pile (B20); and (f) 20° batter pile with an under-ream bulb (B20U1) as shown in Fig. 3.4 have been constructed at test site 1. Similarly, four pile groups: (a) three vertical piles (3VG); (b) three batter piles all inclined at an angle, $\beta = 20°$ to the vertical axis (3BG); (c) four vertical piles (4VG); and (d) four batter piles all inclined at an angle, $\beta = 20°$ to the vertical axis (4BG) as shown in Fig. 3.5 have been constructed as bored cast in-situ reinforced concrete piles at test site 2. All these piles had a length, l = 2.50 m and a diameter, d = 0.20 m. Piles B0U1, B10U1 and B20U1 consist of one under-reamed bulb of 0.50 m diameter. The dimensions of piles considered are selected considering the maximum excitation force level of the oscillator motor assembly used for generating dynamic loads. All the six single piles and four pile groups were bored cast in-situ piles constructed at test site1 and test site 2 in two different phases. No similarity ratio or scaling law was applied in this experimental investigation because all the tests were conducted in the existing field condition.

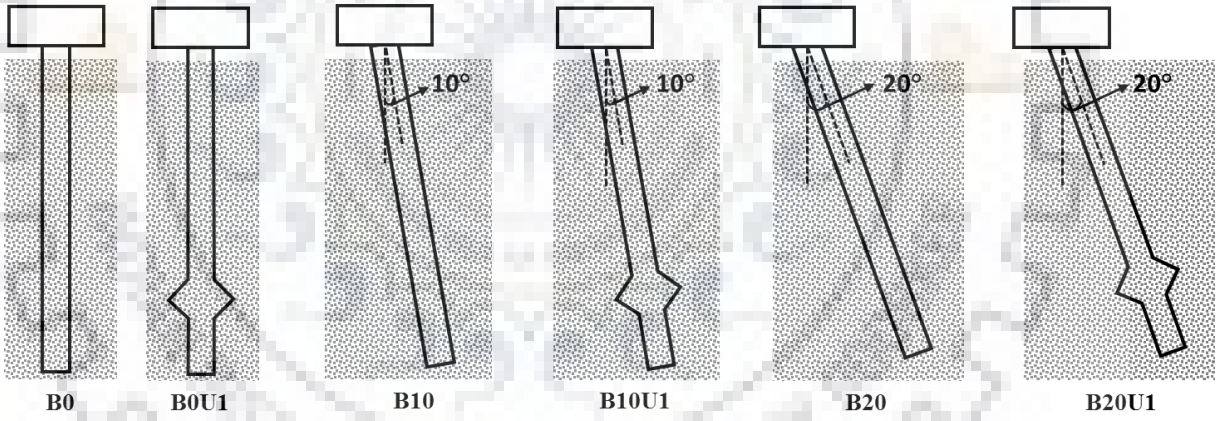

Fig. 3.4 Pile geometries in elevation for (a) single vertial pile (B0); (b) vertical pile with an under-ream bulb (B0U1); (c) 10° batter pile (B10); (d) 10° batter pile with an under-ream bulb (B10U1); (e) 20° batter pile (B20); and (f) 20° batter pile with an under-ream bulb (B20U1)

Vertical boreholes (each of diameter 0.20 m) for the required length of the piles and pile groups were created at the site by auger boring method. However, for the construction of batter piles and pile groups, inclined boreholes (each of diameter 0.20 m) for the required length of the piles were created at the site with the help of a boring guide. Construction of reinforced concrete batter piles by bored cast in-situ method beyond 20° in dry silty sand is practically not feasible. Boring beyond 20° in dry silty sand could also lead to the collapse of the bore hole before casting.

The batter piles that were constructed in the region of interest was only upto 20° and hence the boring guide used in this experiment has special arrangements for guiding the auger at four different inclination settings *i.e.* 5°, 10°, 15° and 20°. Figure 3.6 (a) shows the guide setting for boring a 20º batter pile. The under-reamer used to construct under-reamed bulb is shown in Fig. 3.6 (b). The pile and its cap was designed considering the recommendations of BIS (2010). The dimension of all the pile caps for singel pile were kept the same i.e. 0.70 m × 0.70 m × 0.30 m. In all four pile groups, the centre to centre spacing between the piles, *S* was kept equal to 2*d*. A minimum distance of at least 5*d* (≈ 1.0 m) was maintained between the pile groups. It can be observed from Fig. 3.5 (a-d) that two different dimensions of the pile caps were used for pile groups with three (3VG and 3BG) and four (4VG and 4BG) piles.

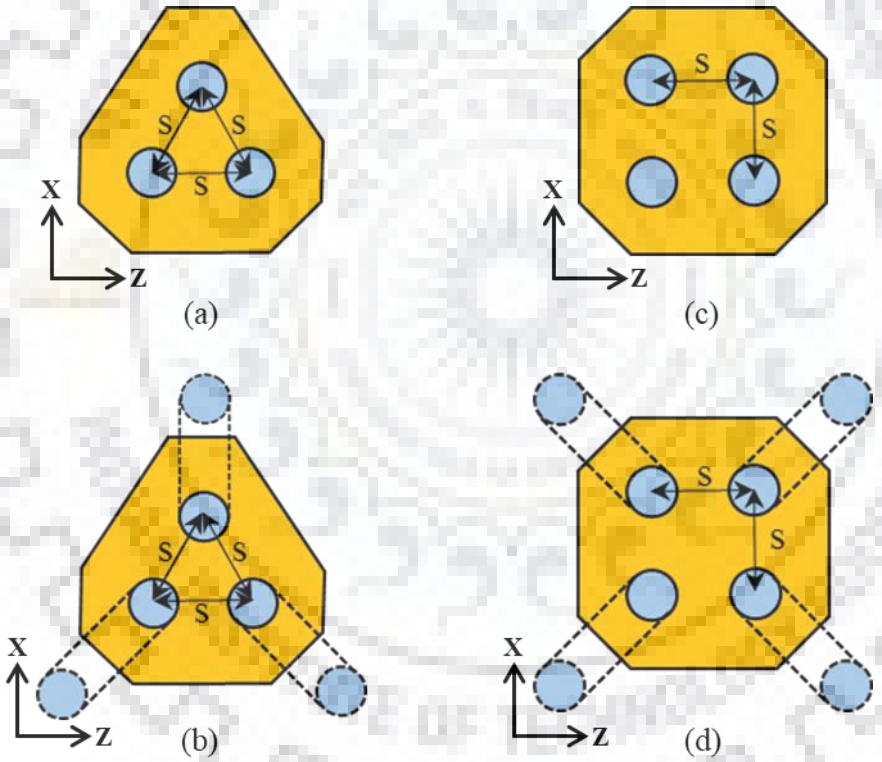

Fig. 3.5 Pile group geometries in plan for (a) 3 vertial pile group (VG); (b) 3 batter pile group (BG); (c) 4 vertial pile group (VG); and (d) 4 batter pile group (BG)

Four numbers of longitudinal thermo-mechanically treated (TMT) bars each of 10 mm diameter were provided in all piles, whereas 8 mm diameter TMT bar in the form of circular rings at the spacing of 150 mm c/c were used for transverse reinforcement to achieve confinement of concrete and support the longitudinal bars of the pile (Fig. 3.6 (c)).

Fig. 3.6 Details of construction procedure: (a) boring guide; (b) underreamer; (c) reinforcement cage for pile; (d) reinforcement cage for pile cap; (e) bolts welded to pile cap reinforcement cage; (f) welding of reinforcement cages; and (g) concreted pile cap with bolts

The clear cover of 20 mm was used for piles (BIS 2010). Separators (used for the clear cover of the pile) were fixed to the reinforcement cage and then were placed into the holes. For the pile cap, 10 mm diameter TMT bars at a spacing of 150 mm c/c with clear cover 60 mm were provided in both directions and at top and bottom of pile cap (Fig. 3.6 (d)) as given in (BIS 2010). Before casting, Four bolts were also welded to the reinforcement cage bars of the pile cap (Fig. 3.6 (e)) to facilitate mounting of the oscillator motor assembly on top of the pile cap. The reinforcement bars of both the pile and the pile cap were welded (Fig. 3.6 (f)), to ensure firm and monolithic connection. The borehole was first filled by pouring the concrete (M25 grade) into the borehole and then pile cap casting mold was filled (Fig. 3.6 (g)). The needle vibrator was used to ensure proper compaction of concrete. Proper care was taken at every stage to ensure good quality of workmanship in order to avoid adverse effects on the performance of the concrete model piles. Before the commencement of the experiment all these cast in-situ reinforced concrete piles and pile groups were cured for a minimum duration of twenty-eight days.

3.2.3 Loading and Response

The sinusoidal dynamic load was generated with the help of an oscillator having two eccentric masses (each of 8.4 kg). The oscillator motor assembly generates the dynamic load in the form of sinusoidal waves which can be represented using Eq. (3.1).

$$F_d = 2m_0 r\omega^2 \times \sin(e/2) \times \sin \omega t \tag{3.1}$$

where, F_d is the dynamic force in N; eccentric mass, m_0 = 8.4 kg; crank radius, r = 0.063 m and ω is the operating frequency in rad/sec. A pictorial representation of the oscillator with the eccentric masses representing e, r and other details is presented in Fig. 3.7 (a-b).

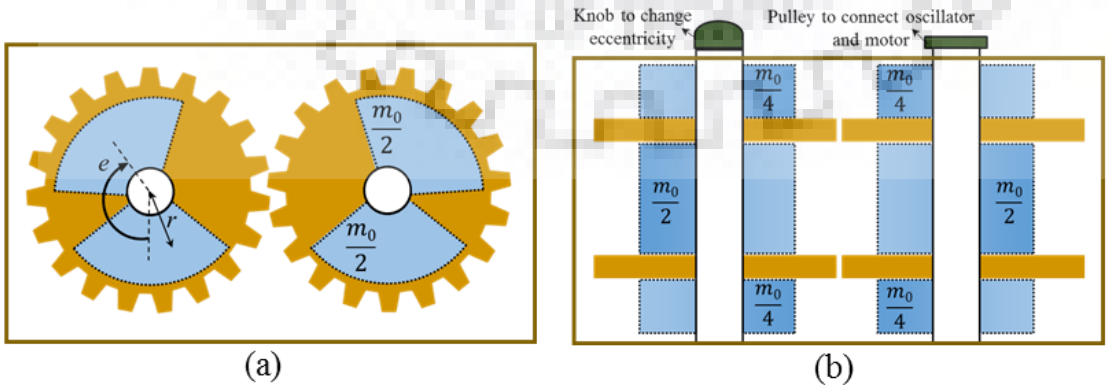

Fig. 3.7 Test setup (a) cross section of the oscillator; and (b) oscillator in plan

A 3HP DC motor with maximum working frequency of 45 Hz (2700 rpm) was used along with the speed control unit to excite the oscillator at the desired frequency. Dynamic tests on single piles have been conducted, at six different eccentricities *i.e.* 10º, 20º, 30º, 60º, 80º and 100º with excitation frequency ranging between f_1=1 to f_n=40 Hz at all considered eccentricity of the oscillator. For dynamic tests on pile groups, five different eccentricities *i.e.* 30º, 60º, 90º, 120º and 150º have been considered. A typical force time history for varying frequency is represented in Fig. 3.8 (a and b) for e = 30 and 150º, respectively. At a particular eccentricity, the single piles were first tested in one of the lateral (X) direction, followed by the another lateral (Z) direction. Further the piles were excited in vertical (Y) direction to measure the dynamic response. However at paticular forcing level, a minimum duration of 48 hours was maintained as the rest period between each test. The tests were conducted on the piles at a higher eccentricity following the same loading direction sequence (*i.e.* first X, second Z and third Y). This loading sequence was maintained so that the pile is subjected to same force level in all three directions before testing it for a higher force level.

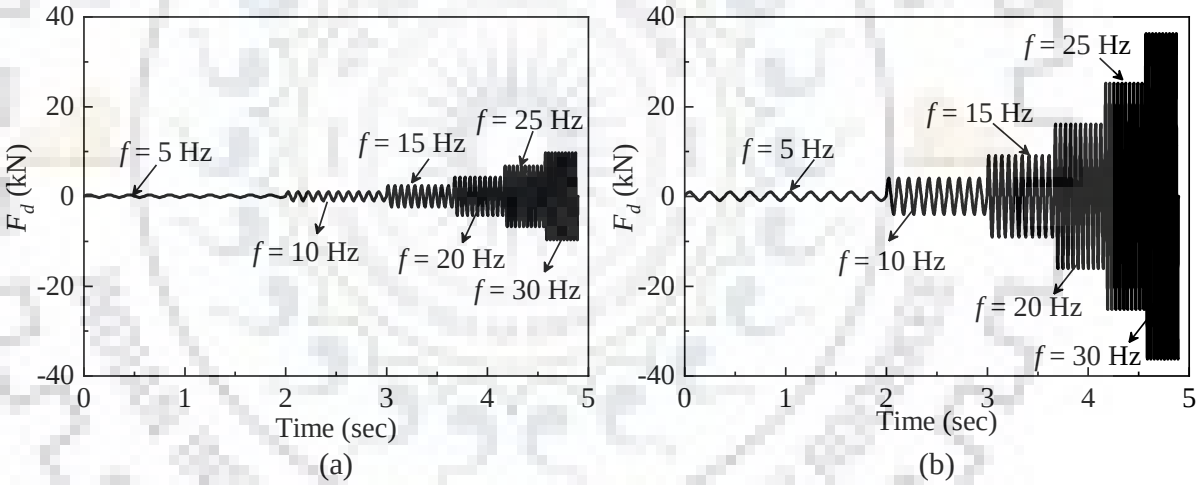

Fig. 3.8 Force-time history for different frequencies at (a) e = 30°; and (b) e = 150°

The assembly of oscillator motor mounted on the pile cap for lateral and vertical excitations is depicted in Figs. 3.9 (a-b) respectively. The oscillator motor assembly used for generating sinusoidal dynamic load consists of a base plate (40 kg), two supporting frames (27.5 kg), four long steel rods (9 kg), four small steel rods (5.5 kg), oscillator (119 kg), a motor base plate (61.5 kg) and a motor (104.5 kg). The oscillator was firmly mounted on pile cap top, with four connecting bolts, on top of which DC motor was mounted. During lateral excitation, 3 accelerometers were placed along the pile cap depth (Fig. 3.9 (a)) whereas, for vertical excitation 2 accelerometers are placed on top of the adjacent faces of the pile cap (Fig. 3.9 (b)). A multi-

channel data acquisition device (Fig. 3.10 (a)) from National Instruments, NI 9233 (24 bit delta sigma (with analog prefiltering) ADC and 102 dB dynamic range) was used along with PCB accelerometers (Fig. 3.10 (b)) with sensitivity 100 mVolts/g (±10%); frequency range between 0.5 and 10000 Hz and measurement range of ±50 g pk to record the dynamic response in terms of acceleration during the experiment. The data acquisition device is further connected to the computer with the help of portable USB carrier NI USB-9162. At each operating frequency 12000 continuous samples of acceleration time history data were recorded with a sampling rate of 2000 Hz in the real-time for all considered cases. A tacheometer (Fig. 3.10 (c)) is used to record the operaing frequency of the system. Schematic representation of the entire test setup for single piles and pile group subjected to both lateral and vertical excitation is presented in Fig. 3.11 (a-b) respectivley.

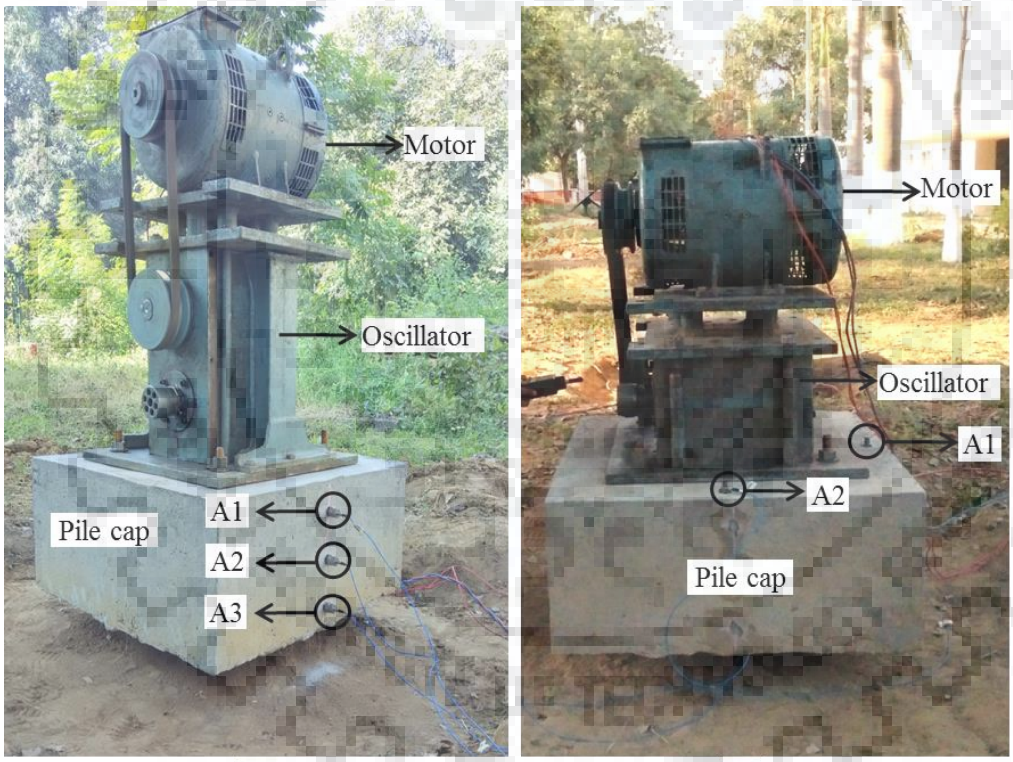

Fig. 3.9 Test setup for (a) lateral vibration; and (b) vertical vibration

In addition, the effect of lateral loading direction on these single piles are also examined. The direction of dynamic loading has been altered by changing the orientation of the oscillator motor assembly. Figures 3.12(a-b) depicts both the direction of excitations considered for this experimental investigation.

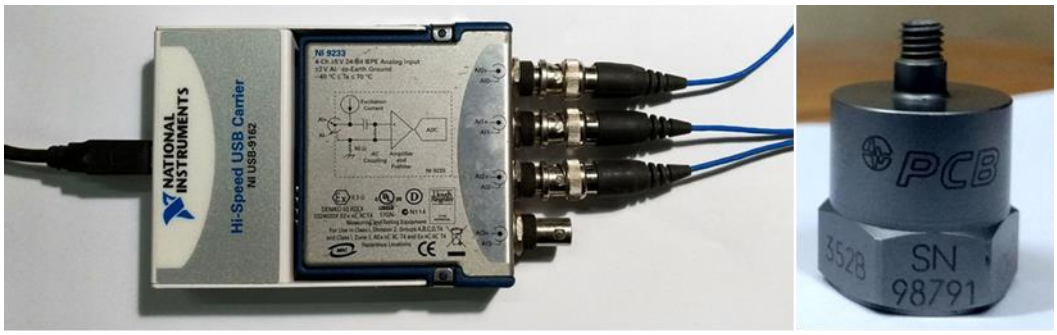

(a) (b)

(c)

Fig. 3.10 Details of other instruments including (a) data acquisition system; (b) accelerometer; and (c) tacheometer

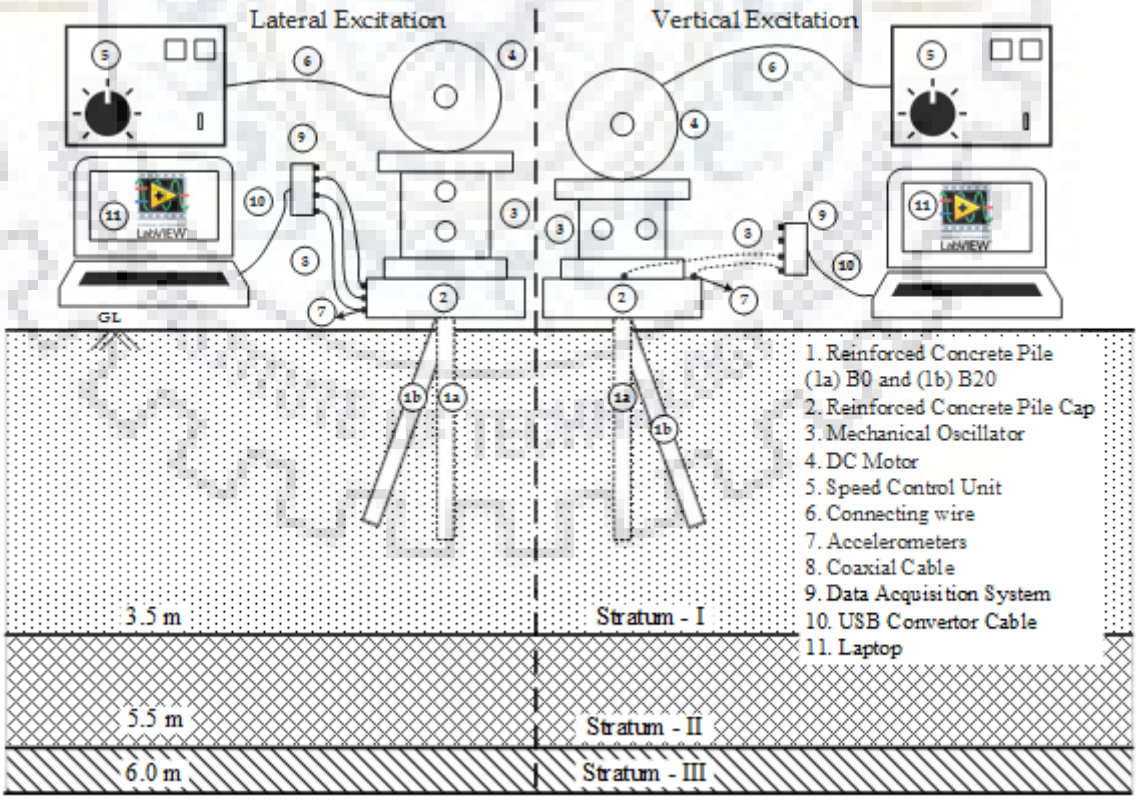

(a)

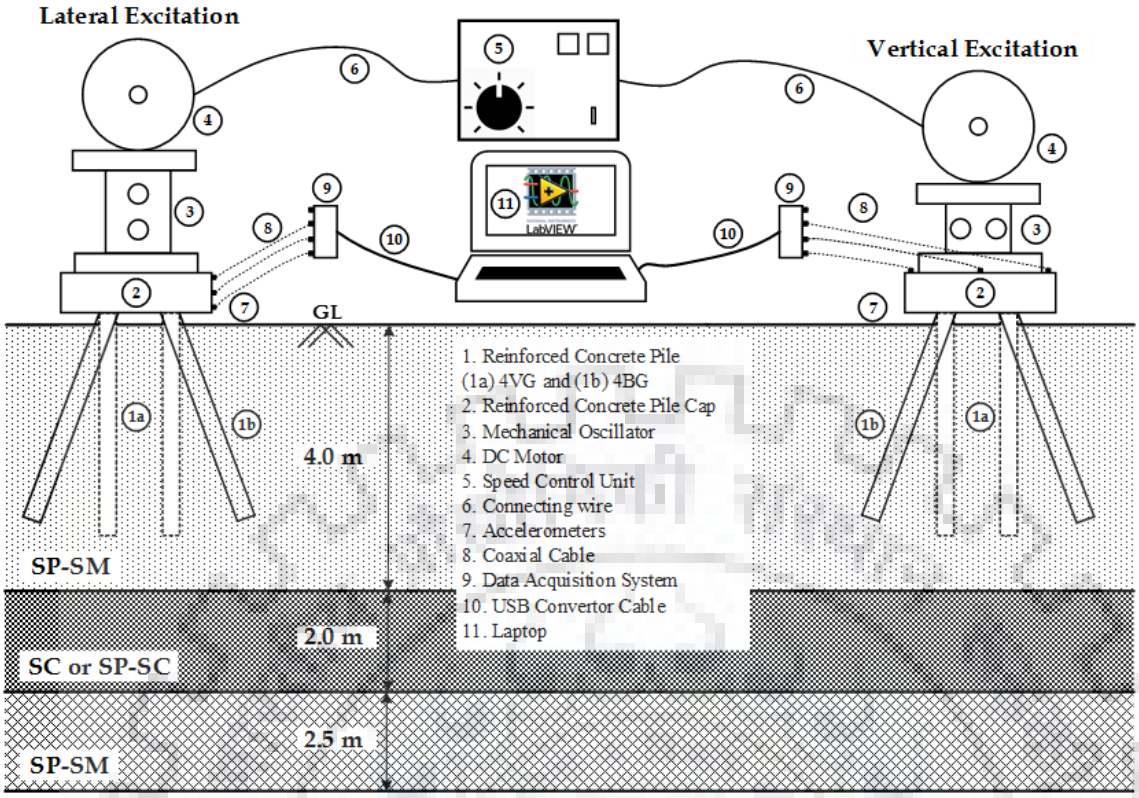

(b)

Fig. 3.11 Schematic representation of the entire test setup for (a) single; and (b) pile group

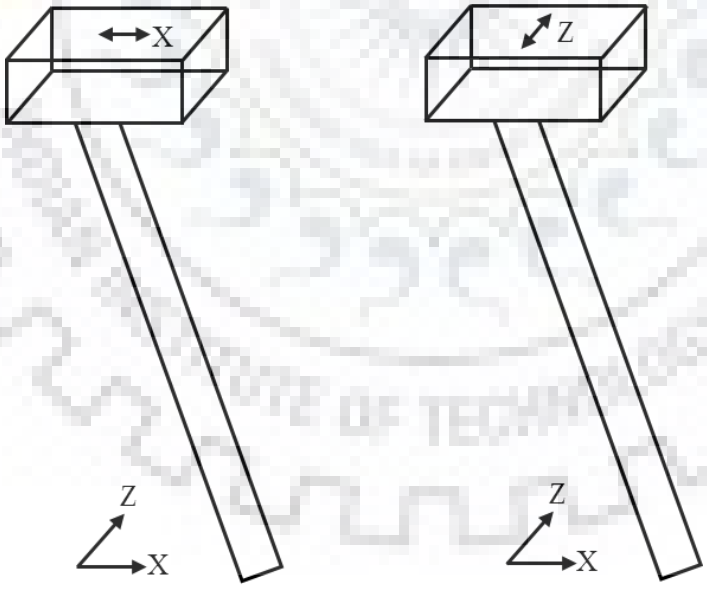

(a) (b)

Fig. 3.12 The direction of lateral loading (a) X; and (b) Z

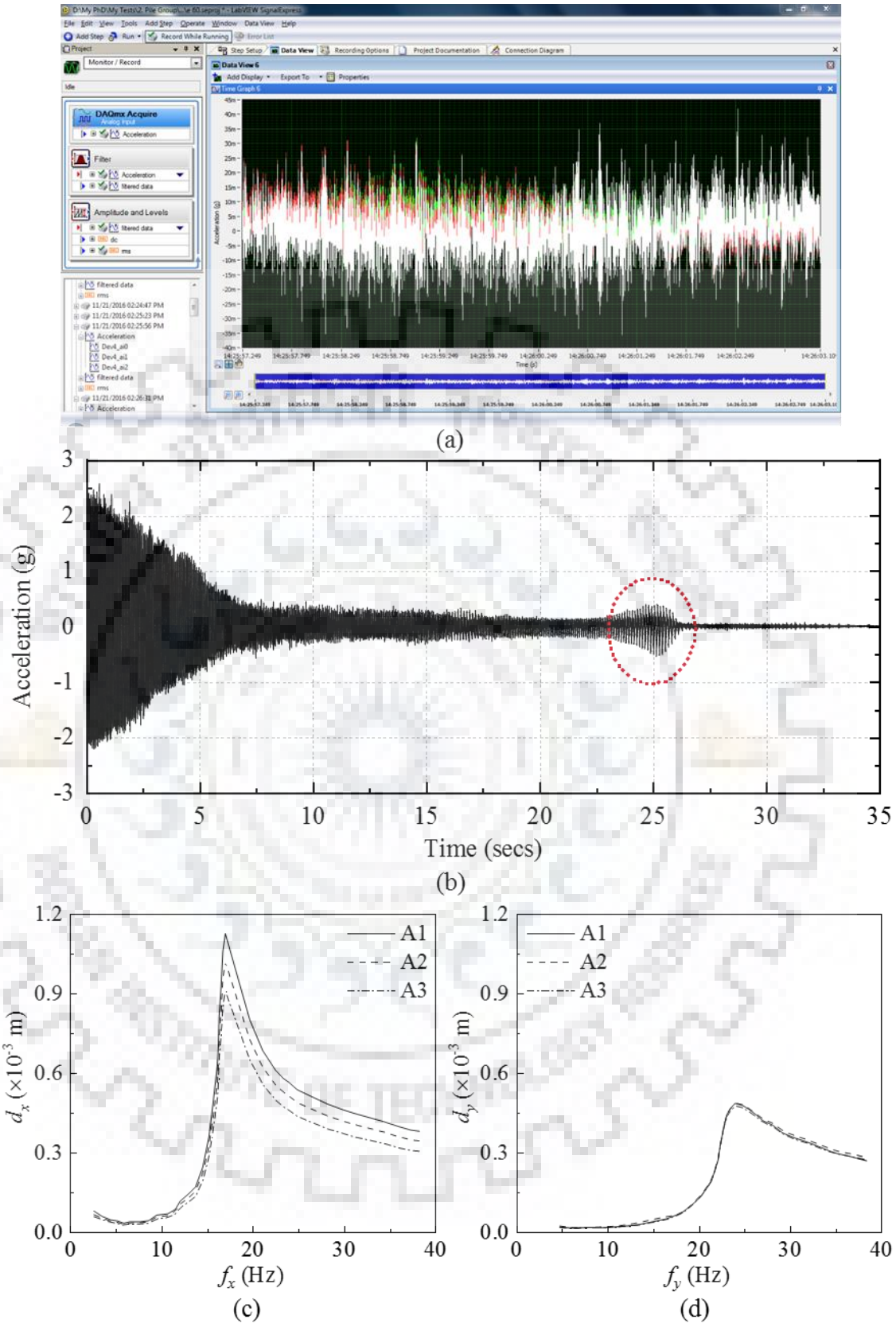

Fig. 3.13 Sample record obtained during (a) dynamic test; (b) typical rundown acceleration record; (c) typical displacement response of 4VG at e = 90° in X; and (d) typical displacement response of 3VG at e = 90° in Y

The acceleration-time histories were recorded and processed in real tim during the experiment at each operating frequency through LabVIEW (2009) software. A typical acceleration time history record obtained during the dynamic test is presented in Fig. 3.13(a). In Fig. 3.13(a), bands in different colors represent the response recorded during the experiment through different accelerometers. When the operating frequency reaches f_n the power supply to the oscillator is withdrawn by switching off the speed control unit and rundown is recorded which captures the entire test in the reverse order (i.e. from 40 Hz to 0 Hz). A typical rundown record thus obtained is presented in Fig. 3.13(b) where the encircled region represents the range of resonant frequency. Since this record is obtained after reaching f_n it has frequency in the reverse order. The rundown record thus obtained has been only used for verifying the resonant frequency obtained. A typical frequency amplitude response obtained from the records in X and Y directions is presented in Fig. 3.13(c) and 3.13(d), respectively. In Fig. 3.13(c) and 3.13(d), A1, A2 and A3 represent the records of three different accelerometers used.

3.3 RESULTS AND DISCUSSION

The dynamic responses of single piles and pile groups, obtained from the recorded acceleration time histories in lateral and vertical directions have been discussed in detail, in terms of resonant frequency, displacement amplitude, induced strain level *etc*., in the following sections.

3.3.1 Single Piles

3.3.1.1 Lateral Response

The dynamic response of single piles without an under-reamed bulb excited, at all considered force levels, both in X and Z directions are presented in terms of frequency (f_x or f_z) against lateral displacement (d_x or d_z) in Figs. 3.14(a-c) and 3.14(d-f) respectively. Similarly, the dynamic response of single piles with an under-reamed bulb excited both in X and Z directions are presented in Figs. 3.15(a-c) and 3.15(d-f) respectively. The recorded frequency versus lateral displacement amplitude variation thus obtained for piles excited in X and Z directions at all considered force levels in terms of exciting frequency of the oscillator (up to 25 Hz so that the difference between peaks are clearly visible). In all the cases the resonant frequency was observed below 25 Hz.

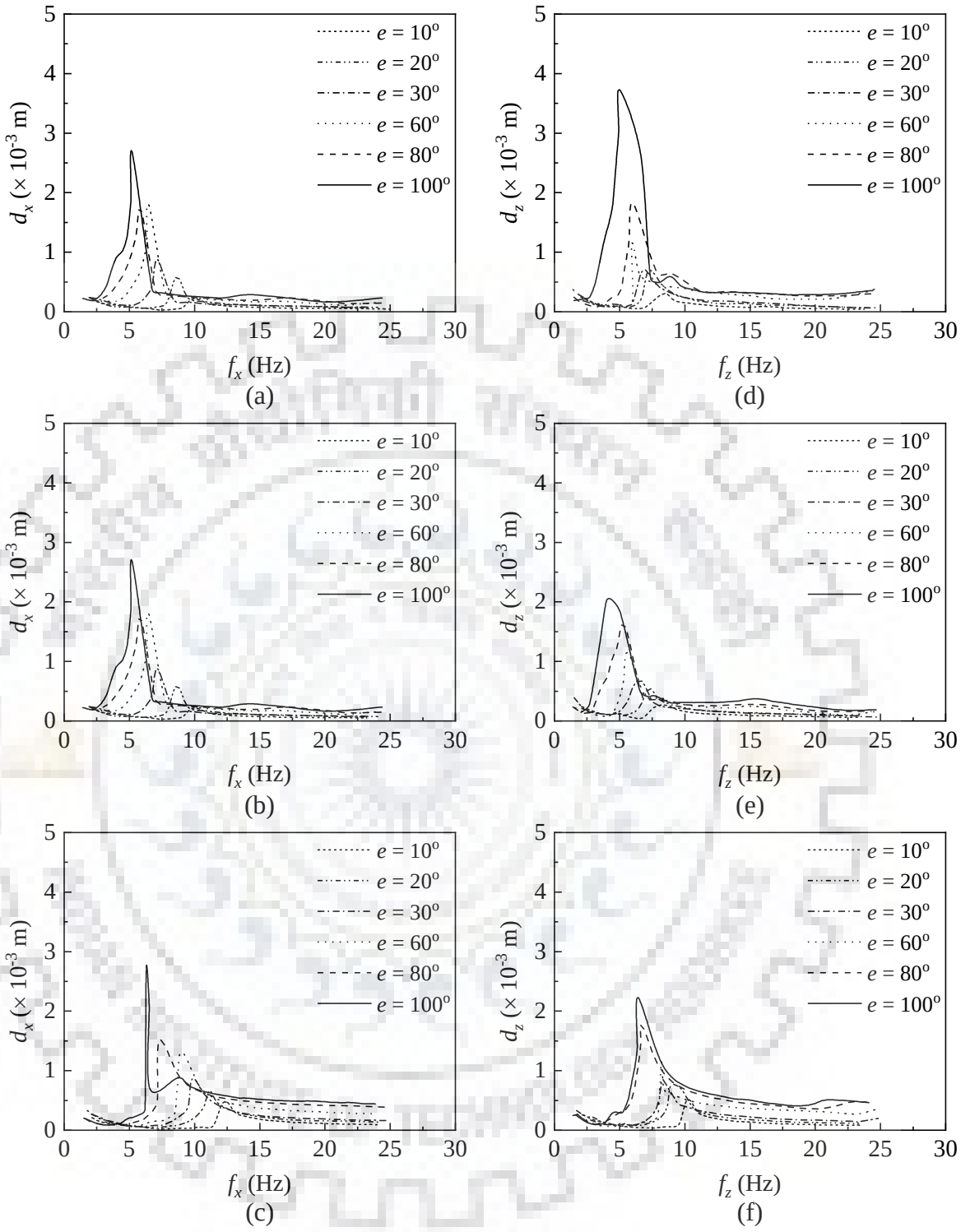

Fig. 3.14 Frequency variation with lateral displacement amplitudes for (a) B0 in X; (b) B10 in X; (c) B20 in X; (d) B0 in Z; (e) B10 in Z; and (f) B20 in Z

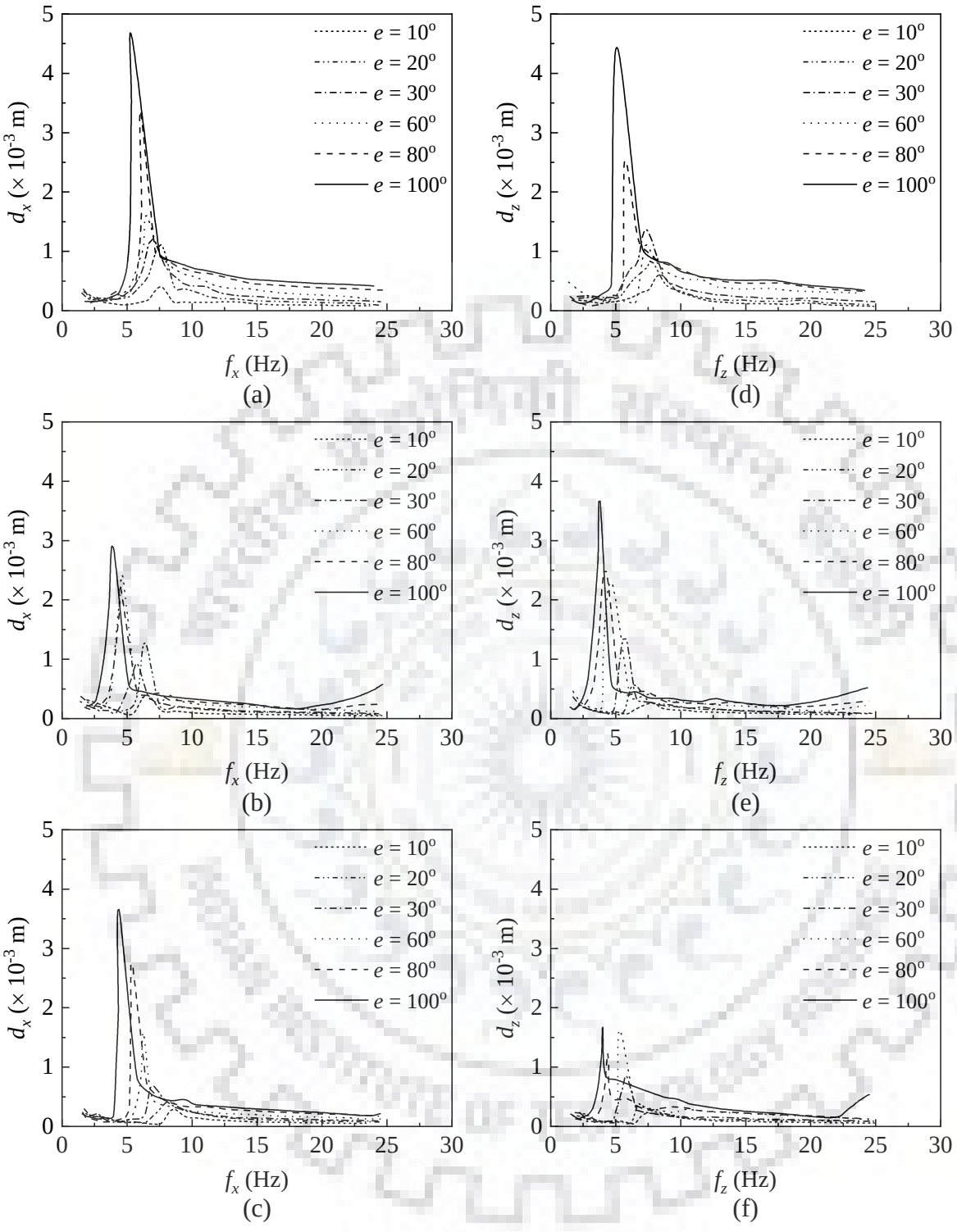

Fig. 3.15 Frequency variation with lateral displacement amplitudes for (a) B0U1 in X; (b) B10U1 in X; (c) B20U1 in X; (d) B0U1 in Z; (e) B10U1 in Z; and (f) B20U1 in Z

The dynamic lateral behavior is also discussed in terms of peak lateral displacement, resonant frequency, ground level displacement, induced shear strain, rotational stiffness and damping ratio. The frequency has been obtained from the rotations (*i.e.* rotations per minute) of the oscillator motor assembly. The reported displacement response of the piles was obtained as the average of the measured acceleration response with the help of three accelerometers. The displacement is obtained, as ratio of acceleration and $4\pi^2 f^2$ where f is the frequency in Hz, according to the procedure suggested by BIS (1981b). When the response of the soil-pile system is similar to a single degree of freedom system then the frequency displacement response consists of only a single peak as observed in Fig. 3.14 and 3.15. A minimal gap (less than 5 cm) was created between the ground surface and bottom of all the pile caps to avoid the friction between them. Rotational mode of vibration is more significant for large freestanding length or slender piles, but in this study, the freestanding length is less than 5 cm and the slenderness ratio is also very less. Hence, only the translation mode is significant as also observed in the experimental records. Based on the observations from the frequency displacement response, further analysis has been carried out considering the soil-pile system as a single degree of freedom. It can be observed from Fig. 3.14 and 3.15 that there is only one peak value in all the cases. The soil-pile system behaves like a single-degree-of-freedom system and hence only one peak is observed unlike a two-degree-of-freedom system. Thus, for the further interpretation, the soil-pile system is considered to be a single-degree-of-freedom system. From the frequency versus displacement amplitude records, the resonant frequency and the peak lateral displacement amplitude for all the considered cases are obtained and reported.

The resonant frequency (f_x' or f_z') and peak displacement amplitude (d_x' or d_z') of piles B0, B10 and B20 at each force level, in both X and Z directions, were obtained from the frequency displacement amplitude records and are reported in the Figs. 3.16(a-b) and 3.16(c-d) respectively. Similarly, the variation of f_x' or f_z' and d_x' or d_z' of piles B0U1, B10U1 and B20U1 with force level are reported in Figs. 3.17(a-b) and 3.17(c-d) respectively. The resonant frequency of the soil-pile system, (f_x' or f_z') significantly reduces (by 37-50%) with the increase in force level (*i.e.* eccentricity) in both the lateral directions. Possible reasons may be, as the eccentricity increases, force level also increases, and degradation in stiffness of the soil mass also increases. Hence, the stiffness of the soil-pile system participating in vibration decreases which leads to decrease in the resonant frequency. The peak displacement, (d_x' or d_z') increases with increase in the force level in both the directions. The increase in d_x' or d_z' at maximum forcing level, was about 11 times than that of minimum forcing level for B0 pile and about 4 times for B20 pile. It is worth mentioning that at all lower eccentricities (*i.e.* $\leq 80°$ eccentricity) there is no significant

difference in the displacement amplitude in X and Z direction of B0. When the pile B0 was excited at e = 100° in Z direction the displacement amplitude was much higher. This may be attributed to the permanent deformation of the soil pile system which was evident through gap formation along the circumference of the piles.

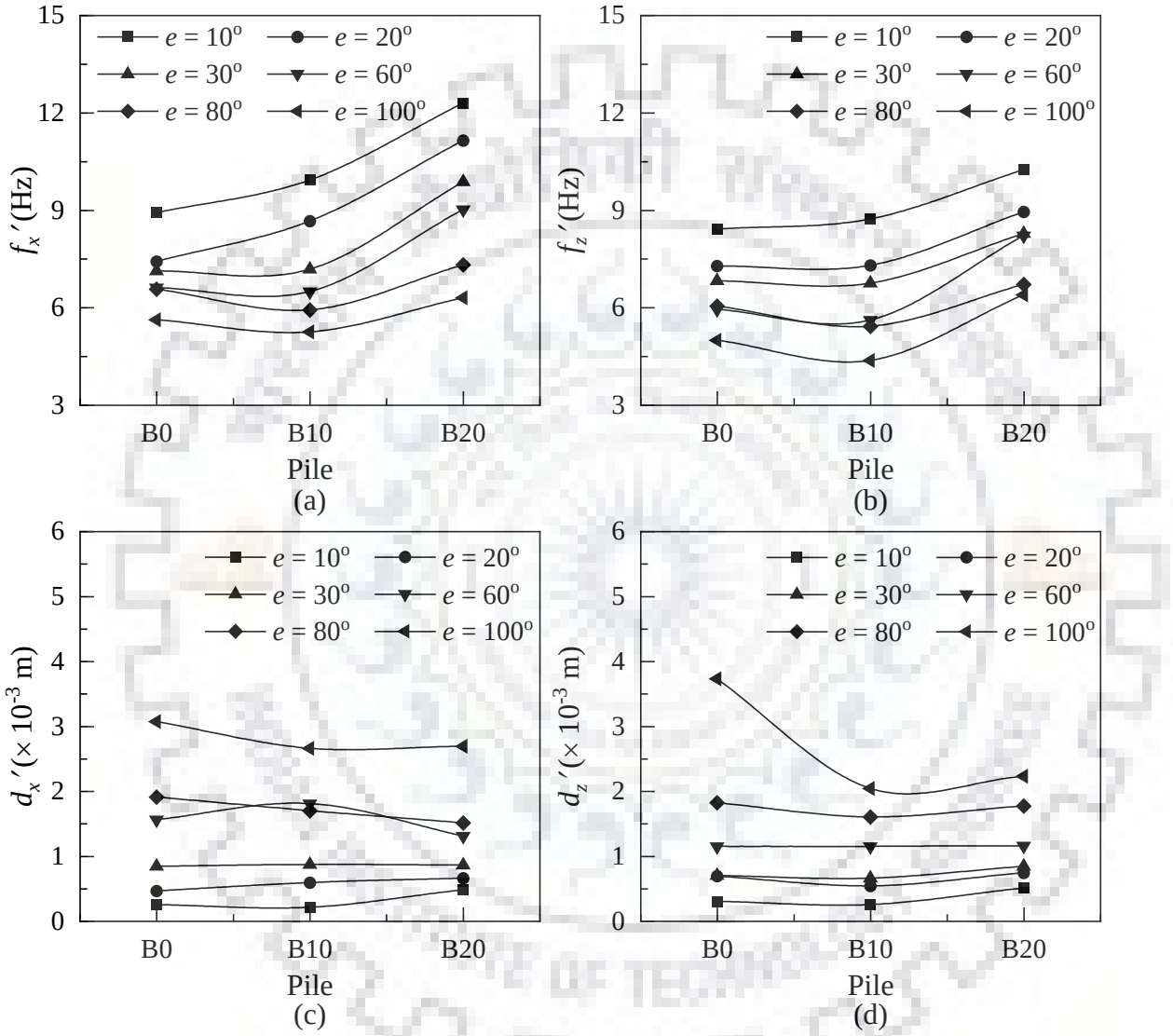

Fig. 3.16 Experimental observations on B0, B10 and B20 (a) resonant frequency in X (b) resonant frequency in Z (c) peak displacement amplitude in X and (d) peak displacement amplitude in Z

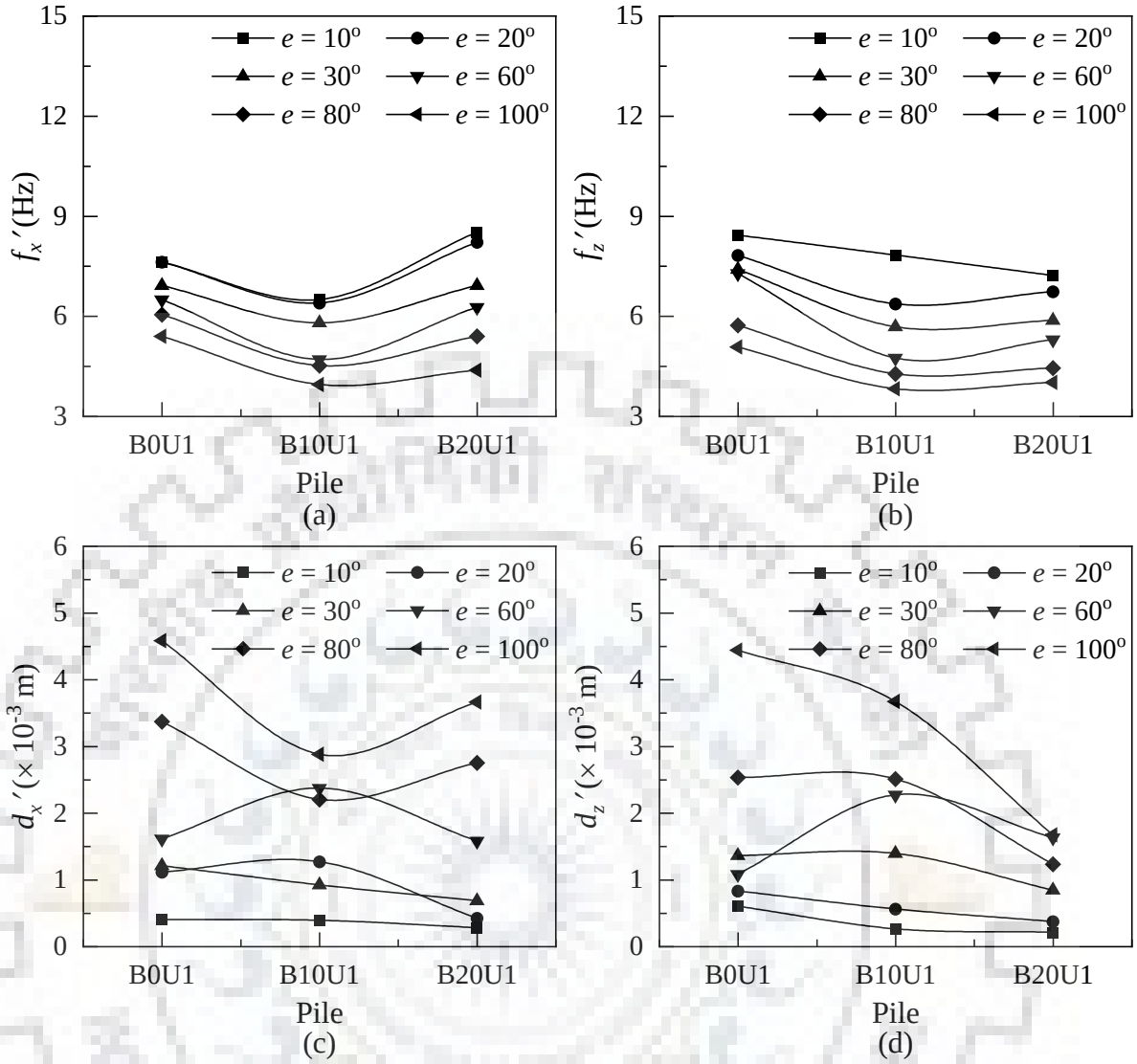

Fig. 3.17 Experimental observations on B0U1, B10U1 and B20U1 (a) resonant frequency in X; (b) resonant frequency in Z; (c) peak displacement amplitude in X; and (d) peak displacement amplitude in Z

Let the top, middle and bottom displacement values in X direction be d_{x1}, d_{x2}, and d_{x3} respectively. The displacement response revealed linear variation in displacement from the top to bottom, d_{x1} the maximum and d_{x3} the minimum in all the cases. When d_{x1}, d_{x2}, and d_{x3} values extend to meet the pile it intersects the pile's centreline at a critical depth as shown in Fig. 3.18. In case of B10U1 and B20U1 the equivalent vertical depth is considered as critical depth. The rotational amplitude, A_θ is obtained from the critical depth and d_{x1}. Knowing the rotational amplitude the displacement at ground level (d_{xg} or d_{zg}) is attained. The ratio of d_{xg} or d_{zg} and pile diameter is defined as the induced shear strain (ε_x or ε_z) in this study. The variation of d_{xg} or d_{zg}

and ε_x or ε_z with force level is reported in detail in the following section. BIS (1981b) suggests a procedure to evaluate the overall stiffness and damping ratio of the soil-pile systems subjected to dynamic lateral tests which is summarized briefly as follows: The resonant frequency obtained from the experimental frequency displacement response is assumed as the damped natural frequency of the system (f_{ndx} or f_{ndz}). Then assuming a damping ratio (ξ), undamped natural frequency (f_{nx} or f_{nz}), magnification factor (μ) and static displacement (δ_{stat}) were arrived. The exciting moment M_d is obtained as the product of the height of c.g. of oscillator mass (0.235 m in this case) to F_d obtained using Eq. 1. Then, the slope of M_d against δ_{stat} gives the stiffness of the soil-pile system for an assumed ξ. Now, ξ is recalculated from the stiffness value obtained. This process is repeated until the difference between both assumed and calculated ξ becomes small enough to be neglected. Thus the value obtained is the ξ_x or ξ_z and the corresponding stiffness is $K_{\theta x}$ or $K_{\theta z}$ which are reported in the following sections.

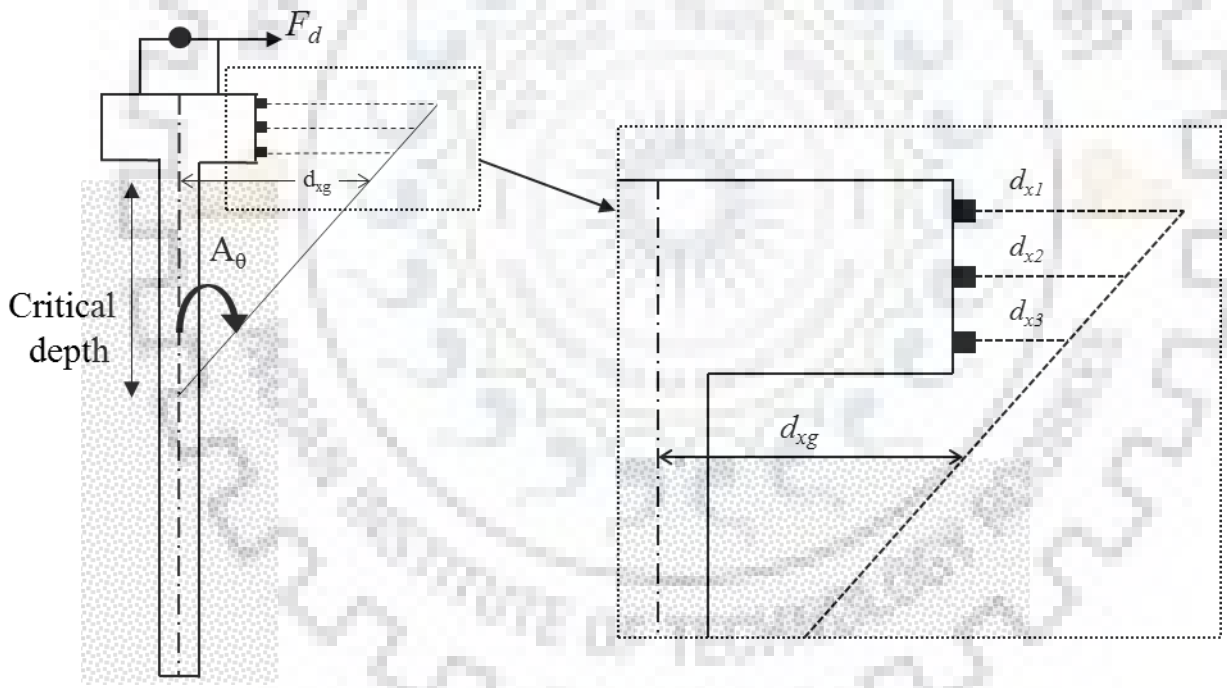

Fig. 3.18 Critical depth for shear strain

Effect on displacement at ground level and induced shear strain

The variation of displacement at ground level (d_{xg} or d_{zg}) against force level for piles B0, B10, and B20 in X and Z directions are presented in Figs. 3.19(a-c) and 3.19(d-f) respectively. Similarly, the variation of d_{xg} or d_{zg} with the force level for piles B0U1, B10U1 and B20U1 is presented in the Figs. 3.20(a-c) and 3.20(d-f) excited in both X and Z directions respectively. It

is evident from these figures that, with the increasing eccentricity (or force level), pile head lateral displacement also increased in all cases. Pile B0U1 has recorded the maximum pile head displacement while excited in both X and Z directions and at all force levels. It is interesting to note that when the piles are excited in X direction at higher force levels (*i.e.* beyond 60º eccentricity), the pile B10U1 had even lesser pile head displacement than pile B20U1. This shows that depending upon the magnitude of force level and soil type even smaller batter angles may provide impressive results. Thus it is clear that batter piles *i.e.* B10U1 and B20U1 helps in reducing the lateral displacement when compared to pile B0U1.

The variation of shear strain (ε_x or ε_z) against force level for piles B0, B10, and B20 in X and Z directions are presented in Figs. 3.21(a-c) and 3.22(d-f) respectively. Similarly, the variation in shear strain along with the force level for piles B0U1, B10U1 and B20U1 is presented in Figs. 3.22(a-c) and 3.22(d-f) excited both in X and Z directions respectively. From these figures, it is evident that the shear strain increases with increasing force level. The increase in shear strain with force level was more prominent in case of B0 and B10 as compared to B20. The shear strain induced in piles B10U1 and B20U1 is higher than that of pile B0U1 upto 60° eccentricity when the piles were excited in X direction. Suddenly, the shear strain induced in B10U1 and B20U1 falls down as compared to that of pile B0U1 beyond 60° eccentricity in X direction. It could be noted that at higher force levels (*i.e.* beyond 20° eccentricity) the shear strain induced in pile B10U1 was the highest when the piles were excited in *Z* direction. The variation in shear strain can be attributed to the amount of passive pressure mobilized during the lateral excitation of the system.

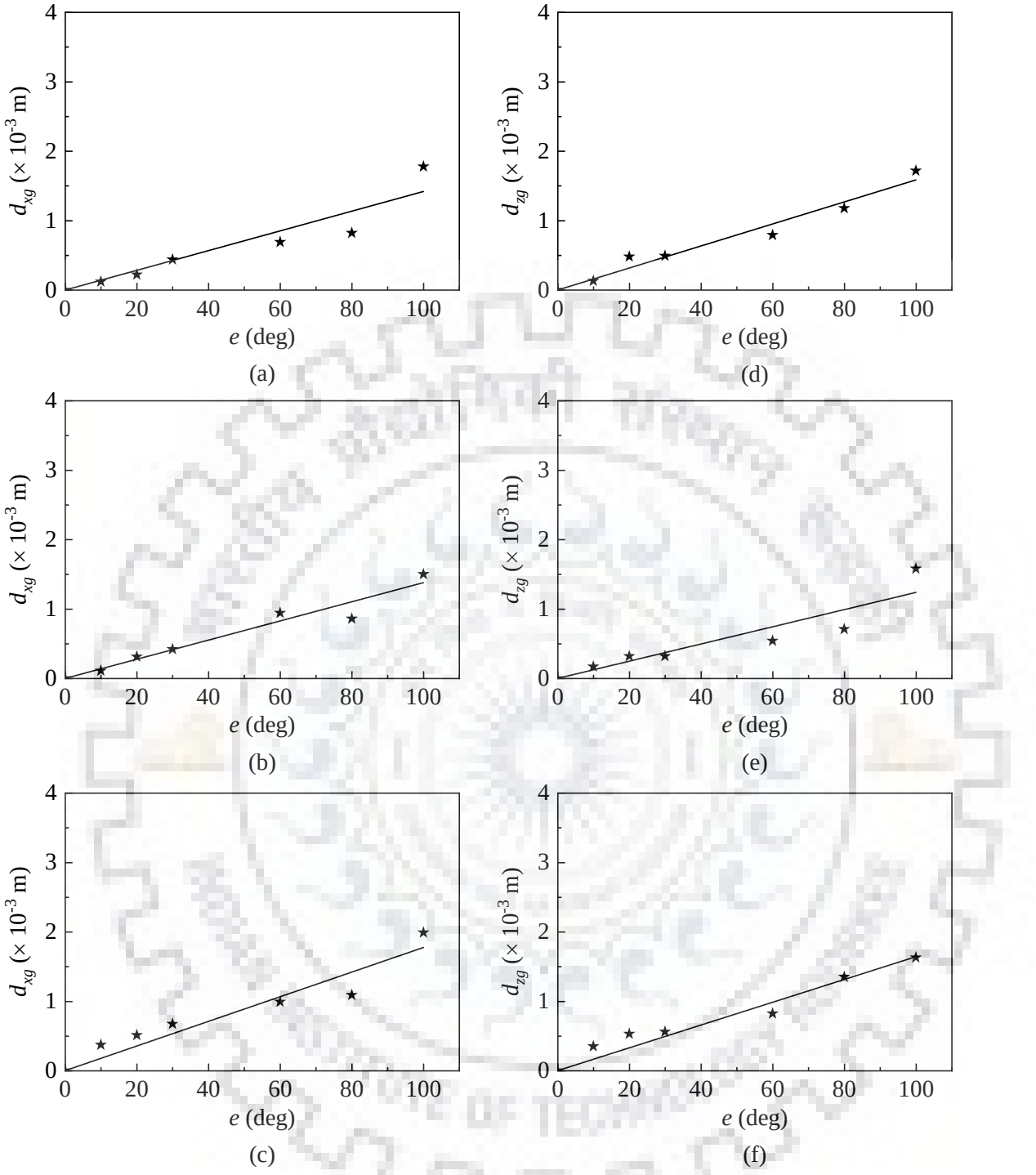

Fig. 3.19 Displacement at ground level of (a) B0 in X; (b) B10 in X; (c) B20 in X; (d) B0 in Z; (e) B10 in Z; and (f) B20 in Z

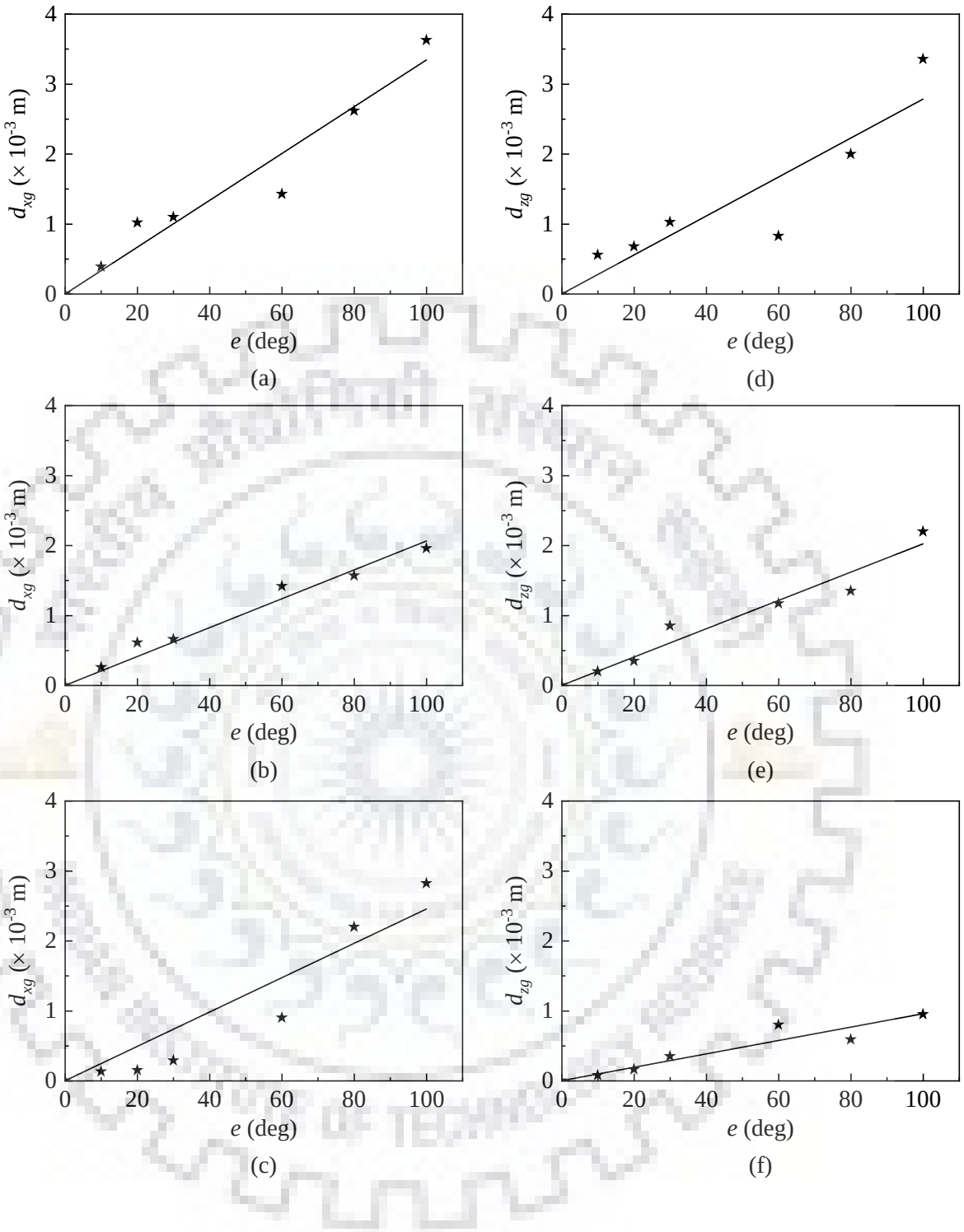

Fig. 3.20 Displacement at ground level of (a) B0U1 in X; (b) B10U1 in X; (c) B20U1 in X; (d) B0U1 in Z; (e) B10U1 in Z; and (f) B20U1 in Z

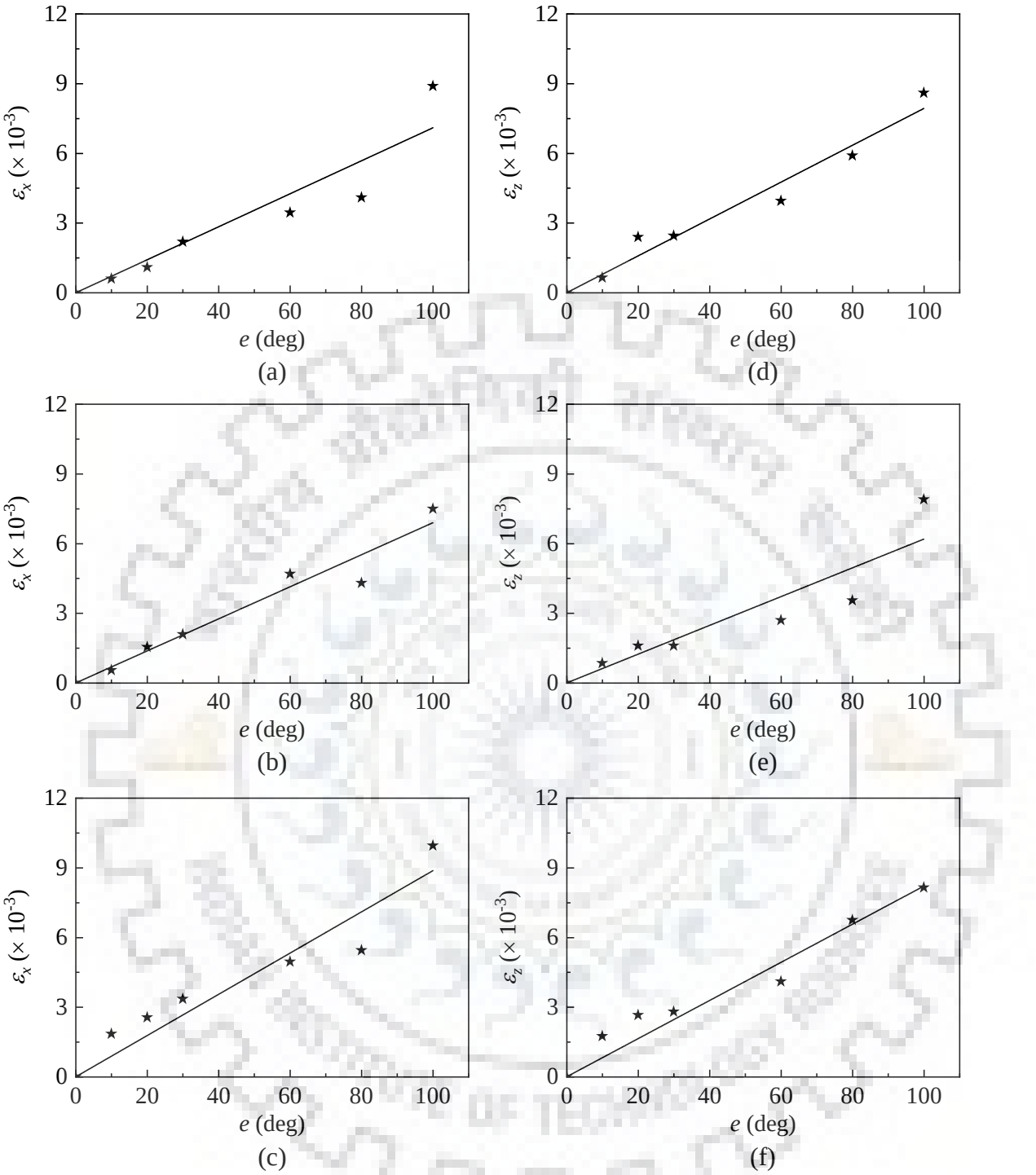

Fig. 3.21 Shear strain variation for (a) B0 in X; (b) B10 in X; (c) B20 in X; (d) B0 in Z; (e) B10 in Z; and (f) B20 in Z

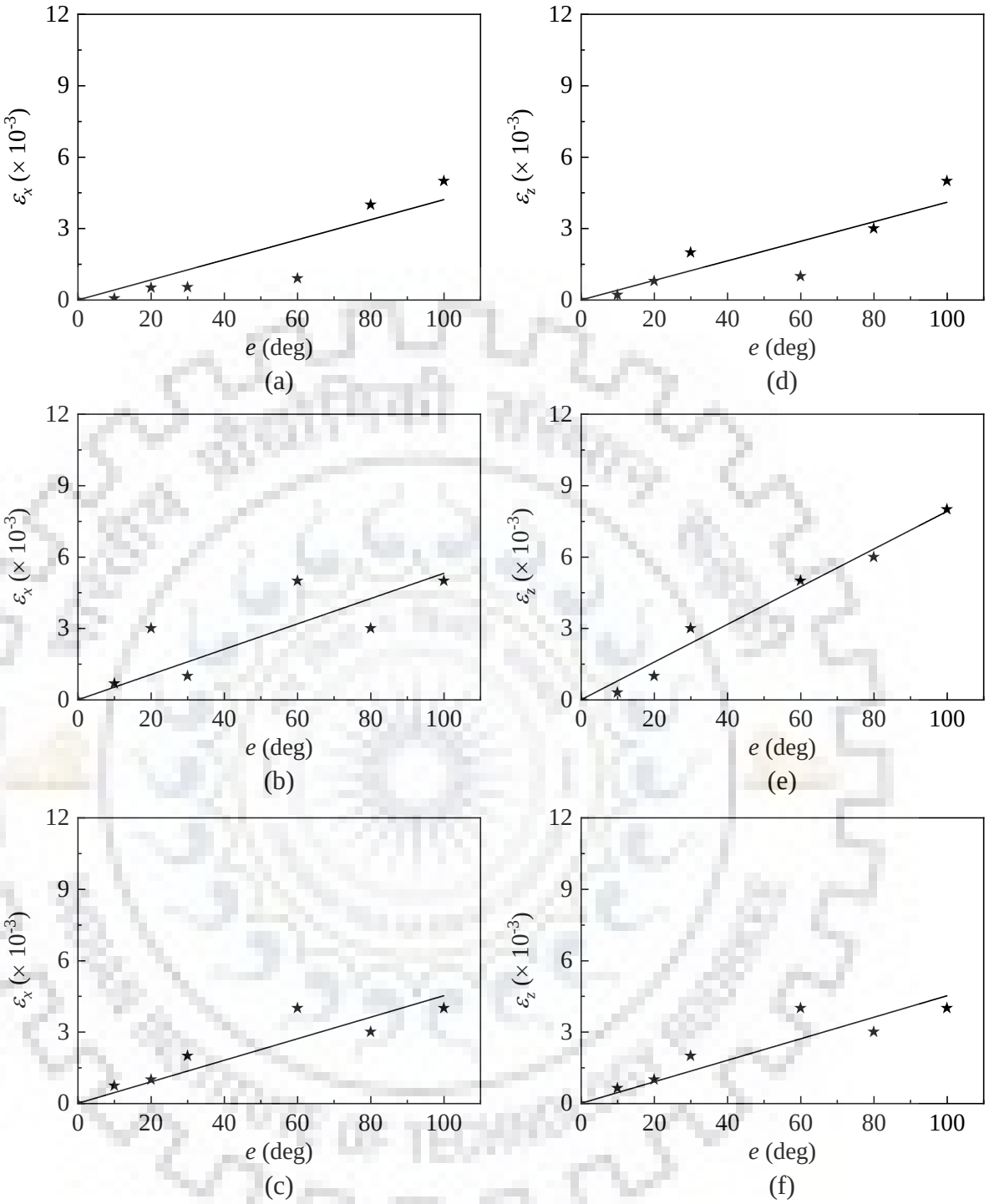

Fig. 3.22 Shear strain variation for (a) B0U1 in X; (b) B10U1 in X; (c) B20U1 in X; (d) B0U1 in Z; (e) B10U1 in Z; and (f) B20U1 in Z

Effect on the rotational stiffness of the soil-pile system

The rotational stiffness of the soil-pile system ($K_{\theta x}$ or $K_{\theta z}$) in X and Z directions for piles B0, B10, and B20 decrease nonlinearly with an increase in the strain level as shown in Figs. 3.23(a-c) and 3.23(d-f) respectively.

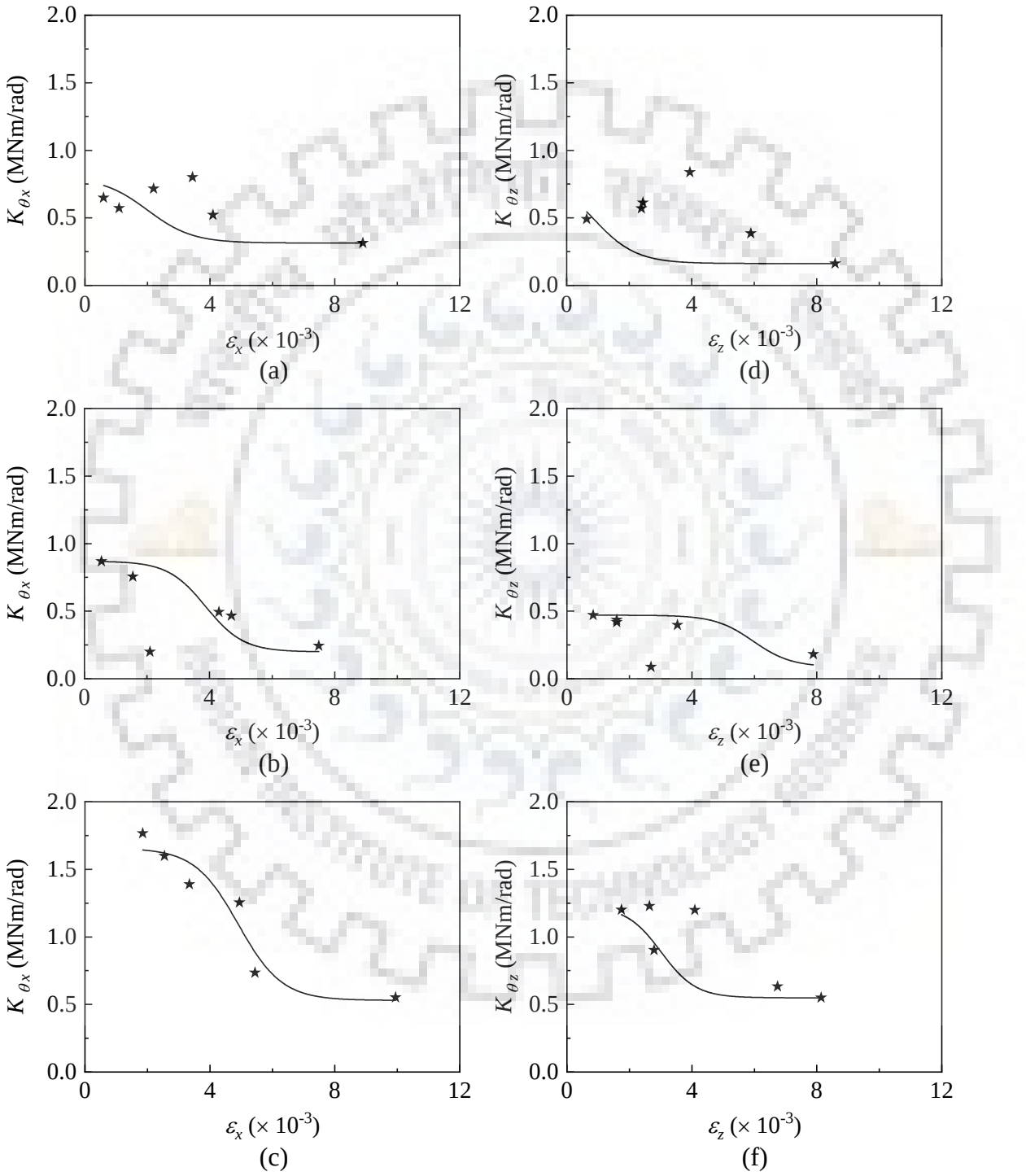

Fig. 3.23 Rotational stiffness for (a) B0 in X; (b) B10 in X; (c) B20 in X; (d) B0 in Z; (e) B10 in Z; and (f) B20 in Z

The variation of rotational stiffness with shear strain follows a similar nonlinear fashion in almost all the cases. The variation of $K_{\theta x}$ is within the range of 1 MNm/rad for both piles B0 and B10, whereas, this ranges further extends upto 2 MNm/rad in case pile B20. It is interesting to note that the nonlinear variation of $K_{\theta z}$ yields lesser value than $K_{\theta x}$ which may be attributed to the fact that in all the piles the initial test at an eccentricity was carried out in X direction and then in Z direction.

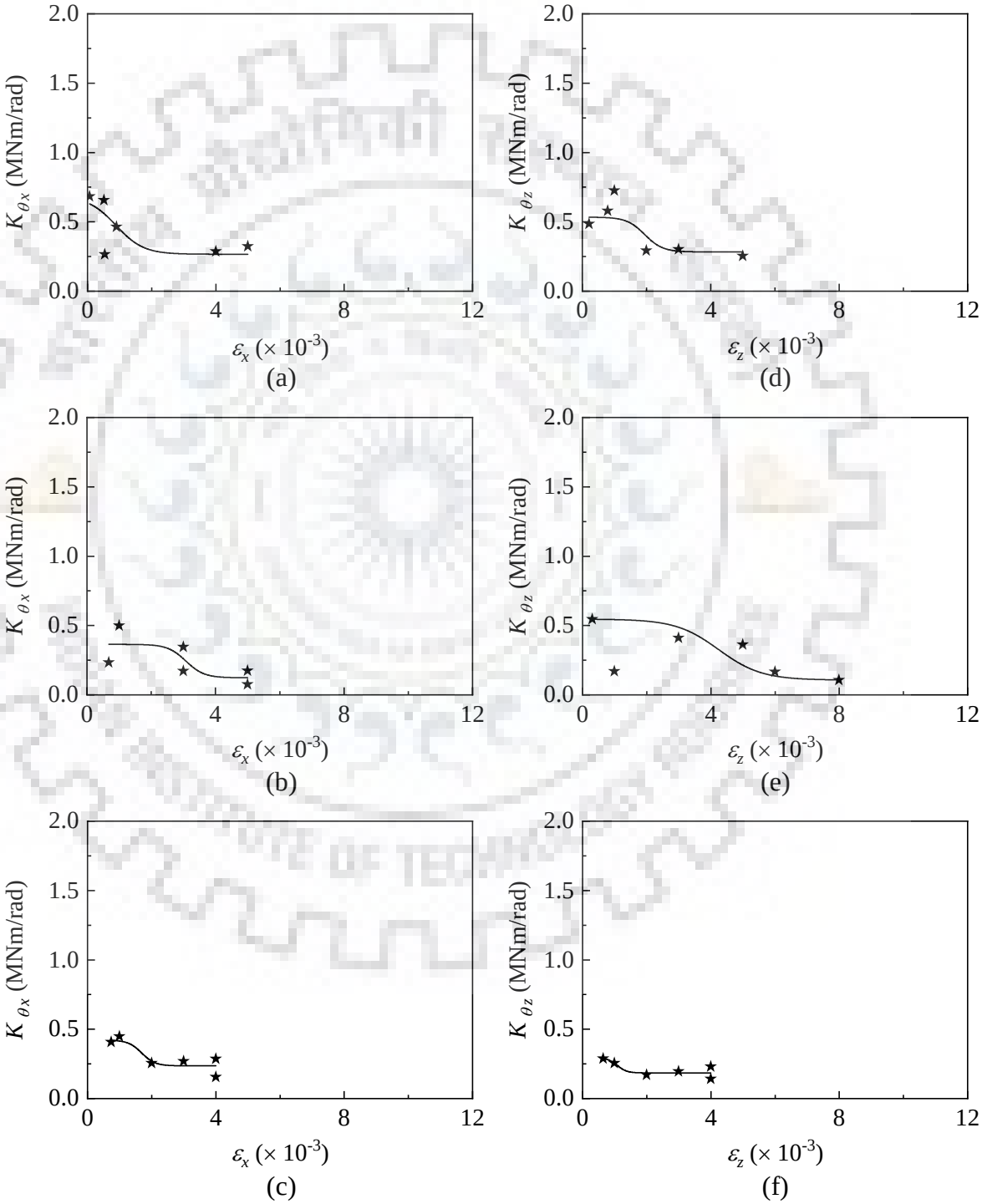

Fig. 3.24 Rotational stiffness for (a) B0U1 in X; (b) B10U1 in X; (c) B20U1 in X; (d) B0U1 in Z; (e) B10U1 in Z; and (f) B20U1 in Z

The variation in the rotational stiffness of the soil-pile system, $K_{\theta x}$ or $K_{\theta z}$ in both X and Z directions along with the force level is shown in Figs. 3.24(a-c) and 3.24(d-f) for piles B0U1, B10U1 and B20U1. It can be observed that variation in stiffness with force level strain does not follow a clear trend in both X and Z directions. This may be attributed to the presence of combined action of batter and under-reamed bulb in piles B10U1 and B20U1. Whereas in case of B0U1 clear trend could not be obtained since the pile reaches inelastic range at an earlier phase compared to other two piles. The rotational stiffness of soil-pile system was maximum for pile B0U1 in almost all the cases. It is interesting to note that the rotational stiffness of pile B10U1 was even lesser than that of pile B20U1 for majority of the cases in X direction and for some cases in Z directions. Rotational stiffness of soil-pile system depends on various parameters, *viz.* batter angle, critical depth, displacement amplitude and the subjected force level (eccentricity setting of the oscillator and operating frequency).

Effect on damping ratio of the soil-pile system

The damping ratios of the soil-pile system (ξ_x or ξ_z) were found to increase nonlinearly with an increase in the force level as presented in Figs. 3.25 (a-c) and 3.25 (d-f) for piles B0, B10, and B20 excited in both the directions (X and Z). Similarly, the variation in the damping ratio for piles B0U1, B10U1 and B20U1 excited both in X and Z directions is presented in Figs. 3.26 (a-c) and 3.26 (d-f) respectively.

ξ_x or ξ_z vary between 5 to 15% for B0 and B20 in both the directions and for B10 in the X direction. In case of pile B10 in X direction the variation is in the range 5% to 10% but in Z direction abruptly the damping ratio increased to 30%. This abrupt change in damping ratio might be due to gap formation between the soil and pile surface which was visible at the ground surface in the form of cracks around the circumference of the pile B10 observed by the authors during the experiment. The damping ratio was found to vary in the range of 5% to 35% for all the three piles in both X and Z directions. When the piles were excited in Z direction the damping ratio obtained for all the piles were equal at 100° eccentricity. The damping ratio of piles B10U1 and B20U1 were less than B0U1 except for 20° and 100° eccentricity in Z direction and beyond 60° eccentricity in X direction. During lateral dynamic excitation at higher force levels the contact between the soil and pile was highly disturbed in such a way that cracks were easily visible on the ground surface and propagated in the direction of excitation of the pile B0U1 which was not observed in piles B10U1 and B20U1.

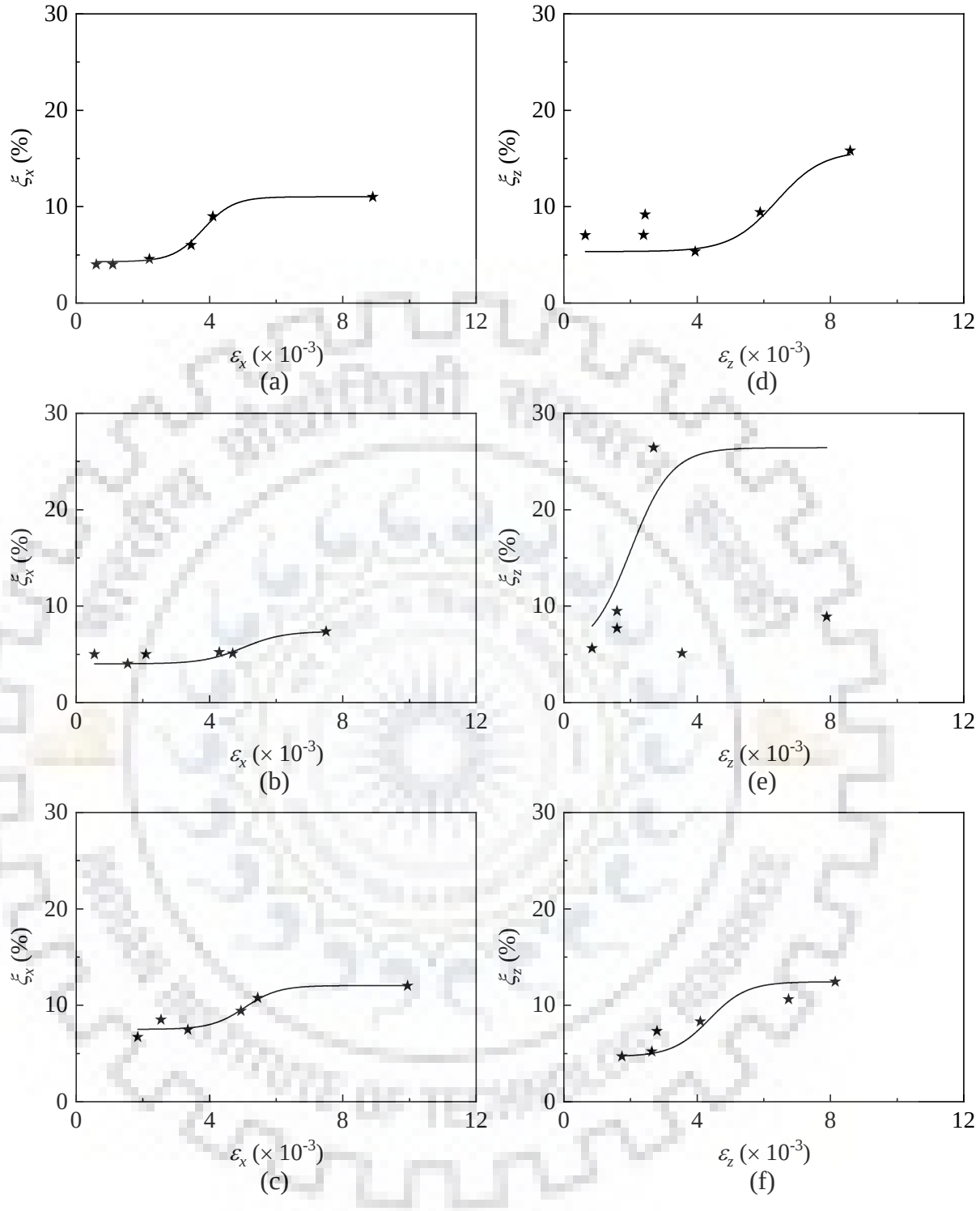

Fig. 3.25 Damping ratio for (a) B0 in X; (b) B10 in X; (c) B20 in X; (d) B0 in Z; (e) B10 in Z; and (f) B20 in Z

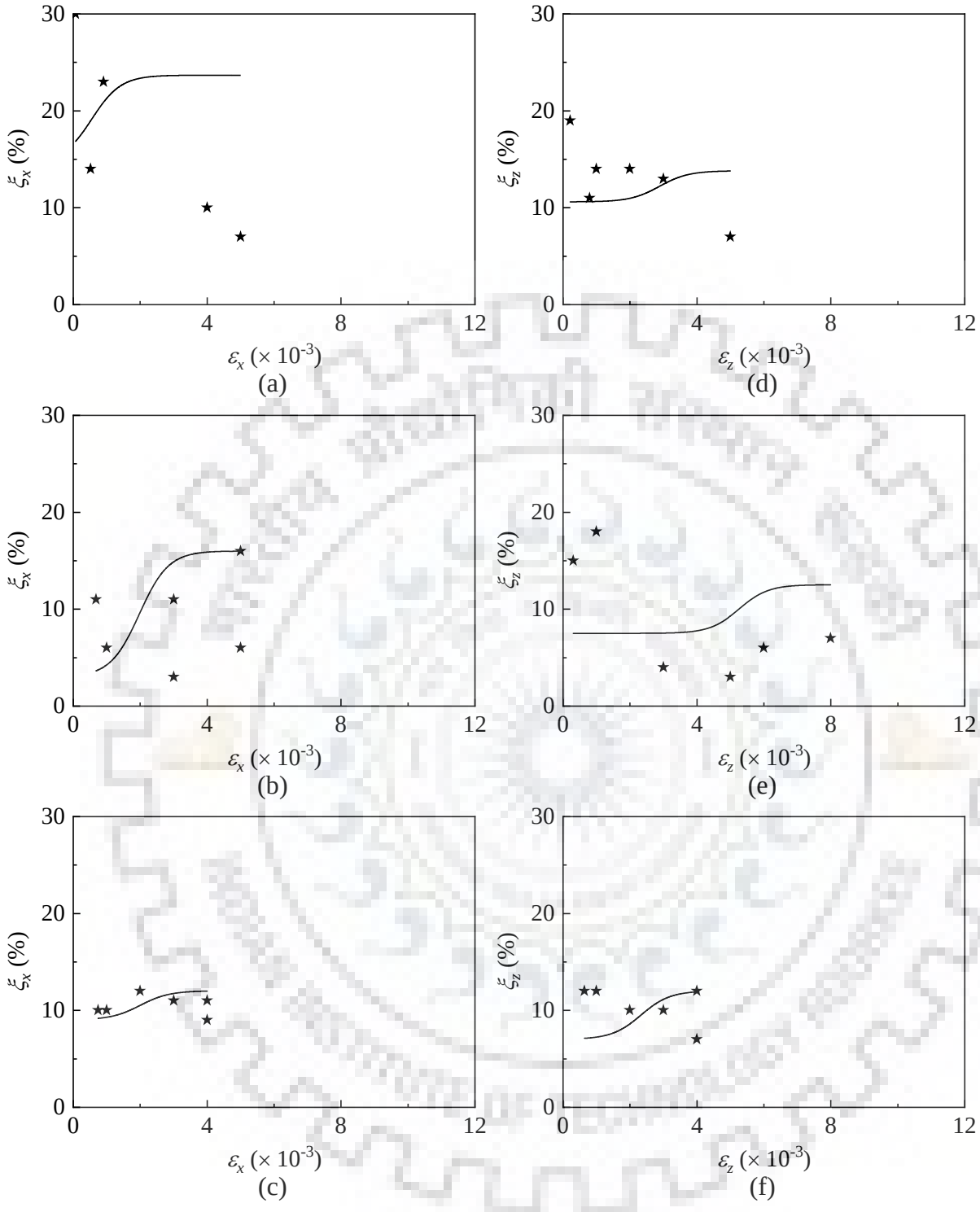

Fig. 3.26 Damping ratio for (a) B0U1 in X; (b) B10U1 in X; (c) B20U1 in X; (d) B0U1 in Z; (e) B10U1 in Z; and (f) B20U1 in Z

The rotational stiffness and damping ratio of the soil-pile system has been evaluated based on a conventional procedure suggested by BIS (1981b). The procedure elaborated in the IS code evaluates the stiffness and damping ratio of soil-pile system of vertical piles in elastic range

accurately. Beyond elastic range (at higher force levels in this case) the adopted procedure may not predict accurate values of these parameters. The reported rotational stiffness and damping ratios were obtained as a function of several other parameters such as batter angle, displacement amplitude, critical depth and exciting force level (eccentricity setting of the oscillator and operating frequency).

3.3.1.2 Vertical Response

In this section, the dynamic vertical response of the all six single piles obtained from the recorded acceleration time histories have been discussed in detail in terms of resonant frequency, vertical displacement amplitude and axial strain. At an eccentricity, the tests in Y direction were conducted after Z direction. Then the eccentricity was increased to a higher value and followed the same loading direction cycle (*i.e.* first X, Z and then Y). However, after excitation in Z direction a duration of at least 48 hours was maintained as the rest period before testing in Y direction.The variations in vertical displacement amplitude with operating frequency are presented in Figs. 3.27 (a-f) for all considered cases. It is obvious from Figs. 3.27 (a-f) that, there is only one clear peak value in all the considered cases, which confirms that the soil-pile system vibrates with its first fundamental frequency (or in the first mode of vibration). Thus, the integrated soil-pile system can be considered as a single degree of freedom system for further interpretation. Parameters including the resonant frequency and vertical displacement are obtained from the frequency displacement plots.

The variation in the resonant frequency (f_y') of all six piles at different force levels considered is shown in Fig. 3.28 (a-b). It is evident from the figure that the resonant frequency (frequency corresponding to peak displacement) decreases with increase in force level for each individual pile. With the increase in force level, f_y' decreases by 43-50%. This may be attributed to the fact that, the increase in force level leads to the increase in the degradation of the soil mass stiffness and hence decrease in resonant frequency. It is also interesting to note that the f_y' of B0 subjected to a particular force level was least in almost all the cases. The variation in the peak vertical displacement (d_y'), at all considered force levels, is shown in Fig. 3.28 (c-d). It is worth noticeable that the peak displacement increases with increase in force level for each individual pile. At e = 100°, d_y' of a pile is almost 4 to 5 times d_y' of the same pile at e = 10°.

Effect on the induced axial strain

Axial strain (ε_y) is obtained as the ratio of d_y' and the effective length of pile, L_e. In case of B0, the total length of pile below the ground level is considered as L_e (Fig. 3.29). Whereas, for piles, B10 and B20 the equivalent vertical length is considered as L_e as indicated in Fig. 3.29.

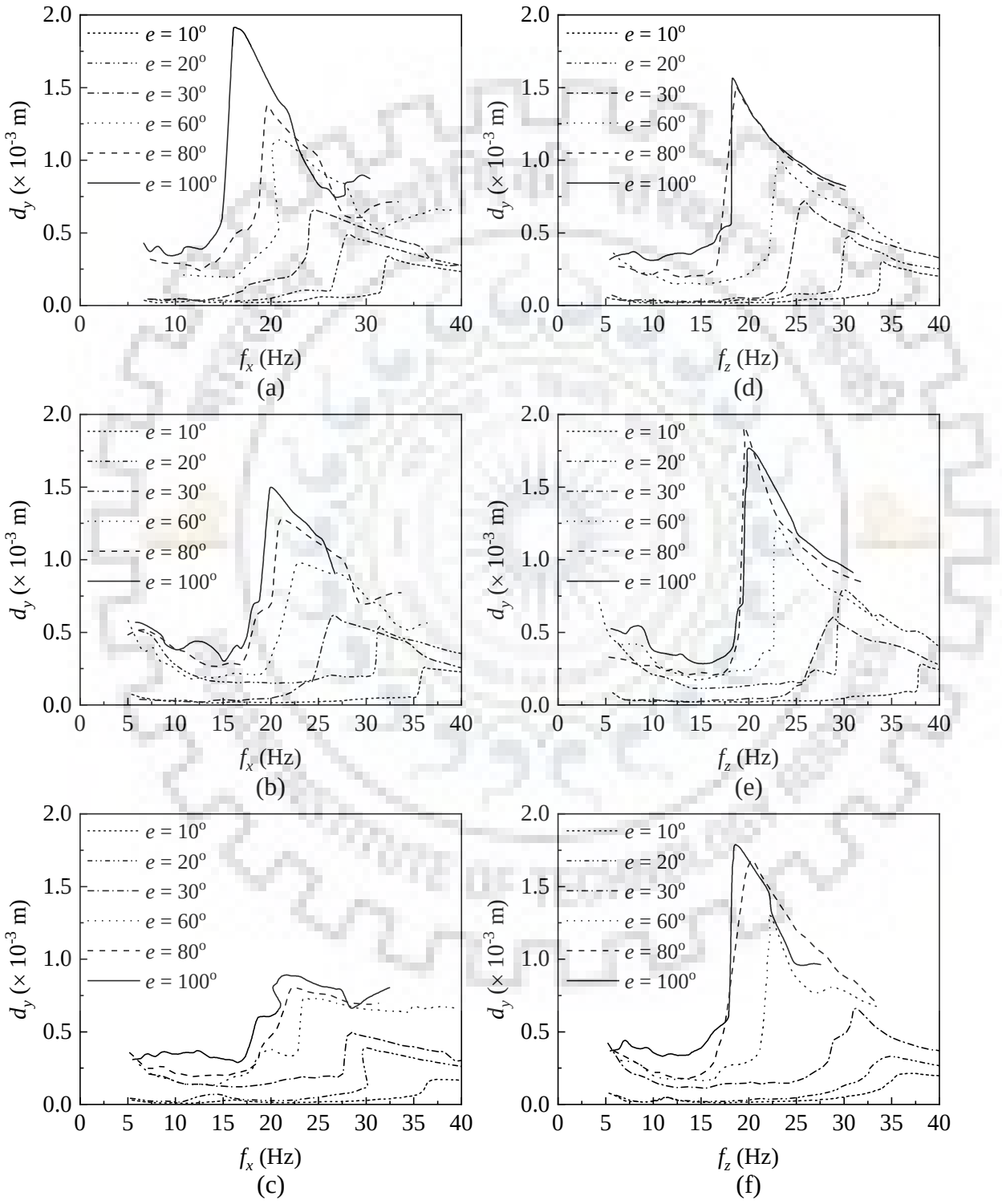

Fig. 3.27 Experimental vertical response of piles (a) B0; (b) B10; (c) B20; (d) B0U1; (e) B10U1; and (f) B20U1

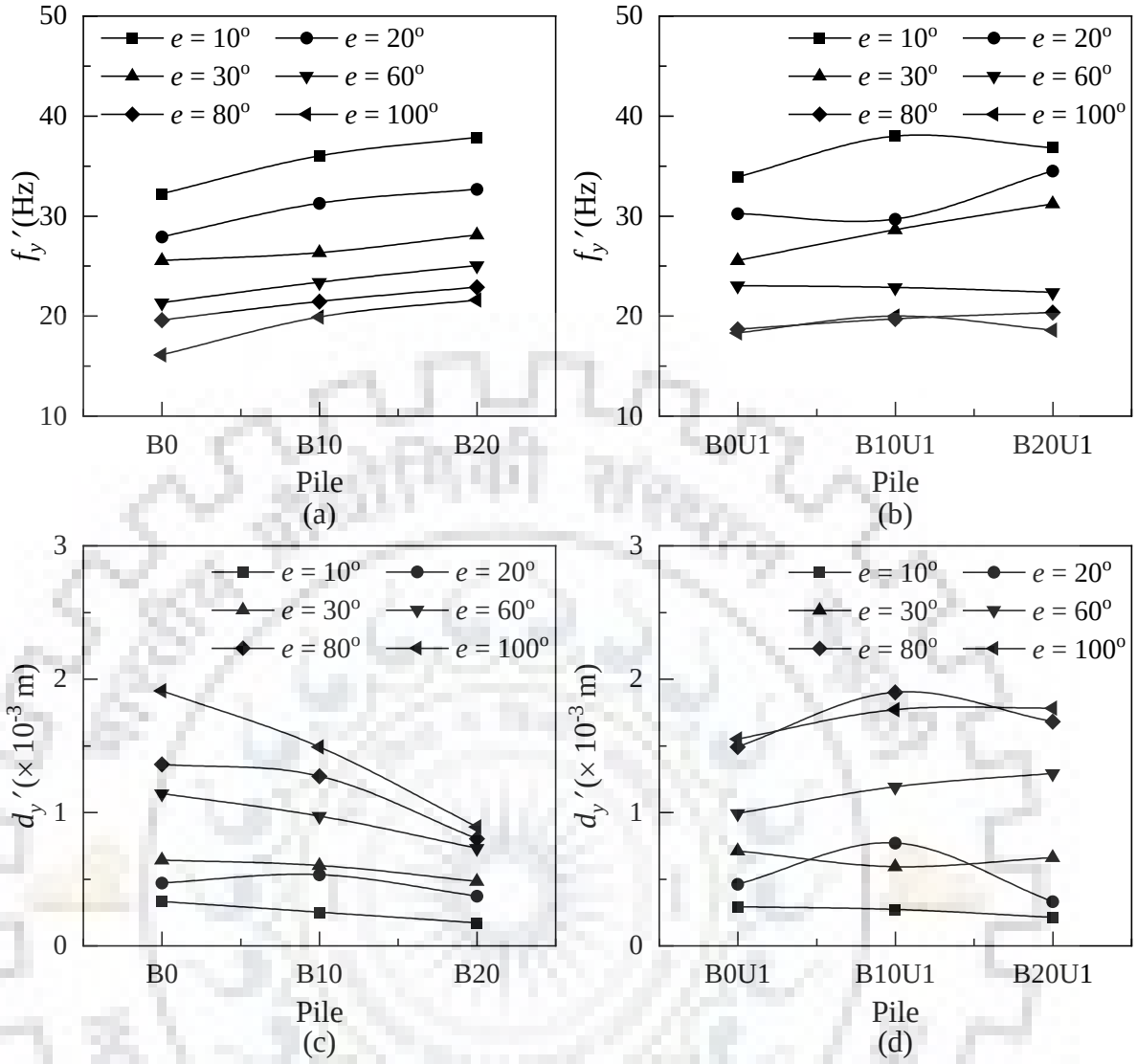

Fig. 3.28 Variation of (a) f_y' in piles B0, B10 and B20; (b) f_y' in piles B0U1, B10U1 and B20U1; (c) d_y' in piles B0, B10 and B20; and (d) d_y' in piles B0U1, B10U1 and B20U1

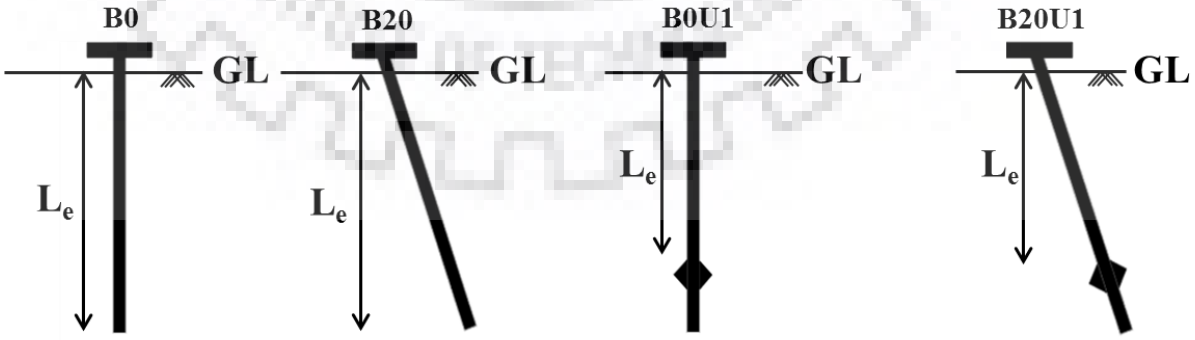

Fig. 3.29 Effective length for axial strain

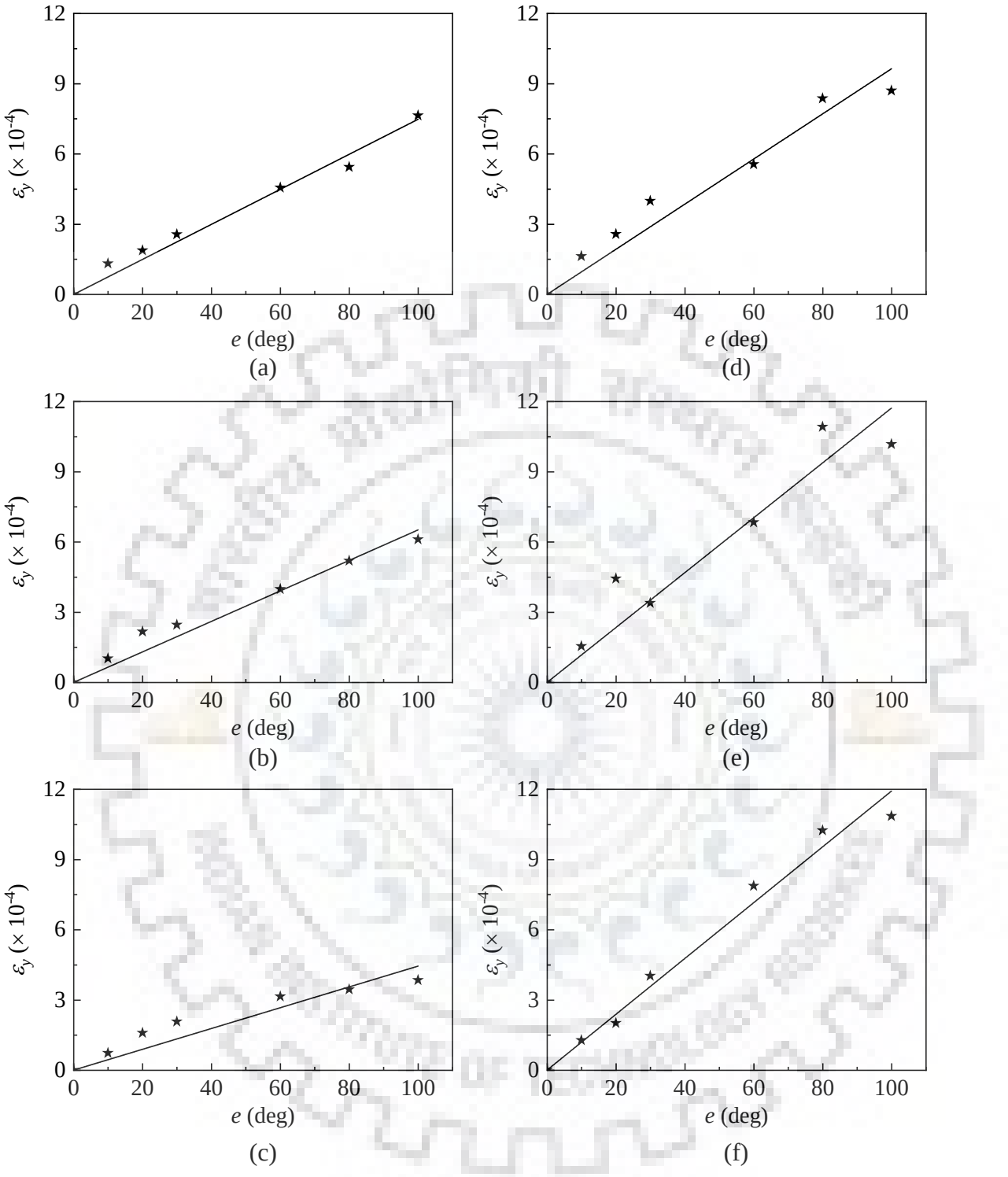

Fig. 3.30 Variation of axial strain of piles (a) B0; (b) B10; (c) B20; (d) B0U1; (e) B10U1; and (f) B20U1

The variation of axial strain induced in these model piles thus obtained is depicted in Fig. 3.30. It can be observed that the axial strain induced is linearly varying with the force level. In all cases, at e = 100° the ε_y is almost 4 times higher than ε_y of the same pile at e = 10°.

3.3.2 Pile Groups

The results have been presented for all four pile groups with varying force levels ranging from e = 30 to 150º. The dynamic response is presented in terms of frequency versus displacement plots in all the excitation directions considered. The response of the considered pile groups is further interpreted in terms of resonant frequency and peak displacement for varying load intensity. The following sections give a clear idea of the dynamic performance of the vertical and batter pile groups subjected to lateral and vertical vibrations. All four pile groups were tested for five different force levels in increasing order in all excitation directions individually.

3.3.2.1 Lateral Response

Effect of load intensity

The operating frequency, f, was obtained from the oscillator-motor assembly in terms of rotations per minute (rpm). The acceleration measured along the depth of the pile cap has been used to obtain the lateral displacement. The variation in recorded frequency versus lateral displacement at all considered force levels in terms of exciting frequency of the oscillator is presented in Fig. 3.31(a-d) for all pile groups. The displacement values reported in Fig. 3.31(a-d) were obtained as the average of the three values recorded from A1, A2 and A3. The response of these pile groups in the X direction is presented in terms of resonant frequency, f_x' and peak displacement, d_x' in Fig. 3.32(a) and 3.32(b), respectively.

It can be observed from Fig. 3.32(a) that with the increase in force level, resonant frequency in X direction, f_x' decreases for almost all the cases. The drop in f_x' from e = 30 to 150° for 3VG and 4VG is 20 and 14% whereas in case of 3BG and 4BG the drop is 38 and 33% respectively. The f_x' of 3BG increased by 5 to 35% of f_x' in 3VG. Similarly, f_x' of 4BG increased by 9 to 43% of f_x' in 4VG. The f_x' of the batter pile group was higher than their respective vertical pile group at all force levels. Similar observation was also reported by Subramanian and Boominathan (2016) in their experimental investigation on lateral dynamic behaviour of scaled pile group (vertical and batter) embedded in clay. However, this difference in f_x' was marginal at higher force levels and significant towards lower force levels.

It is obvious from Fig. 3.32(b) that with the increase in force level, d_x' increases in all the pile groups. With the force level varying from e = 30 to 150°, the increase in d_x' was 1.8 and 2.5 times in 3VG and 4VG respectively. In case of 3BG and 4BG, d_x' at e = 150° increased by 3.3 to 4.0 times d_x' at e = 30°. At all considered force levels, d_x' in batter pile group was lesser when

compared to their respective vertical pile group. The d_x' of 3BG reduced by 19 to 51% of d_x' in 3VG. Similarly, d_x' of 4BG reduced by 29 to 54% of d_x' in 4VG. The d_x' of 4VG reduced by 5 to 24% when compared to 3VG. Whereas, compared to 3VG d_x' of 4BG reduced by 37 to 66%. The decrease in resonant frequency and increase in the displacement with increasing force levels may be attributed to the fact that when the system is subjected to larger lateral loads, the lateral stiffness of the system reduces due to the degradation in stiffness of the surrounding soil mass only.

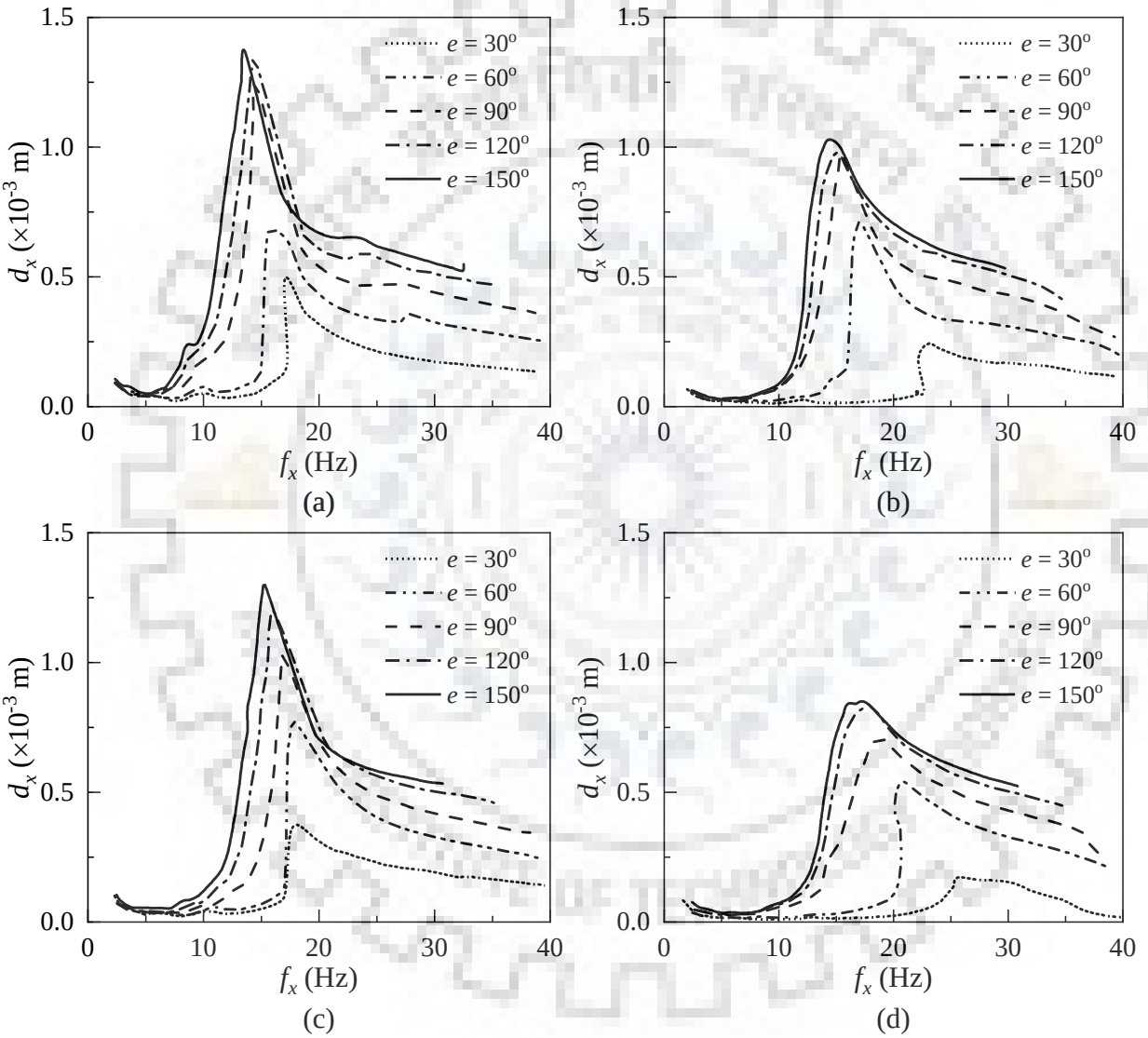

Fig. 3.31 Frequency displacement response in X direction for (a) 3VG; (b) 3BG; (c) 4VG; and (d) 4BG

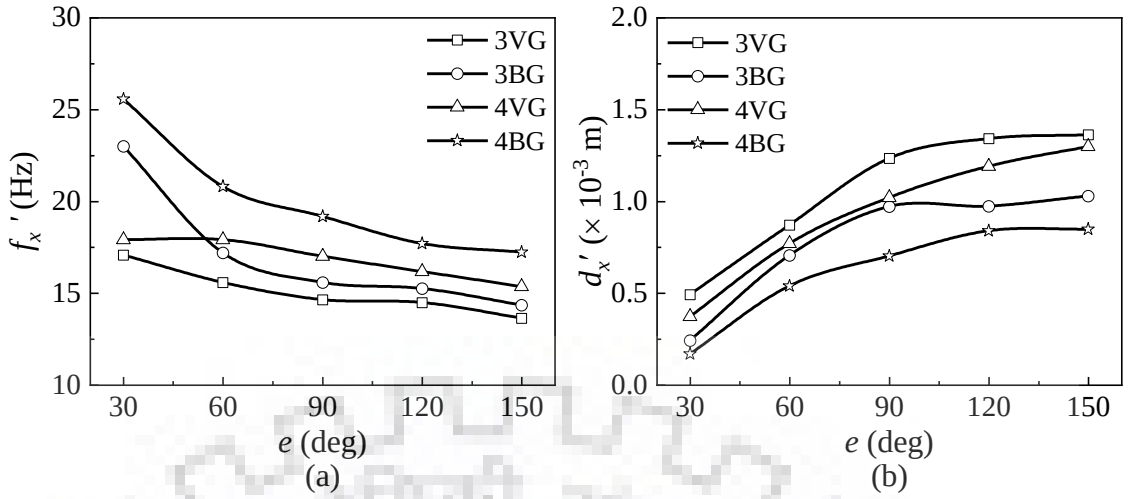

Fig. 3.32 Variation of (a) resonant frequency; and (b) peak displacement in X direction

Effect of loading direction

In case of pile groups with three piles arranged in the triangular pattern, the effect of the loading direction was investigated at all considered force levels. The direction of dynamic loading was altered by changing the orientation of the oscillator motor assembly. An attempt was made to compare the dynamic behaviour of two pile groups excited both in lateral (X) and transverse (Z) directions. The variation in frequency versus displacement of both 3VG and 3BG in the Z direction is presented in Figs. 3.33(a) and 3.33(b), respectively.

The response of 3VG and 3BG excited in both X and Z directions have been compared in terms of resonant frequency and peak displacement in Figs. 3.34(a) and 3.34(b), respectively. With the increase in force level from e = 30 to 150°, the resonant frequency in Z direction, f_z' of both 3VG and 3BG decreased at an average rate of 22%. The f_z' of 3BG is higher than that of 3VG by 8 to 13%. Similarly, peak displacement in Z direction, d_z' at e = 150° increased by 2.2 times d_z' at e = 30° in both 3VG and 3BG. d_z' of 3BG reduced by 24% of d_z' recorded for 3VG. Thus, the change in the direction of lateral dynamic loading leads to modified dynamic response of the pile group with three piles arranged in a triangular pattern.

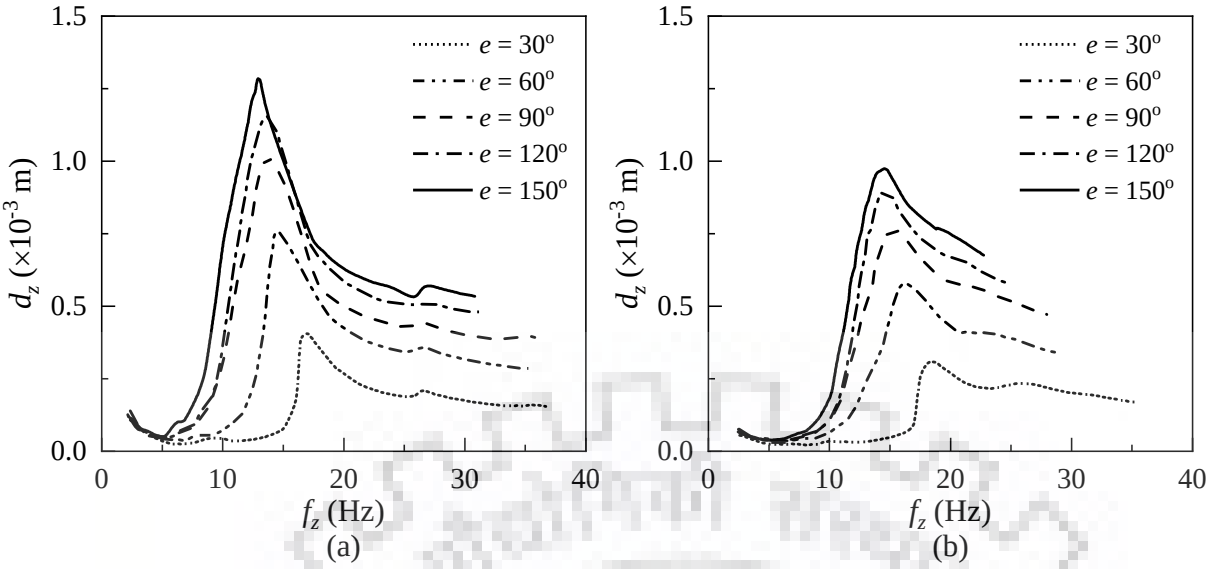

Fig. 3.33 Frequency displacement response in Z direction for (a) 3VG; and (c) 3BG

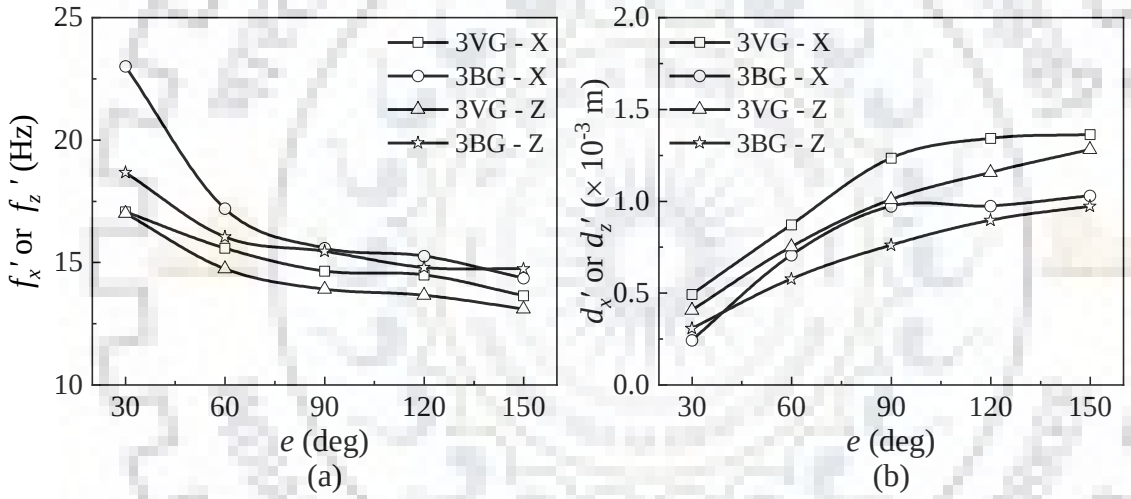

Fig. 3.34 Variation of (a) resonant frequency; and (b) peak displacement in X and Z directions

3.3.2.2 Vertical Response

The frequency was obtained from the rotation (rpm) of the oscillator-motor assembly. The acceleration measured at adjacent faces on top of the pile cap has been used to obtain the vertical displacement. The variation in the recorded frequency versus vertical displacement at all considered force levels in terms of exciting frequency of the oscillator is presented in Fig. 3.35(a-d). The displacement value reported in Fig. 3.35(a-d) is obtained as the average of the three values recorded from A1, A2 and A3. The variation in the resonant frequency, f_y' and the peak vertical displacement, d_y' in Y direction with the increasing force level for all four pile groups is presented in Fig. 3.36(a) and 3.36(b), respectively. Figure 3.36 shows that with the increase in force level,

the resonant frequency decreases and the peak displacement increase in all the cases. With the increase in force level from 30 to 150°, f_y' of 3VG, 3BG, 4VG, and 4BG decreased by 27, 29, 30 and 14% respectively. d_y' at highest force level was 1.5 times the lowest force level in case of pile groups with vertical piles. The increase in d_y' of 3BG and 4BG at e = 150° was 2.6 and 1.4 times d_y' at e = 30° respectively. The f_y' of 3BG was 25 to 33% higher than 3VG whereas, the increase was 18 to 46% higher in 4BG compared to 4VG. The d_y' of 3BG was 9 to 40% lesser than 3VG whereas the decrease of only 15 to 22% was observed in 4BG compared to 4VG. In comparison with 3VG, d_y' of 4BG reduced by 43% on an average. When the system is subjected to larger vertical loads, the resonant frequency decreases and displacement increases. This variation is due to the mobilization of skin friction along the pile length and tip resistance at the base leading to the significant reduction in vertical stiffness of the system.

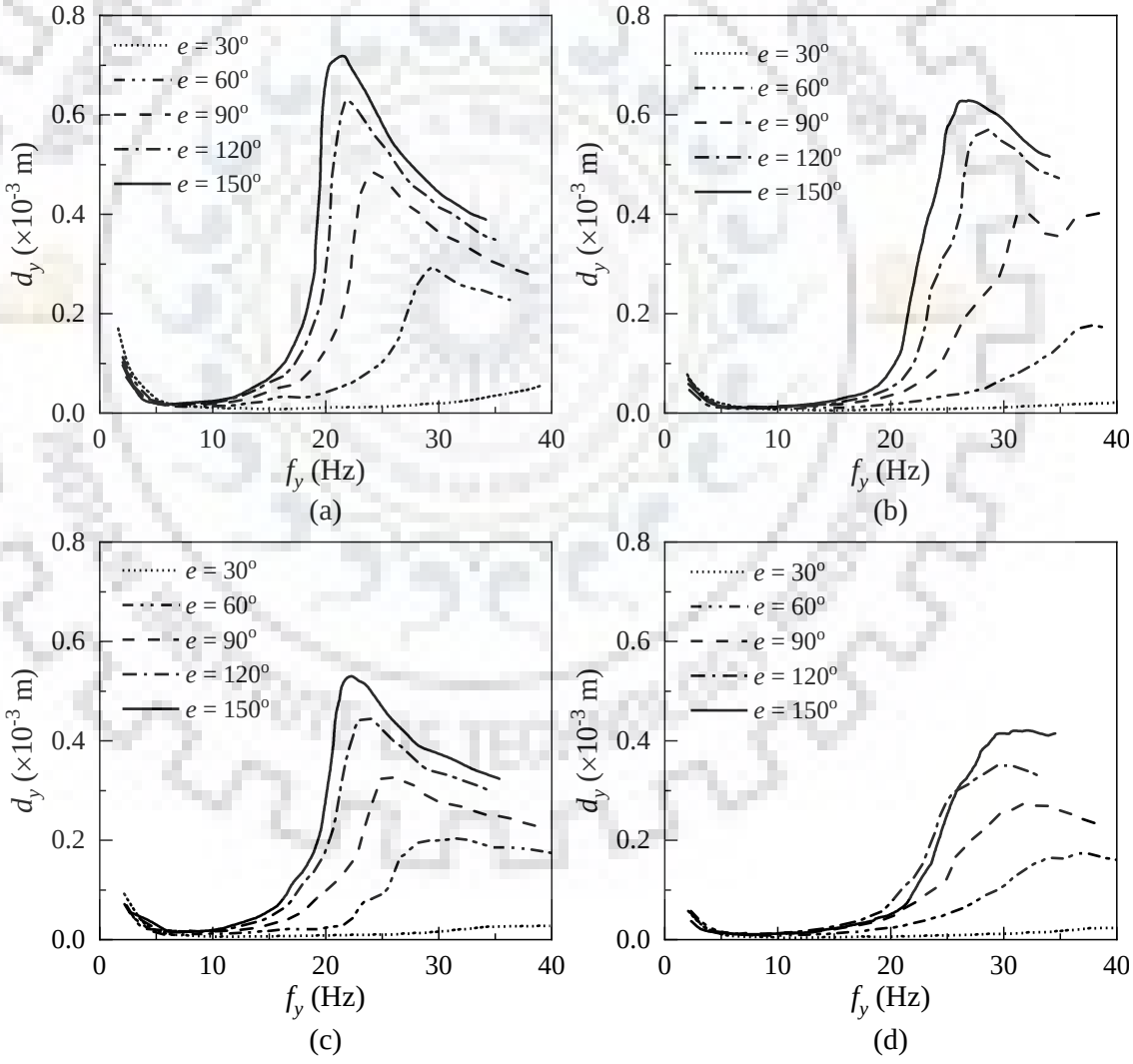

Fig. 3.35 Frequency displacement response in Y direction for (a) 3VG; (b) 3BG; (c) 4VG; and (d) 4BG

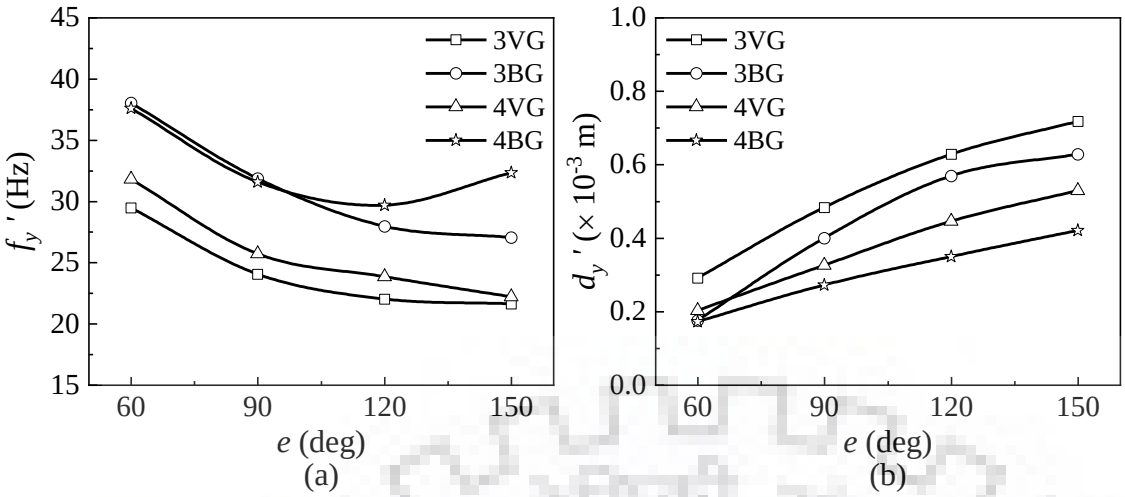

Fig. 3.36 Variation of (a) resonant frequency; and (b) peak displacement in Y direction

3.3.2.3 Estimation of Pile Group Efficiency

In order to estimate the efficiency of pile group, comparisons were made to the experimental work carried out on single vertical and batter piles, subjected to lateral and vertical dynamic loads at a nearby site with similar soil profile, by the authors. The frequency response of single vertical pile (B0) and batter pile (B20) is compared to the response of the pile groups to understand the efficiency of vertical and batter pile groups in Fig. 3.37 (a and b) and Fig. 3.37 (c and d) for X or Z and Y directions, respectively.

d_x' of 3VG decreases by 56% compared to its respective B0. Similarly, d_x' of 3BG decreases by 62 and 67% compared to its respective B20 and B0 respectively. Further, d_z' of 3VG decreases by 66% compared to its respective B0, whereas d_z' of 3BG decreases by 56 and 74% in comparison to their respective B20 and B0. Similarly, d_x' of 4VG recorded a decrease of 58% compared to its respective B0. But, in case of 4BG, d_x' decreased by 68 and 72% in comparison to their respective B20 and B0.

d_y' of 3VG and 4VG decreases by 62 and 72% respectively when compared to B0. Similarly, d_y' of 3BG and 4BG decrease by 29 and 53% respectively when compared to B20 and the decrease is about 67 and 78% respectively when compared to B0. In all three directions (*i.e.* X, Y and Z), there is a significant reduction of displacement in pile groups compared to the response of their respective single piles.

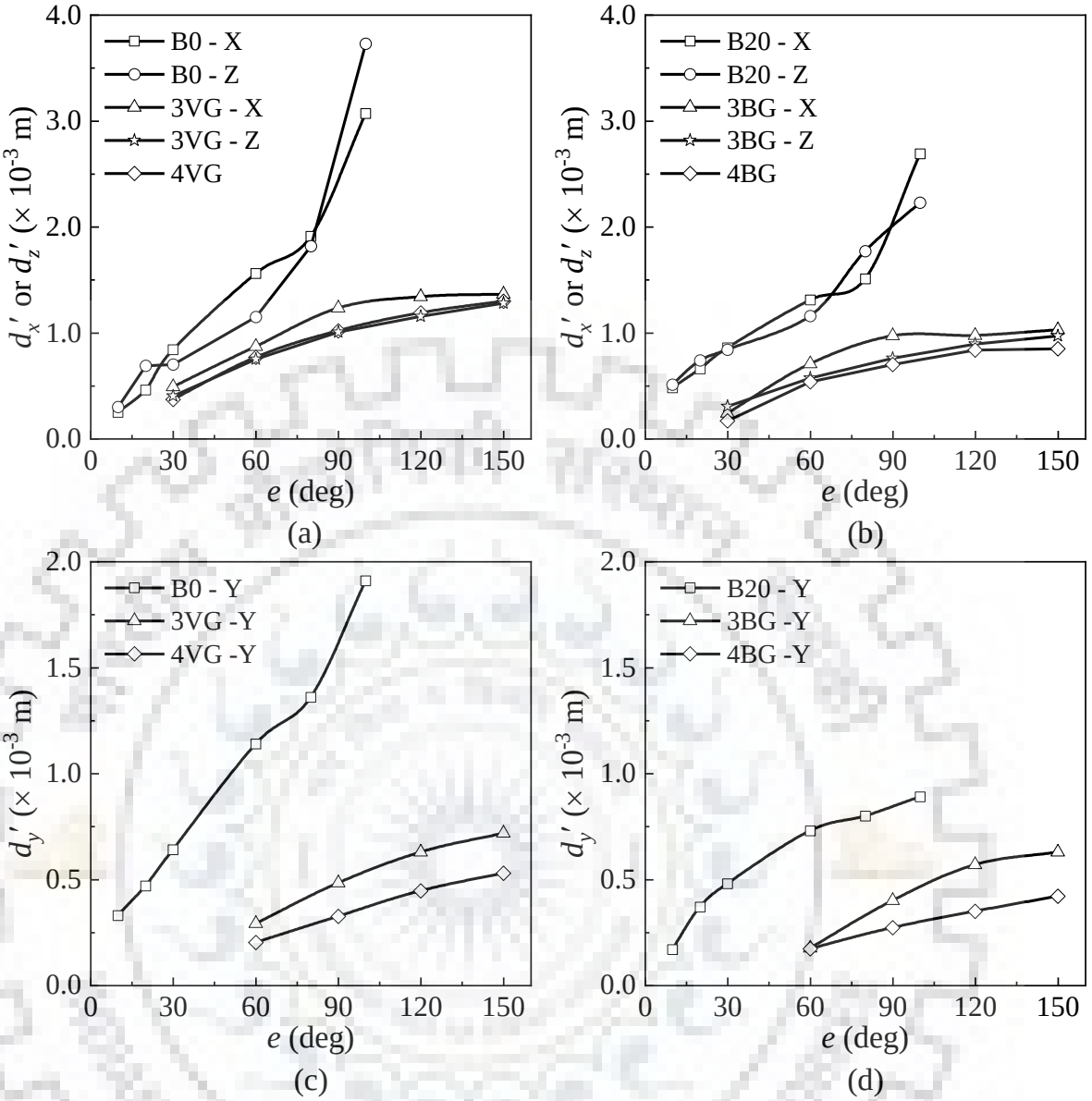

Fig. 3.37 Peak displacement of single piles and their corresponding pile groups: (a) vertical pile and its group in X and Z; (b) batter pile and its group in X and Z; (c) vertical pile and its group in Y; and (d) batter pile and its group in Y

3.4 SUMMARY

An extensive experimental study has been performed to estimate the dynamic behaviour of batter piles, batter pile with an under-reamed bulb and batter pile groups. The effect of exciting force level intensity and the effect of loading direction has been explored for all considered cases. The results obtained from the present study have been presented in the form of variation of resonant frequency, peak displacement amplitude, induced strain level etc.

3.4.1 Dynamic Behaviour of Single Piles

Field tests were conducted on bored cast in-situ vertical (B0), batter (B10 and B20), vertical pile with an under-reamed bulb (B0U1) and batter piles with an under-reamed bulb (B10U1 and B20U1) installed in silty sand, subjected to dynamic lateral and vertical vibrations, individually. It was found that the soil-pile system vibrates like a single degree of freedom system, as only one peak amplitude was observed in the frequency displacement plot for all the piles in both lateral and vertical directions.

Resonant frequency of the soil-pile system decreases with an increase in the force level in both lateral (X and Z) and vertical (Y) directions. With the increase in force level, the degradation of stiffness in soil mass also increases. Thus, at the particular force level, when the mass participation increases, the resonant frequency of the system automatically decreases. The highest resonant frequency was observed for 20° batter pile (B20), regardless of the force level and direction of excitation, and this signifies the importance of batter pile subjected to dynamic lateral load over the vertical pile. The peak displacement and shear strain / axial strain increase linearly with the increase in the force level. The percentage decrease in peak lateral displacement amplitude is higher in case of B10U1 than in B20U1 in X direction whereas the percentage decrease in the peak lateral displacement is higher in B20U1 than in B10U1 in Z direction.

The rotational stiffness decreases nonlinearly, while the damping ratio increases nonlinearly with an increase in shear strain. This, on the other hand, means that with increasing force level, rotational stiffness decreases and damping ratio increases nonlinearly. The variation of rotational stiffness and damping ratio of all the soil-pile system along with the force level excited both in X and Z directions does not seem to have a significant role in determining the lateral behaviour of combined batter and under-reamed pile. This may be attributed to the soil mass participation above and below the under-reamed bulb and the pressure distribution on both the lateral sides of the piles along the direction of loading.

It is clear that the direction of loading (X or Z) has a significant influence on the dynamic performance of single piles. This may be attributed to the soil mass participation, stiffness degradation and the pressure distribution on the two directions of loading in the horizontal plane.

3.4.2 Dynamic Behaviour of Pile Groups

An extensive experimental study has been performed on four reinforced concrete pile groups (two vertical pile groups and two batter pile groups) with the pile cap constructed on the same soil conditions by bored cast in-situ method and tested for its dynamic response in lateral and vertical directions individually. The variation of peak displacement as well as the resonant frequency for different force levels and loading directions are explored. All the observations reported in the present study are based on recorded deformations at the pile cap.

The resonant frequency decreases and the peak displacement increases with the increase in the exciting force level in all the excitation directions. With the increase in force level, there is a significant reduction in resonant frequency in all directions. In the lateral direction, with the increase in force level maximum reduction in peak displacement of about 38% (for 3BG) was observed, whereas, in vertical direction maximum reduction was about 30% (for 4VG). The peak displacement of batter pile groups was always lower than the vertical pile groups. In lateral and vertical directions, a maximum reductions of 54% (for 4BG) and 40% (for 3BG) in peak displacement were observed when compared to their respective vertical pile group. A minimum reduction of 56% in peak displacement was observed in the pile group when compared to a single pile. In comparison to single piles, the reduction in peak displacement was higher by 8 to 14% in the batter pile groups compared to the vertical pile groups.

Chapter 4

DYNAMIC RESPONSE OF BATTER PILES AND PILE GROUPS : NUMERICAL SIMULATION

4.1 INTRODUCTION

In this chapter, an attempt is made to understand the dynamic behaviour of batter piles and pile groups through numerical simulation using FE method. To this end, 3D FE models of batter piles and pile groups of similar geometry considered for experimental investigation in the previous chapter has been developed. Material properties of soil and pile, dimension of the pile with its cap and applied dynamic loading are kept similar to the experimental investigation. The results obtained from the numerical simulations are validated with the experimental results. The influence of loading direction and intensity of exciting force level are also explored. In addition, an attempt is also made to understand the bending moment distribution along the pile length through a hybrid modelling approach. The following sections elaborate the finite element modelling strategies adopted in this study and the results obtained.

4.2 FINITE ELEMENT MODELLING

Dynamic behaviour of vertical and batter piles and pile groups have been studied using 3D FE modelling in commercially available FE package Abaqus/CAE (2016). 3D FE models are more rigorous but prohibitive for the nonlinear dynamic study due to requirement of huge storage and computational effort. All the FE analyses have been conducted considering two stages of loading. In first stage, the in-situ stresses in the soil including piles under gravity load have been evaluated using a static analysis. In the second stage, nonlinear time history analyses have been performed on the coupled soil pile system using dynamic implicit method based on Hilbert-Hughes-Taylor (HHT) formulation. In dynamic implicit method, the solution is predicted at the current time step based on the result at an incremental time step prior to the current step.

The soil mass is an infinite media and for the FE analysis it is represented as perfect half space medium, where the model dimension and boundary conditions are chosen in such a way that their effects are minimal on the domain of interest. In this study, based on a sensitivity analysis and past researcher's recommendation, the extent of 3D FE soil model has been

considered as 80*d* (*d* = diameter of pile) in lateral dimensions, and 67.5*d* along depth (as shown in Fig. 4.1) for FE simulation.

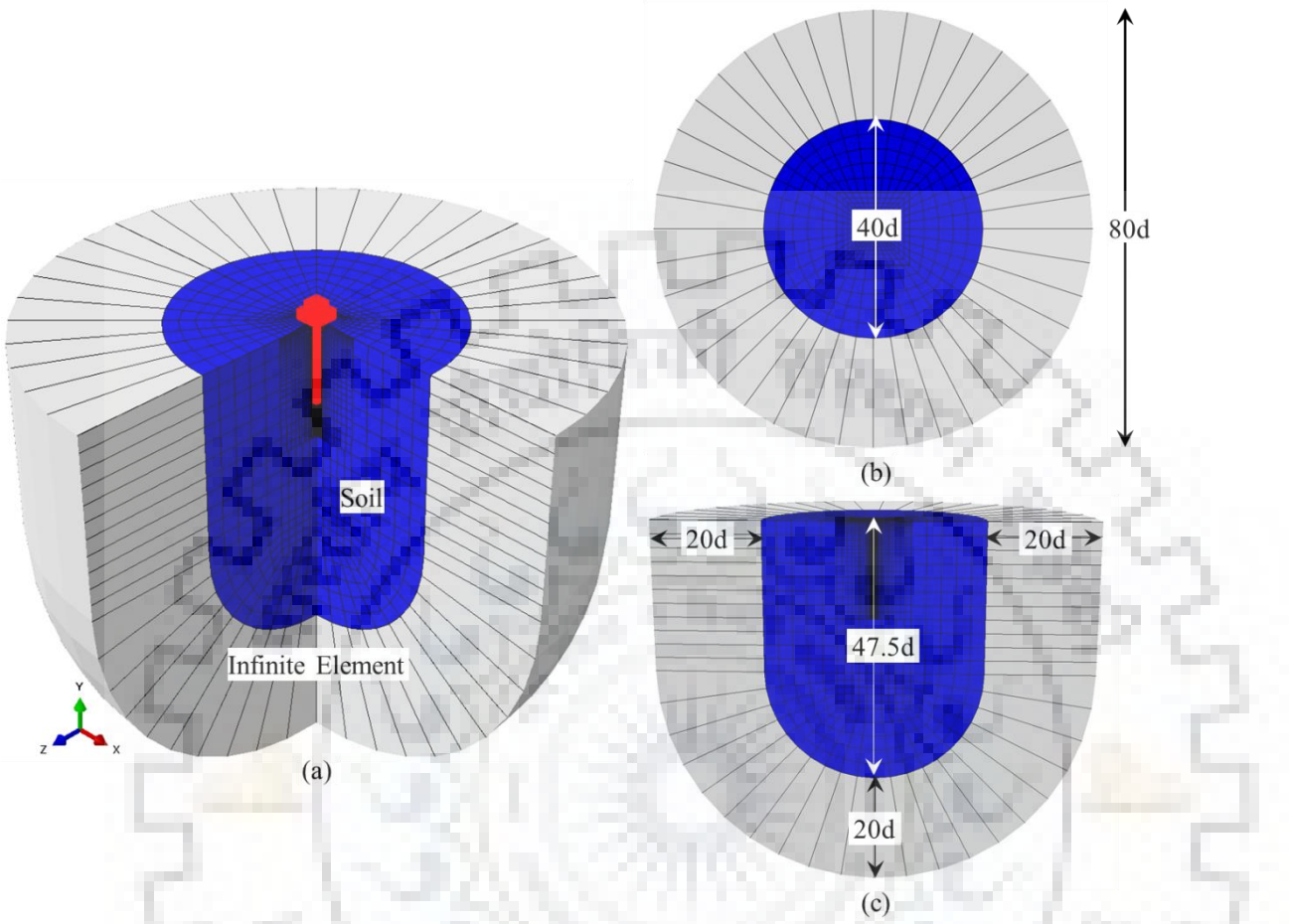

Fig. 4.1 Typical 3D FE model showing (a) soil pile system for B0; (b) top view; and (c) cross section

The piles and pile group have been assigned properties of the M25 grade of concrete (γ_c = 25 kN/m^3; v_c = 0.20 and E_c = 25 GPa). The oscillator motor assembly mounted on the top of the pile cap (with mass ≈ 367 kg) has been modelled explicitly in the FE model. The material properties of soil obtained from field tests at different depths have been used in FE model. The soil mass in each layer was assumed to have the same value of v_s = 0.30. The soil mass has been modelled using an elasto-plastic constitutive model with the Mohr-Coulomb yield criterion, assuming non-associated flow rule. The Mohr-Coulomb material model is adequate for identification of the parameters influencing the dynamic response and the results obtained from this study can serve as a strong reference for more complex soil material models. The angle of internal friction value corresponding to SPT-N value has been obtained from (BIS 1981a). The

elasto-plastic material model can simulate the inelastic energy dissipation whereas, mass and stiffness proportional Rayleigh damping has been used to account for the energy dissipation during the elastic response. Rayleigh damping, specified in terms of coefficients, α_{rd}, and β_{rd}, has been used in the present study, as shown in Eqns. 4.1 and 4.2:

$$\alpha_{rd} = \frac{2\omega_i\omega_j}{\omega_i + \omega_j}\xi \tag{4.1}$$

$$\beta_{rd} = \frac{2\xi}{\omega_i + \omega_j} \tag{4.2}$$

where ξ is damping ratio, and ω_i and ω_j correspond to the range of rotational frequencies of interest. Rayleigh damping parameters for both the soil mass and pile were estimated as α_{rd} = 2.65321, β_{rd} = 0.00032 assuming the damping ratio of 5%. The ω_1 and ω_2 values were estimated as 29.30 rad/s and 282.70 rad/s corresponding to the 1st mode and highest frequency of interest, respectively.

For simulation of wave propagation problems, the maximum size of the element has been restricted to 1/8th to 1/12th of the wavelength of the propagating wave (Kuhlemeyer and Lysmer 1973; Lysmer and Drake 1972), whereas, the suggested element size was in the range of 1/10th to 1/20th of the wavelength of the propagating waves for large propagating distances (Semblat and Brioist 2000). The 3D FE model of the soil mass, pile and pile cap have been discretized with 8-node brick element with reduced integration (C3D8R) elements (Fig. 4.2a). However, in 3D FE model for pile groups a few 4-node tetrahedral element (C3D4) elements (Fig. 4.2c) have been used for discretizing the pile cap. In the present study, smaller mesh size in the order of 1/12th of the desired wavelength (50 Hz) has been used for soil mass near the pile, whereas mesh size has been increased near the boundaries. Discretizing the soil mass into smaller and larger element sizes gave the advantage in predicting the vibration response with comparatively less computational efforts. The FE mesh used in the present study for 3VG and 3BG have been shown in Fig. 4.3 and 4.4, respectively. Similarly, Fig. 4.5 and 4.6 show the FE mesh for 4VG and 4BG, respectively. The surfaces of piles and soil have been connected by tie constraint to avoid any slippage and de-bonding. The different parts of 3D FE model developed in the present study is shown in Fig. 4.7(a-c).

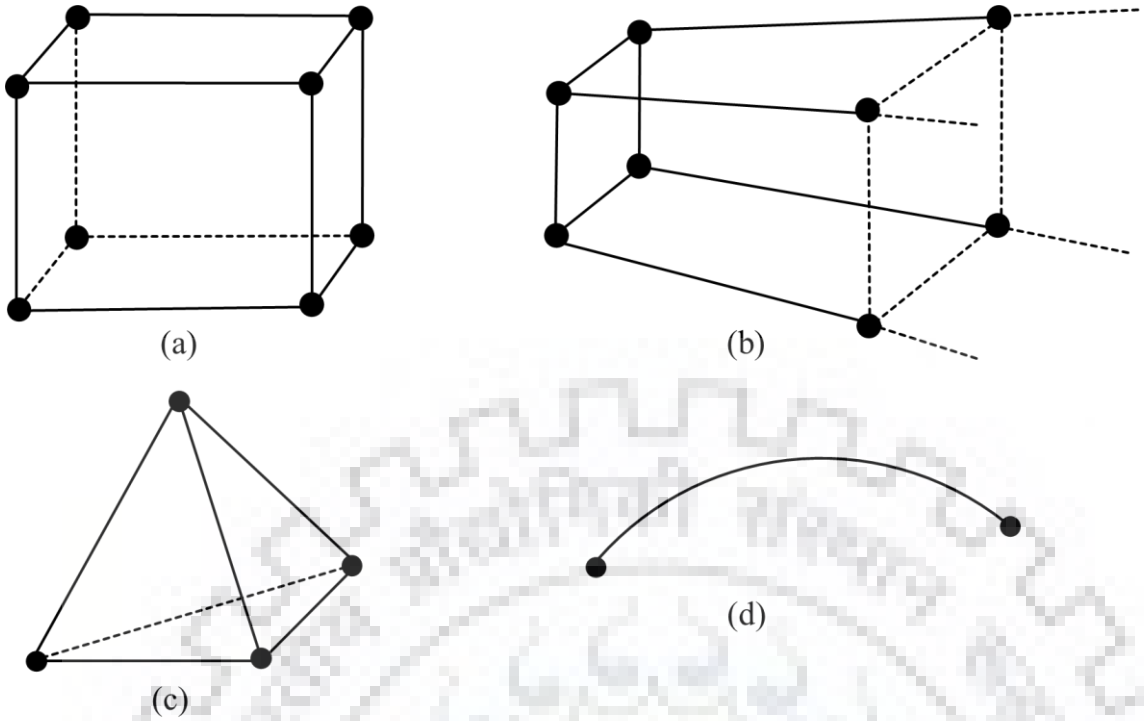

Fig. 4.2 Elements used in 3D FE model: (a) C3D8; (b) CIN3D8; (c) C3D4; and (d) B33

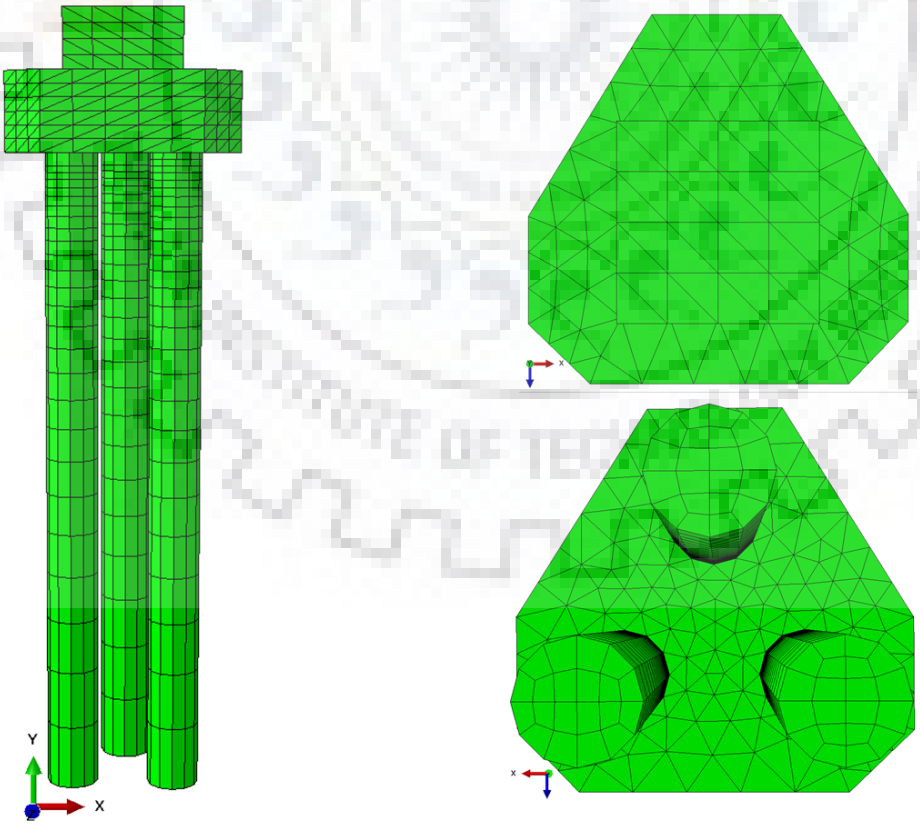

Fig. 4.3 Pile group with cap and machine assembly for 3VG

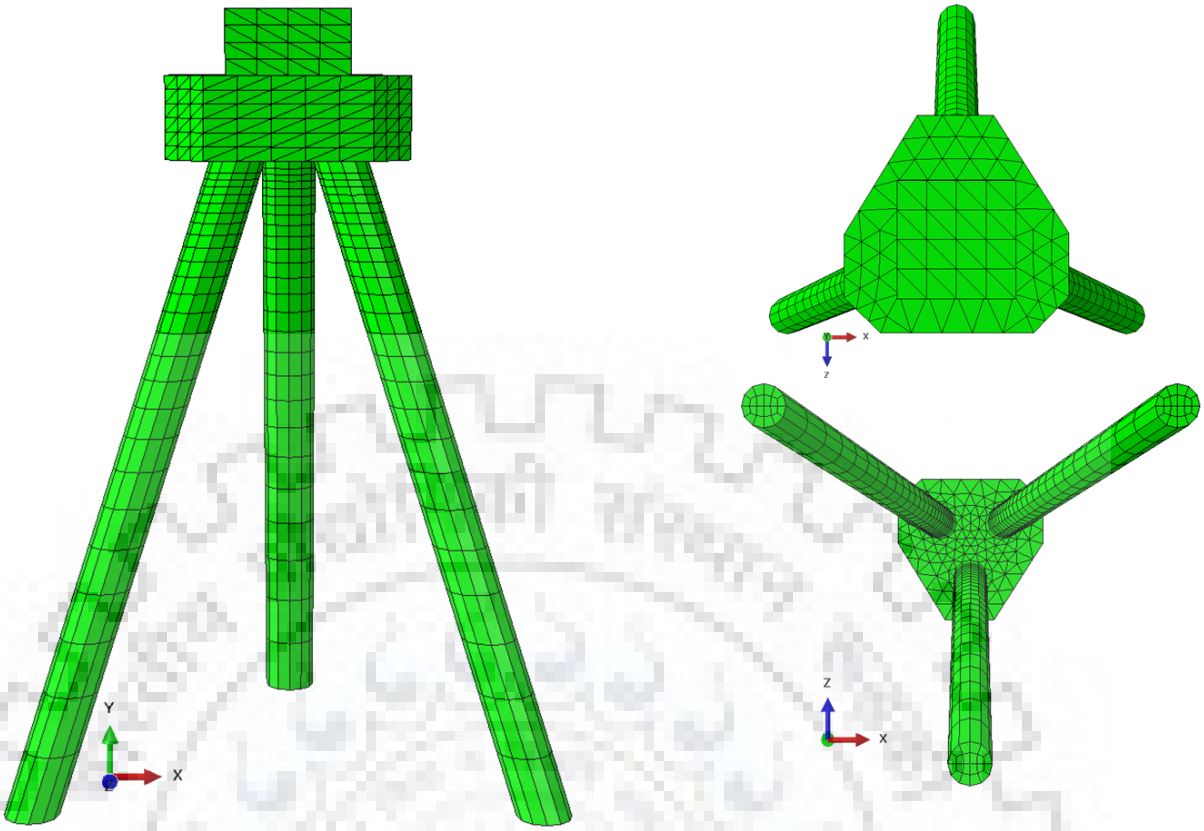

Fig. 4.4 Pile group with cap and machine assembly for 3BG

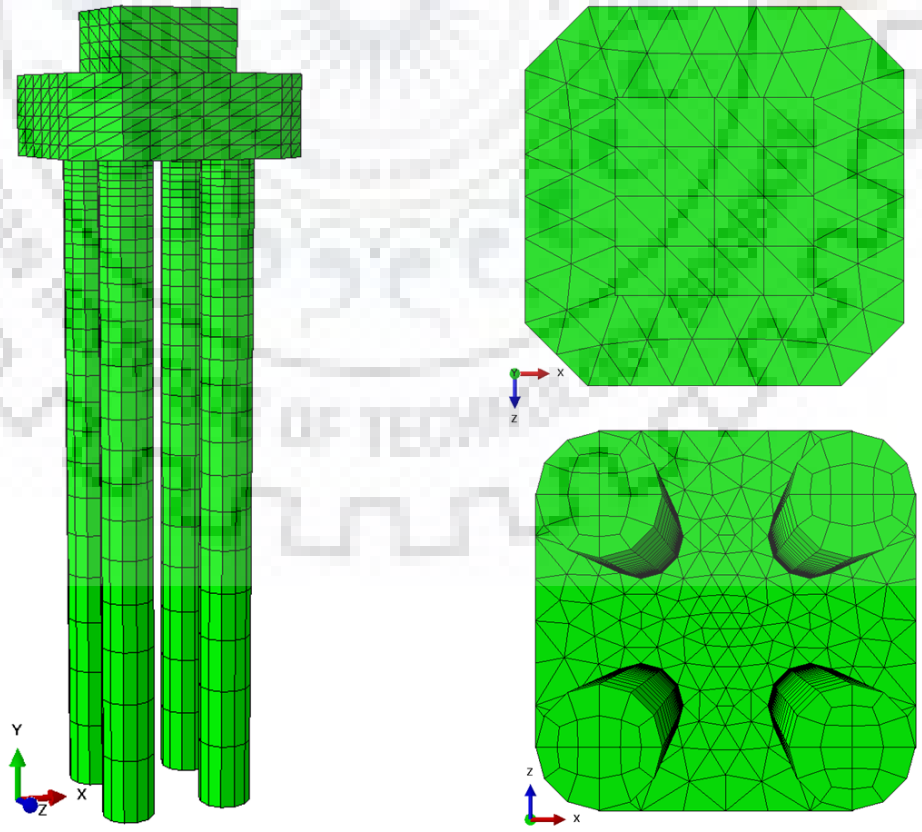

Fig. 4.5 Pile group with cap and machine assembly for 4VG

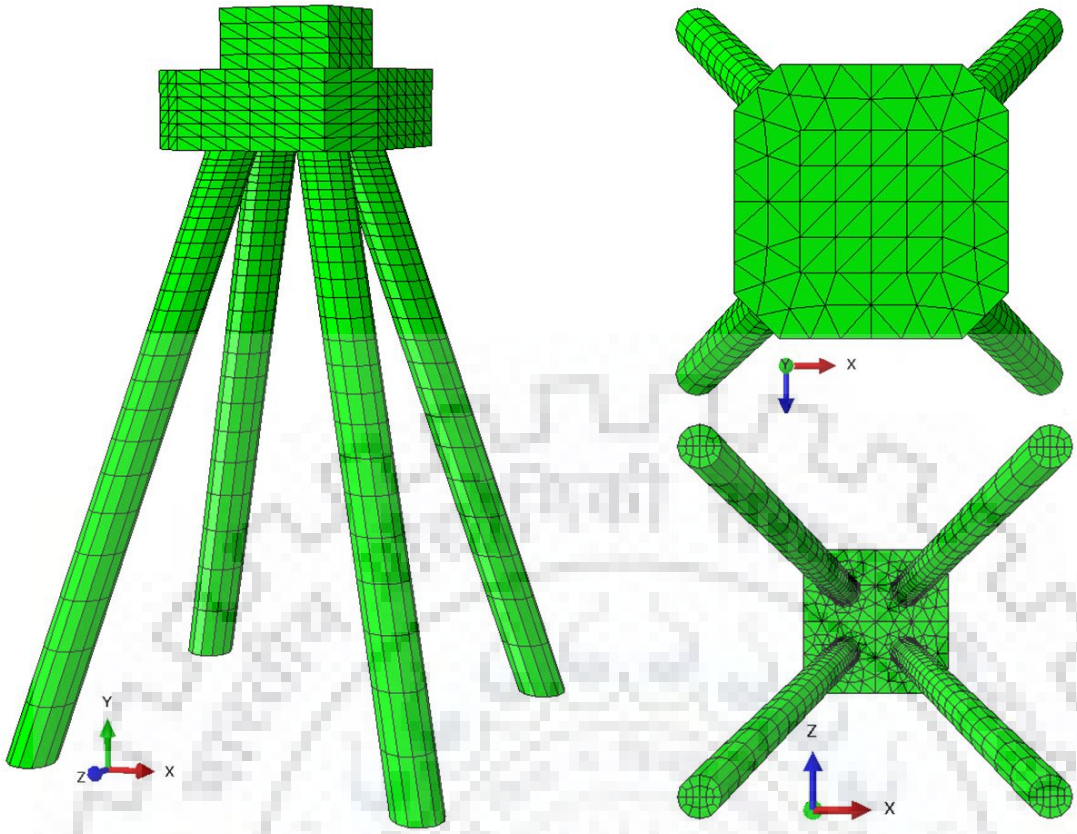

Fig. 4.6 Pile group with cap and machine assembly for 4BG

In order to avoid wave reflections at the boundaries either absorbing boundaries or infinite elements are used (Semblat 2011). Infinite elements are always used in conjunction with finite elements for boundary value problems, where the unbounded domains or region of interest is smaller in size as compared to surrounding medium. Infinite elements exhibit linear behaviour only and provide stiffness in static solid continuum analyses. In implicit dynamic analysis using direct integration, infinite elements provide "absorbing" boundaries to the FE model through the effect of a damping matrix with suppressed stiffness matrix. At the start of the implicit dynamic analysis, infinite elements maintain the static force on boundary computed at the end of static analysis. Hence, during the dynamic response, the far-field nodes in the infinite elements will not displace (Abaqus/CAE 2016). It is important to choose the length of the mesh edge (or outer nodes) in the infinite direction appropriately with respect to the domain of interest (say "Pole") where the loads are applied. For effective use of infinite element during FE analysis, the node along each edge pointing in the infinite direction must be positioned at a distance equal to two times the distance between the pole and the node on the same edge at the boundary between finite and infinite elements.

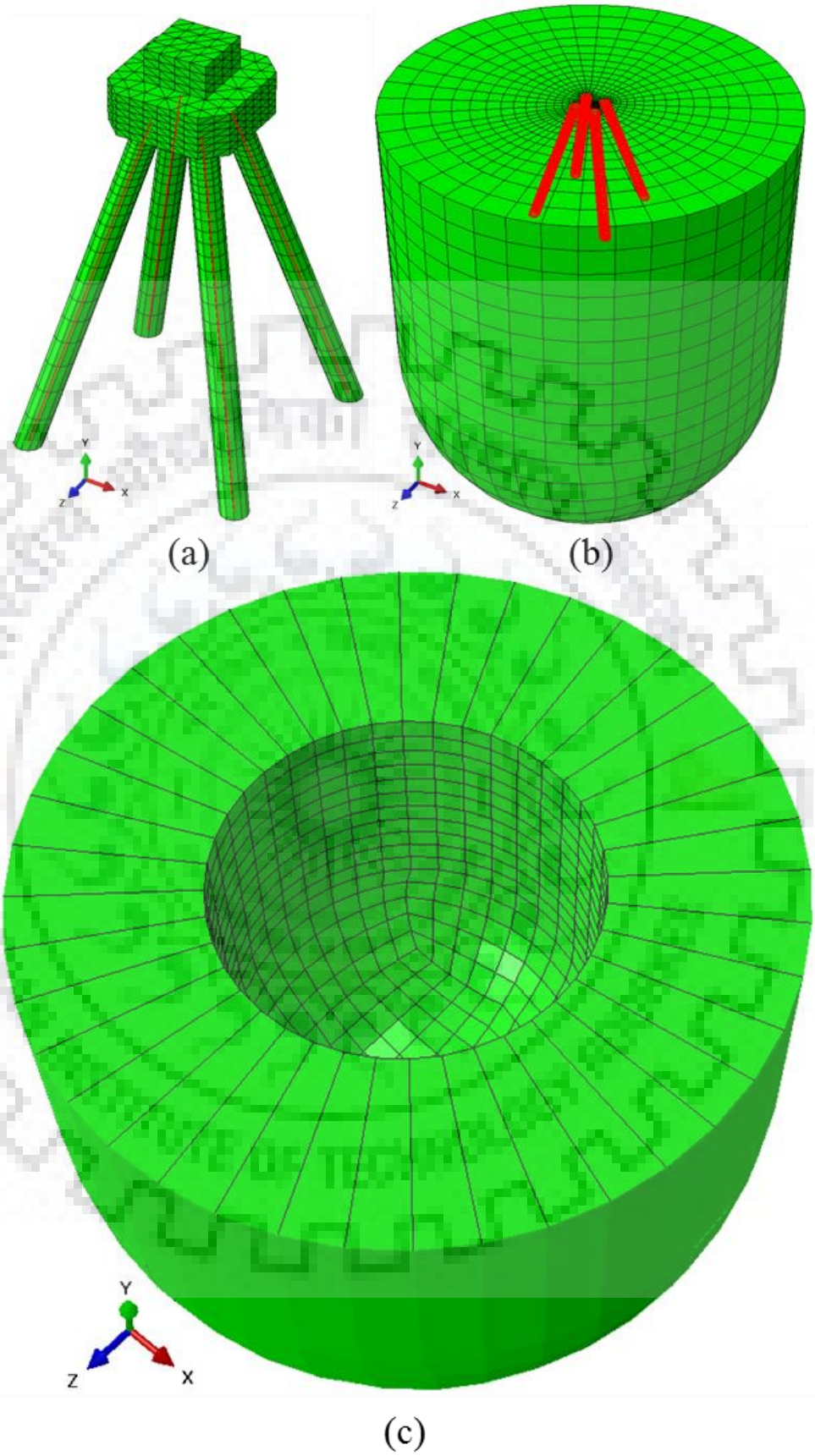

Fig. 4.7 Different parts of 3D FE model (a) hybrid pile group with machine; (b) soil mass with cut for pile group; and (c) outer infinite domain

In the present study, amongst the total FE model, the outer 20*d* solid volume consists of infinite elements (as shown in Fig. 4.1). Eight-node linear one-way infinite brick (CIN3D8) elements (Fig. 4.2b) have been used at the boundaries. Standard finite elements have been used to model the region of interest, with the infinite elements modelling the far-field region. One side of these infinite elements say four nodes are connected to the solid elements of the soil mass and the side consisting of other four nodes are aligned outward from the soil mass. During dynamic step, infinite elements introduce additional normal and shear tractions (proportional to normal and shear components of the velocity of the boundary) on the finite element boundary. These boundary damping constants are chosen to minimize the reflection of dilatational and shear wave energy back into the finite element mesh.

In the 3D FE model, dynamic lateral load generated during the experiment has been applied, on top surface of oscillator motor assembly firmly mounted on the pile cap, in the form of sweep load for different force levels. Figures 4.8 show the force-time history similar to the one generated by the oscillator motor assembly at $e = 60^{o}$ till 50 Hz.

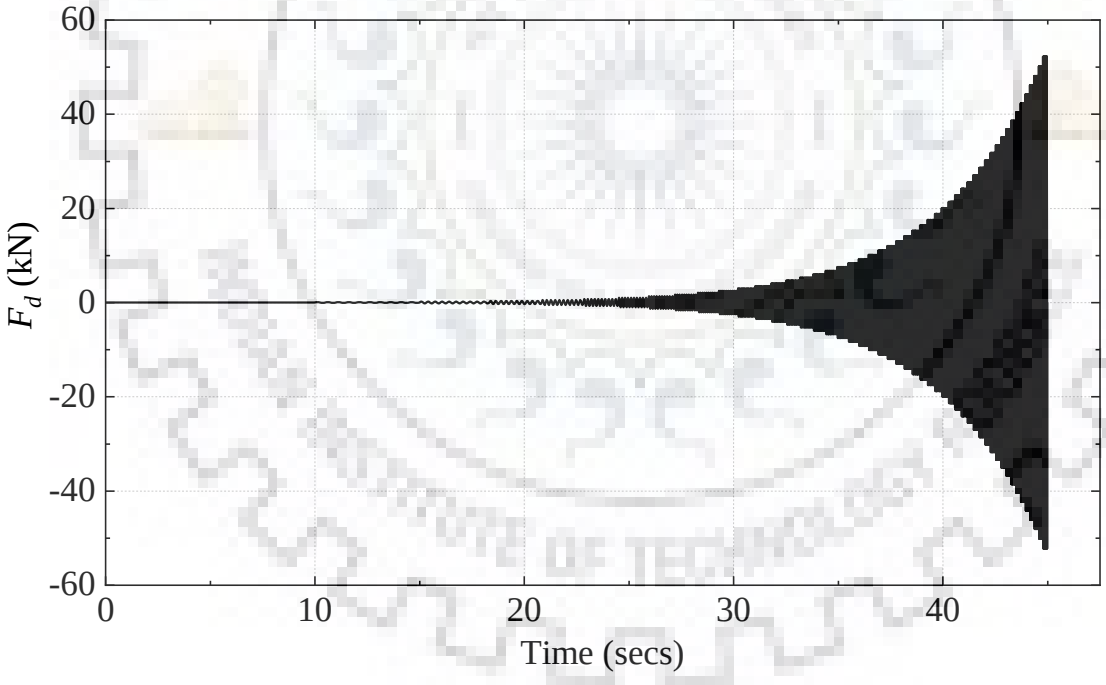

Fig. 4.8 Typical force time history applied on top surface of oscillator motor assembly

A hybrid modelling approach (Banerjee 2009; Banerjee et al. 2014; Banerjee et al. 2016; Zhang and Liu 2017) has been adopted to obtain the bending moment along the length of the pile (Fig. 4.9). In this hybrid approach, beam elements are embedded into the solid pile. For this purpose, 2-node beam element in space with cubic interpolation (B33) has been used (Fig. 4.2d).

In embedded constraint, the pile has been considered as surrounding host element, whereas the beam element has been considered as an embedded element. In Abaqus software, the nodes of the embedded element are automatically constrained (to follow geometric relationship) to the nearest nodes of surrounding host element that contains embedded nodes. This method offers a major advantage in capturing the response of piles in terms of bending moment.

Fig. 4.9 Hybrid modelling approach to obtain bending moment in pile

The responses of the 3D FE models have been obtained in terms of displacement time histories at mid height of pile cap, displacement and bending moment profile along the pile length for all considered cases. Figures 4.10 and 4.11 show the variation in displacement and bending

moment at the pile head of B0, respectively, for applied force-time history corresponding to e = 60º.

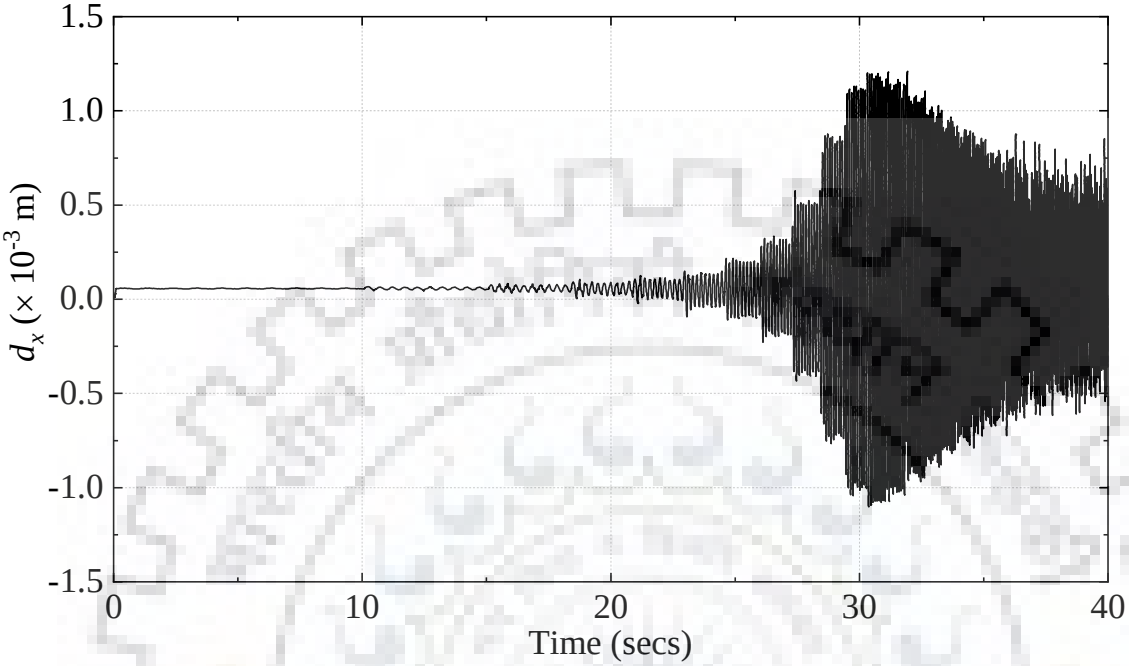

Fig. 4.10 Typical displacement time history at pile head of B0 at e = 60º

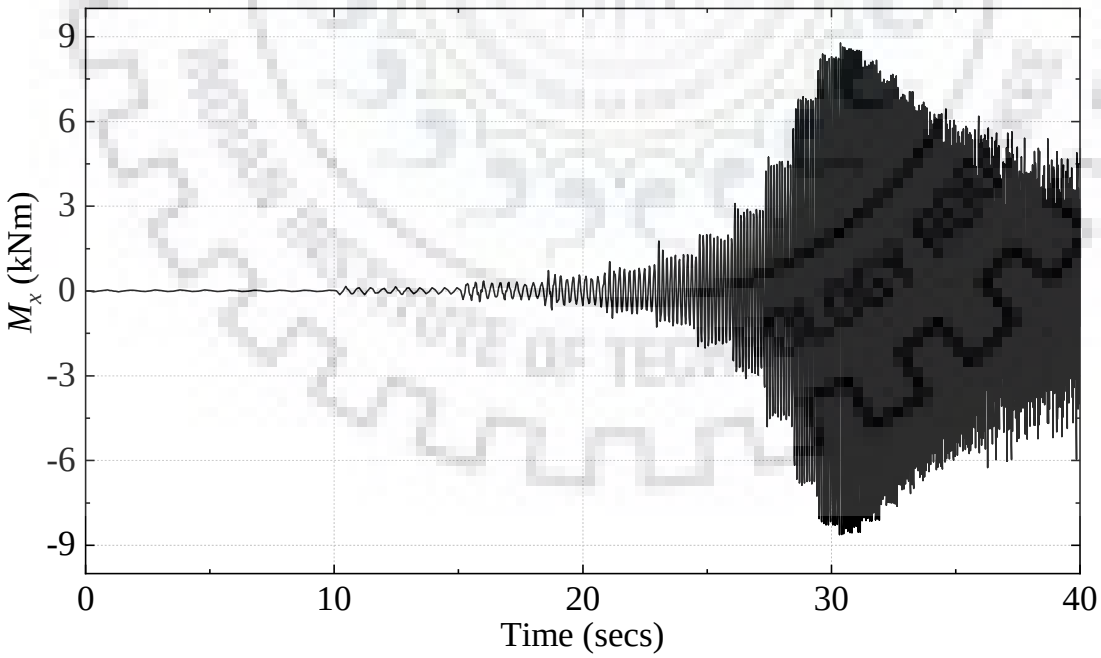

Fig. 4.11 Typical bending moment time history at pile head of B0 at e = 60º

Table 4.1 Summary of elements used in 3D FE models

Element Type	3D FE Model for						
	B0	**B10**	**B20**	**3VG**	**3BG**	**4VG**	**4BG**
B33	26	26	26	78	78	104	104
C3D8R	23480	25573	25606	23278	22981	31739	36899
CIN3D8	740	740	740	740	740	740	740
C3D4	0	0	0	3836	3609	3929	4154
Total No. of Elements	24246	26339	26372	27932	27408	36512	41897
Total No. of Nodes	27513	29703	29794	28510	28659	38314	43792

The computational facility available at the Department of Earthquake Engineering, IIT Roorkee was used to conduct the dynamic analysis of 3D FE models of all piles and pile groups. The summary of type and number of elements used in the developed 3D FE models is presented in Table 4.1. Time required to conduct the 3D FEA on a single model at an exciting force level was 25 hours (aprox.) for single piles and 30 hours (aprox.) for pile groups (PC specification: 64 GB DDR4 RAM, Intel(R) Xeon(R) Gold 5118 CPU @ 2.30 GHz (2 Processors). The results thus obtained from the 3D finite element analyses are presented and discussed in the following sections.

4.3 RESULTS AND DISCUSSION

The results obtained from the dynamic analysis of batter piles and pile groups are elaborated in detail in the following sections.

4.3.1 Single Piles

Typical displacement contours of piles B0, B10 and B20 excited at e = 60° in X direction is presented at a time step corresponding to the resonant frequency (i.e. peak displacement) in Figs. 4.12, 4.13 and 4.14 respectively. From the figures it can be observed that the displacement contours on the surrounding soil mass is symmetric in case of B0 whereas in case of B10 and B20 the contours are slightly unsymmetrical. However, it can also be observed that in case of B10 and B20 the influence area on the positive X direction is larger than the other direction.

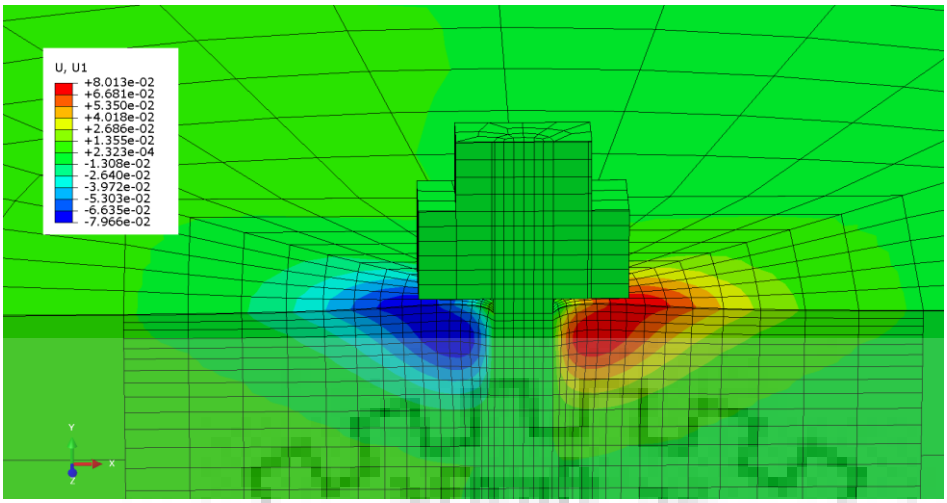

Fig. 4.12 Displacement contour for B0 excited in X direction at *e* = 60°

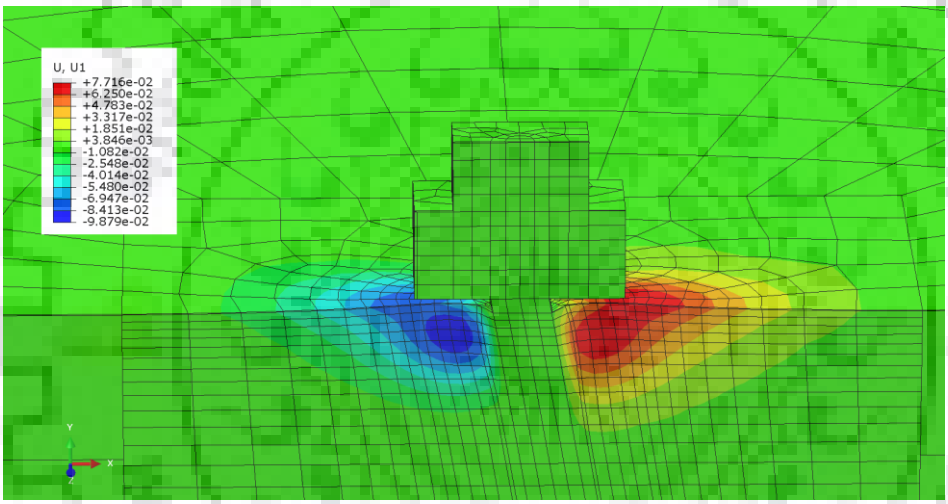

Fig. 4.13 Displacement contour for B10 excited in X direction at *e* = 60°

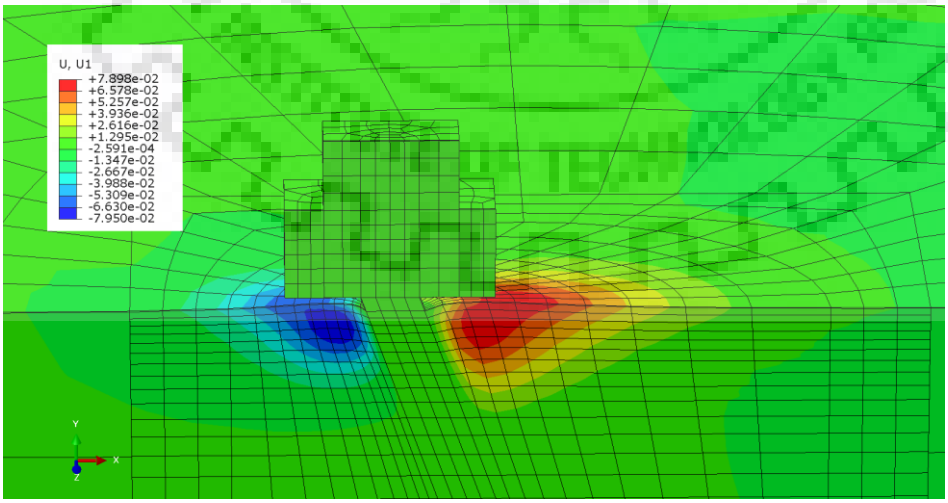

Fig. 4.14 Displacement contour for B20 excited in X direction at *e* = 60°

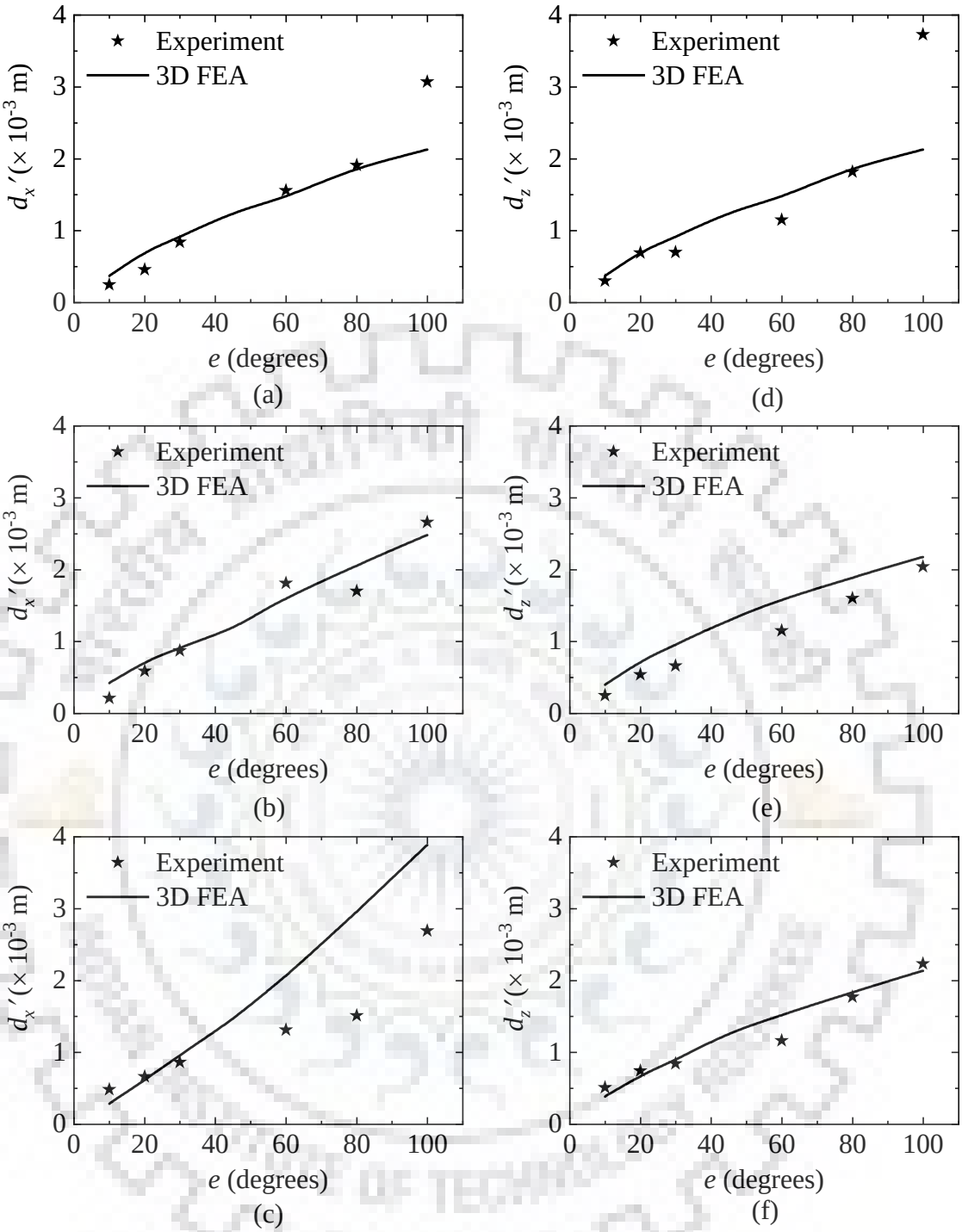

Fig. 4.15 Comparison of experimental and 3D FEA results in: X direction (a) B0; (b) B10; and (c) B20; and Z direction (d) B0; (e) B10; and (f) B20

In order to validate the results from 3D FEA, the peak displacement corresponding to the resonant frequency (d_x' or d_z') has been obtained from the displacement time history measured at the pile head of 3D FEA and compared to the peak displacement obtained experimentally in Fig.

4.15 (a-c) and 4.15 (d-f) for piles B0, B10 and B20 excited in X and Z directions respectively. It can be observed from the figure that both the experimental and 3D FEA are in good agreement.

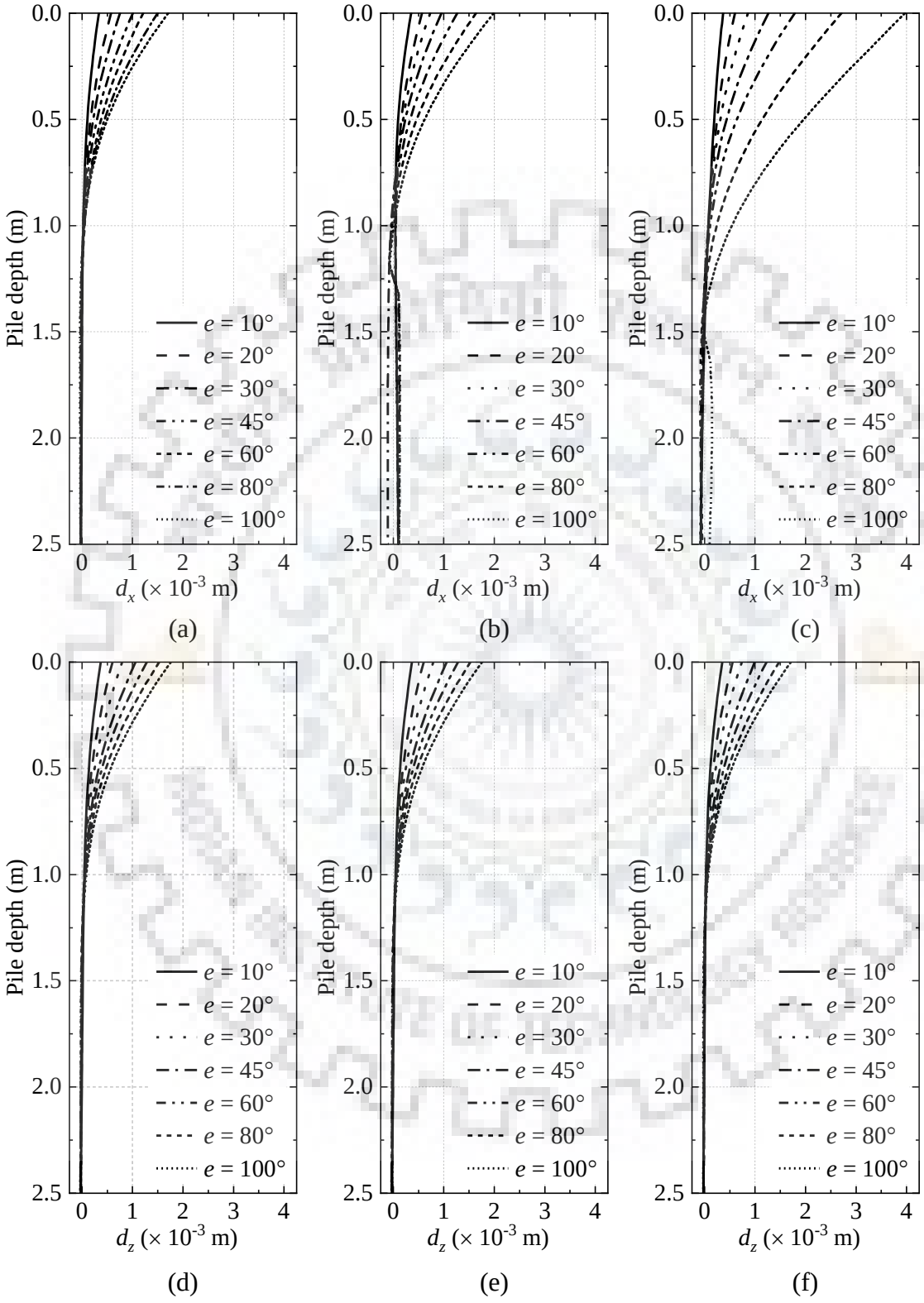

Fig. 4.16 Variation of displacement along pile depth in: X direction (a) B0; (b) B10; and (c) B20; and Z direction (d) B0; (e) B10; and (f) B20

The variation of lateral displacement (d_x or d_z) along the depth of the pile is obtained for all considered cases as shown in Fig. 4.16 corresponding to the resonance region (peak displacement from displacement time history obtained at pile head). It can be observed that B20 excited in X direction experienced large lateral displacement. However, the displacement in Z direction for both B10 and B20 is almost equal to the displacement experienced by B0.

The bending moment capacity of the circular pile section with varying axial load is estimated using Section Designer (ETABS 2018). The capacity envelope of the RC pile has been developed using the material properties, size and reinforcement, used in the experimental investigation. Mander's model for confined concrete (Mander et al. 1988) and elasto-plastic constitutive model for steel has been used. Figure 4.17 show the ultimate moment capacity of the pile cross section along with the reinforcement detailing used in the experimental investigation. It can be observed that the ultimate moment capacity of the considered section is around 11kNm.

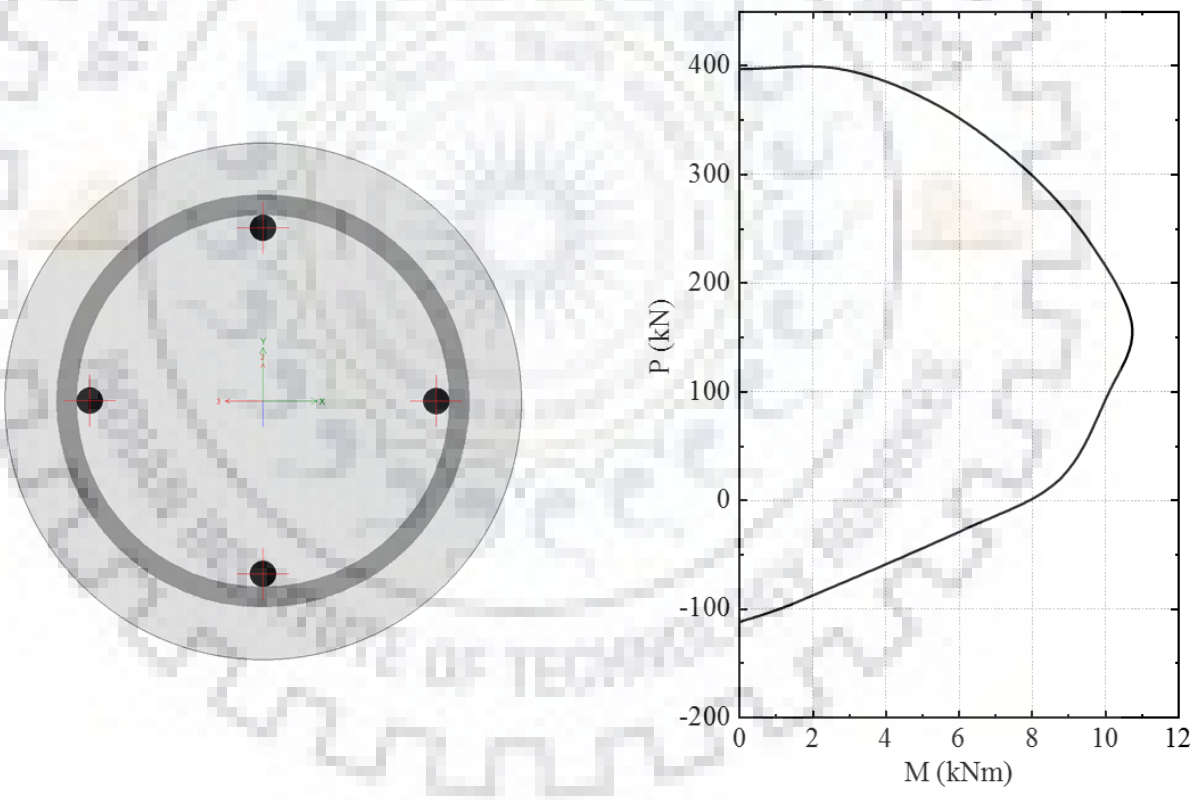

Fig. 4.17 Pile: (a) cross section; and (b) ultimate moment capacity

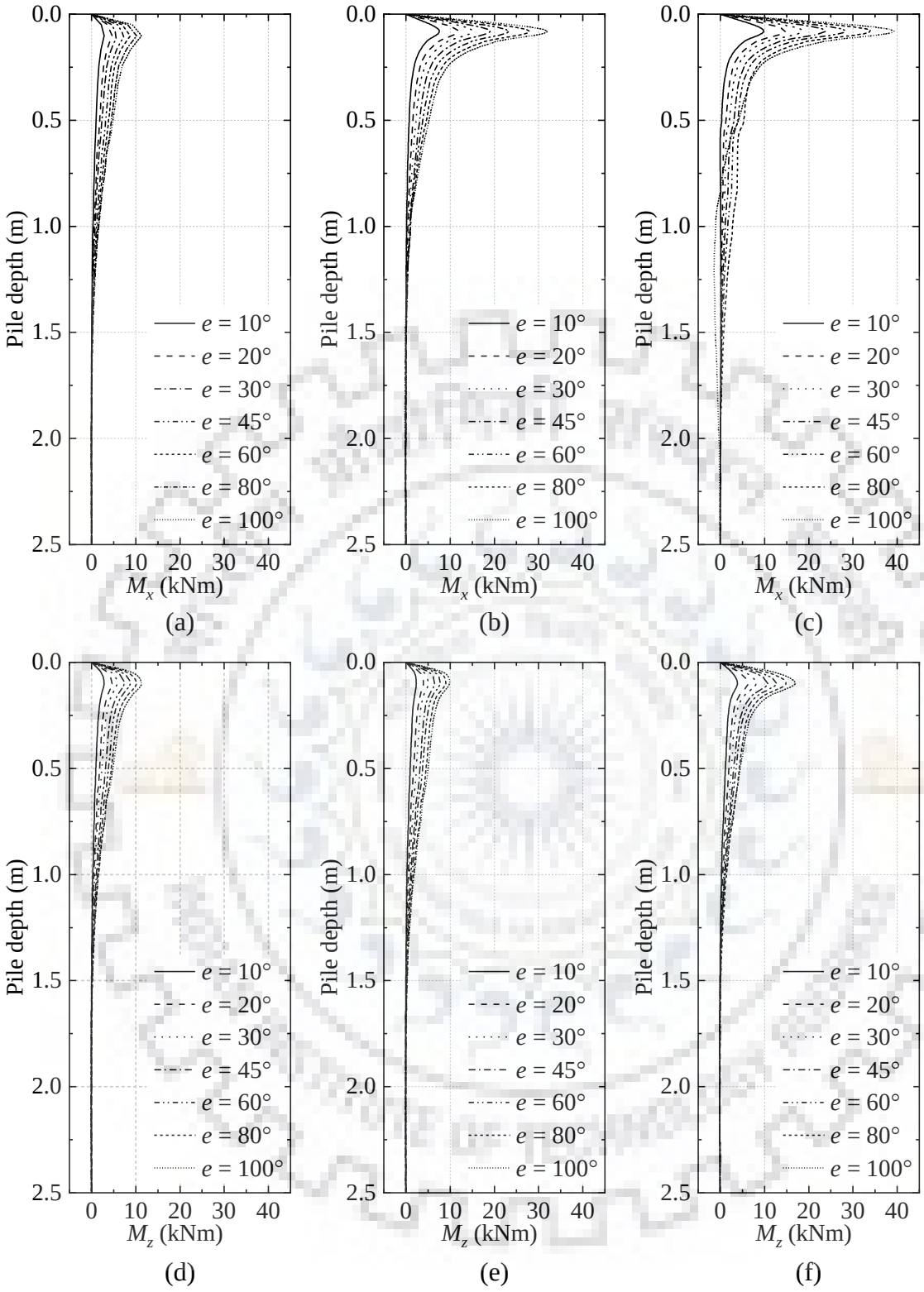

Fig. 4.18 Variation of bending moment along pile depth in: X direction (a) B0; (b) B10; and (c) B20 and Z direction (d) B0; (e) B10; and (f) B20

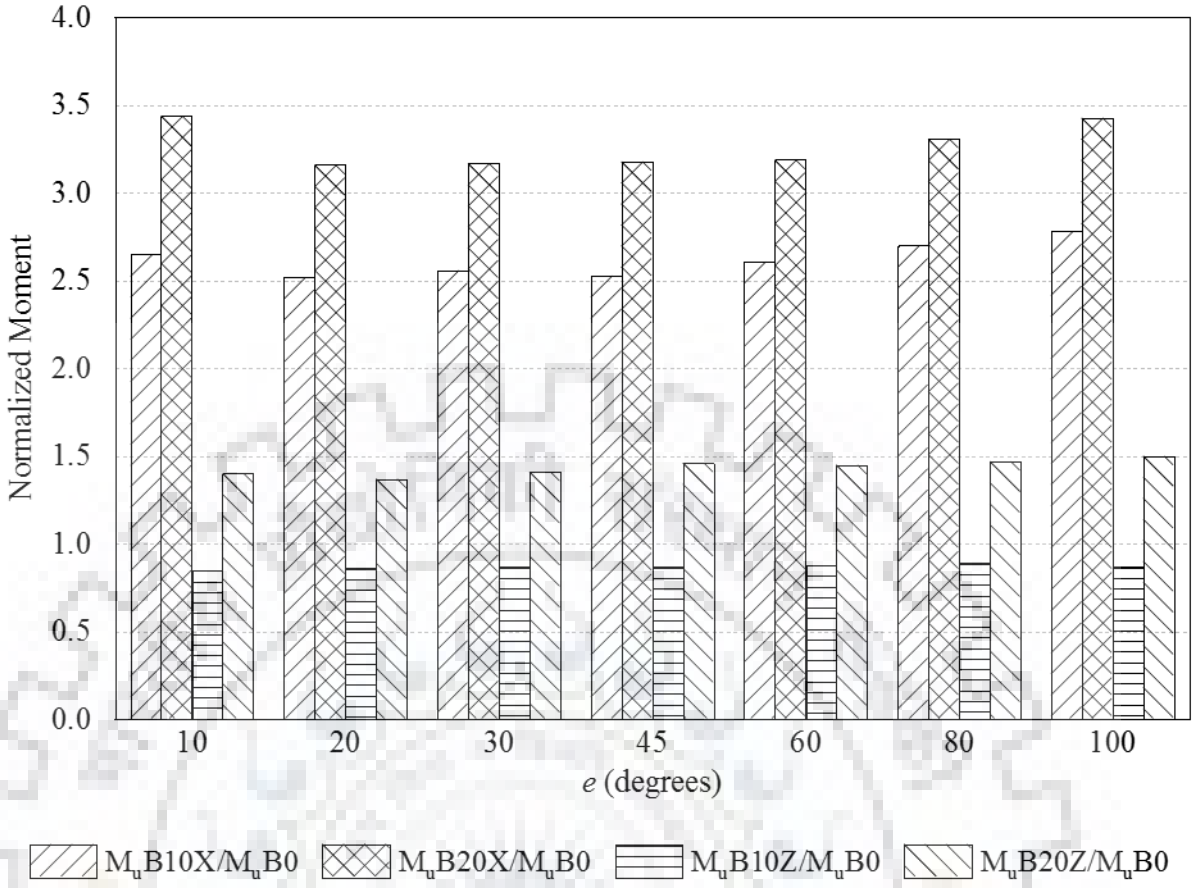

Fig. 4.19 Comparison of normalized maximum bending moment in single piles

With the help of adopted hybrid approach the variation in bending moment (M_x or M_z) along the pile depth corresponding to the resonance region (peak moment from bending moment time history obtained at pile head) has been obtained for all considered cases as presented in Fig. 4.18. It can be observed from this figure that piles B10 and B20 attract more bending moment especially when excited in X direction. The normalized peak bending moment at a particular eccentricity is obtained as the ratio of maximum bending moment in batter pile to the maximum bending moment in vertical pile. The variation of normalized bending moment is presented in Fig. 4.19. It can be seen that B10 and B20 attract bending moment as much as 3 times the bending moment in vertical pile in X direction. It is also interesting to note that in Z direction B10 experiences slightly lower bending moment when compared to B0.

In order to understand the effect of material model a parametric study has been conducted considering the soil mass as linear elastic material. The variation of peak displacement from experiments, linear and non-linear (using Mohr-Coulomb failure criteria) material models is presented in Fig. 4.20(a-c) for piles B0, B10 and B20. It can be observed from the figure that

linear material model overestimates the displacement response at all force levels considered in the present study.

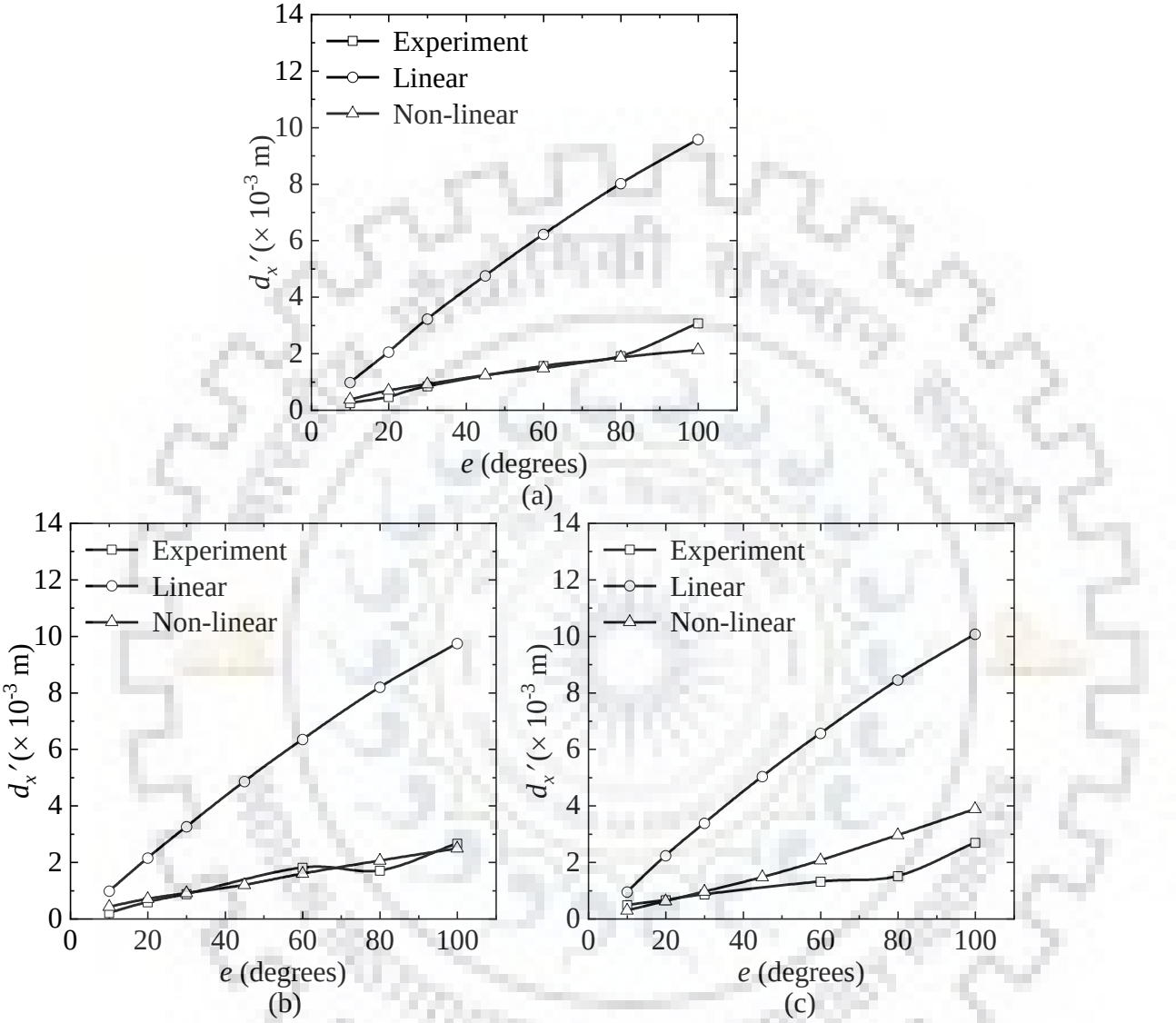

Fig. 4.20 Effect of material model in: (a) B0; (b) B10; and (c) B20 excited in X direction

In addition, an attempt is also made to understand the effect of E_p/E_s value through a parametric study considering the soil mass as linear elastic material. For this purpose three value of E_p/E_s is considered, keeping E_p to be constant. The variation of peak displacement for all three cases is presented in Fig. 4.21(a-c) for piles B0, B10 and B20. It can be observed from the figure that as the E_p/E_s ratio decreases, the displacement response of the piles increases. This might be due to the fact that in the present study, the dynamic loading is applied on top of the pile cap unlike seismic loading and the L/d ratio of pile geometry considered as 12.5 lies between short and slender pile.

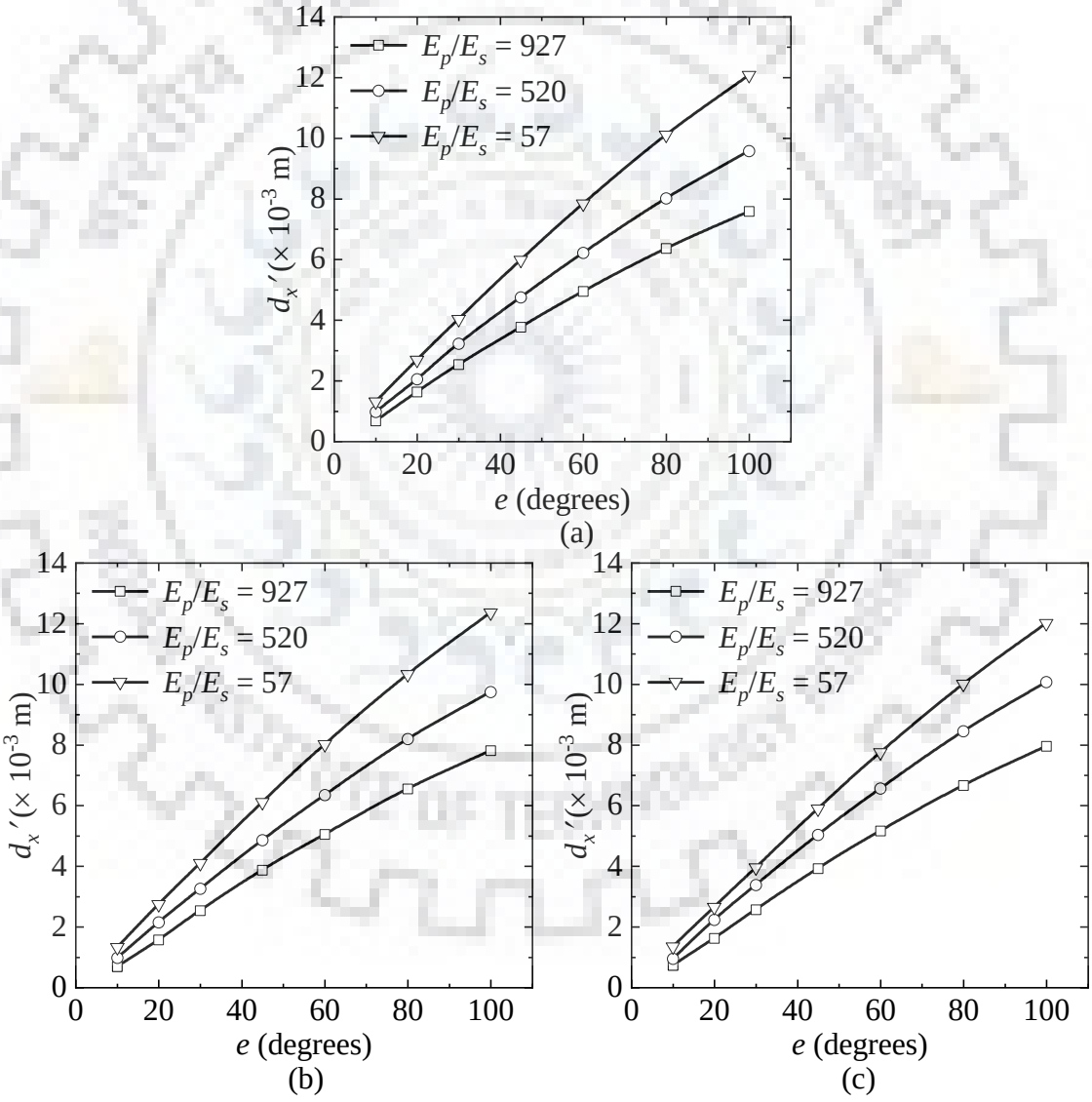

Fig. 4.21 Effect of E_p/E_s for: (a) B0; (b) B10; and (c) B20 excited in X direction

4.3.2 Pile Groups

Typical displacement contours of pile groups 3VG, 3BG, 4VG and 4BG excited at e = 60° in X direction is presented at a time step corresponding to the resonant frequency in Figs. 4.22(a-d). From the figures it can be observed that the displacement contours on the surrounding soil mass for 3VG and 4VG is slightly deeper when compared to the displacement contours of 3BG and 4BG. The influence zone is higher in case of batter pile groups (3BG and 4BG) when compared to vertical pile groups (3VG and 4VG).

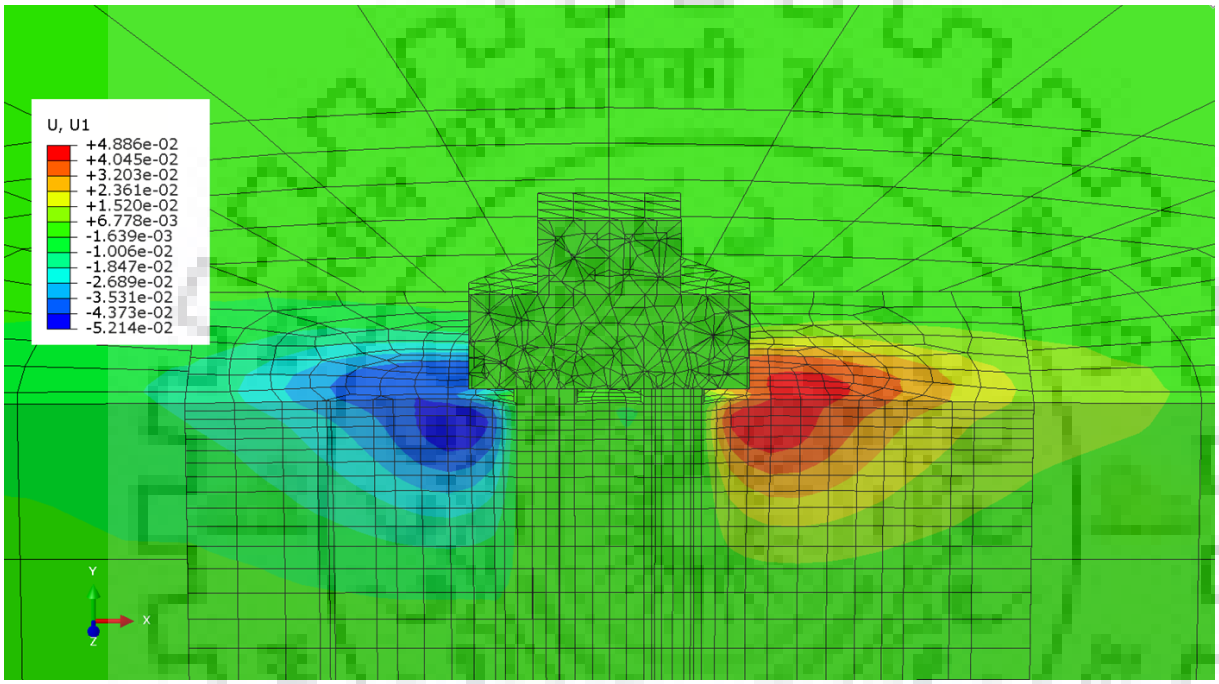

(a)

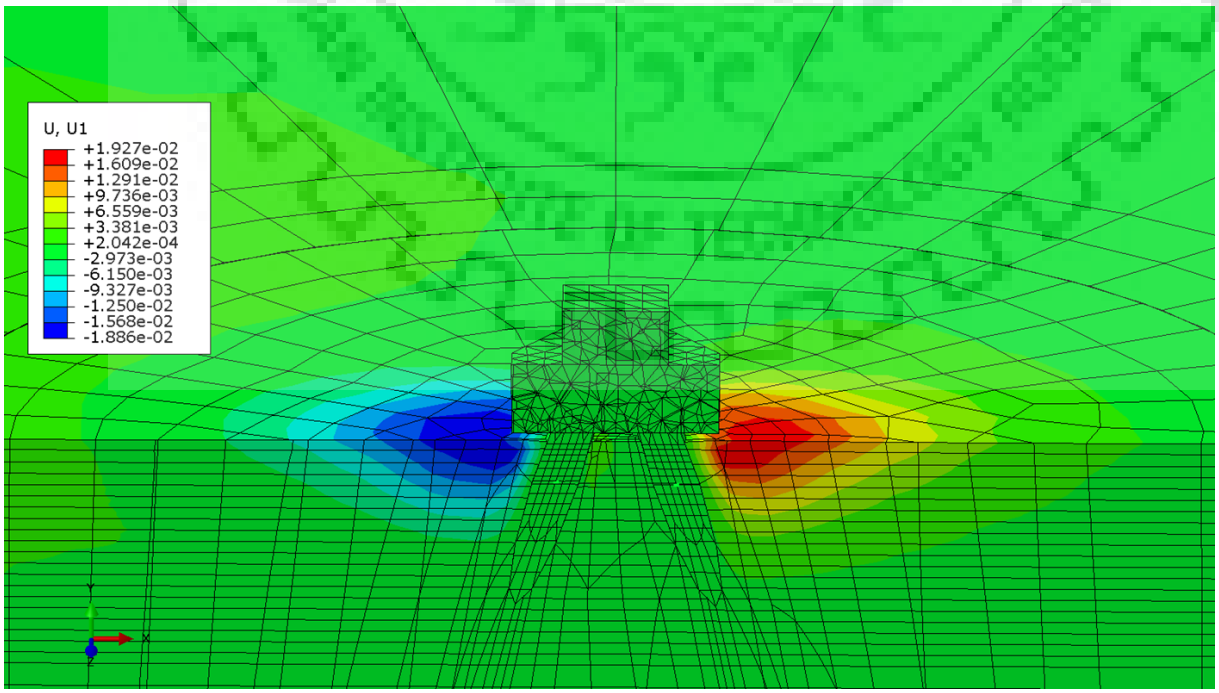

(b)

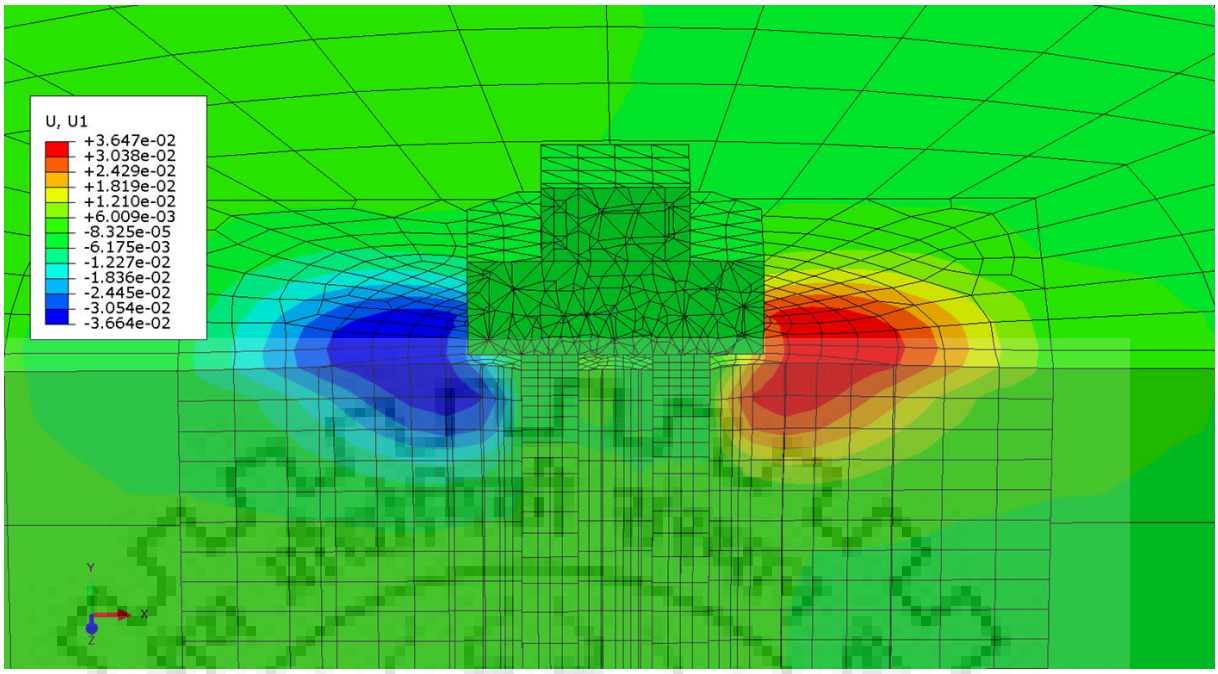

(c)

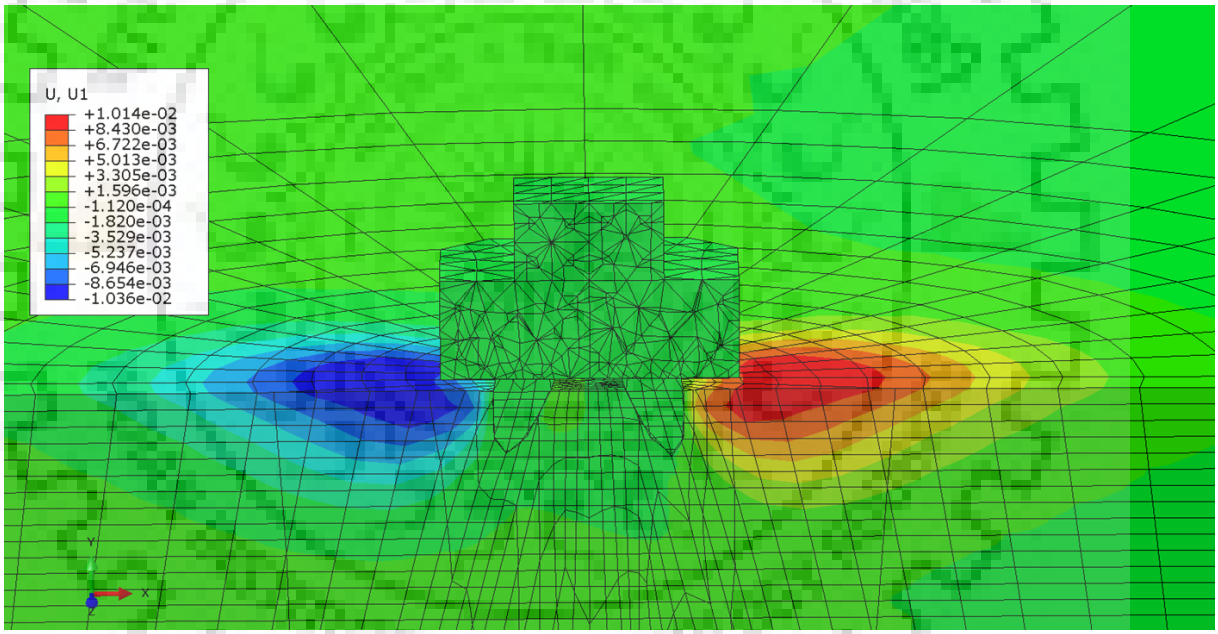

(d)

Fig. 4.22 Displacement contour for pile groups excited in X direction at e = 60° (a) 3VG; (b) 3BG; (c) 4VG; and (d) 4BG

In order to validate the results from 3D FEA, the peak displacement corresponding to the resonant frequency (dx' or dz') has been obtained from the displacement time history measured at the pile head of 3D FEA and compared to the peak displacement obtained experimentally in Fig. 4.23 (a-d) for all four pile groups excited in X direction. It can be observed from the figure that both the experimental and 3D FEA are in good agreement.

However, the variation in displacement and bending moment along pile length of individual piles in a group is not discussed due to their random distribution. This might be due to the fact that the dynamic load is applied on top of pile cap unlike seismic loading usually applied at the base of the model and the displacement or bending moment profiles obtained along the pile length.

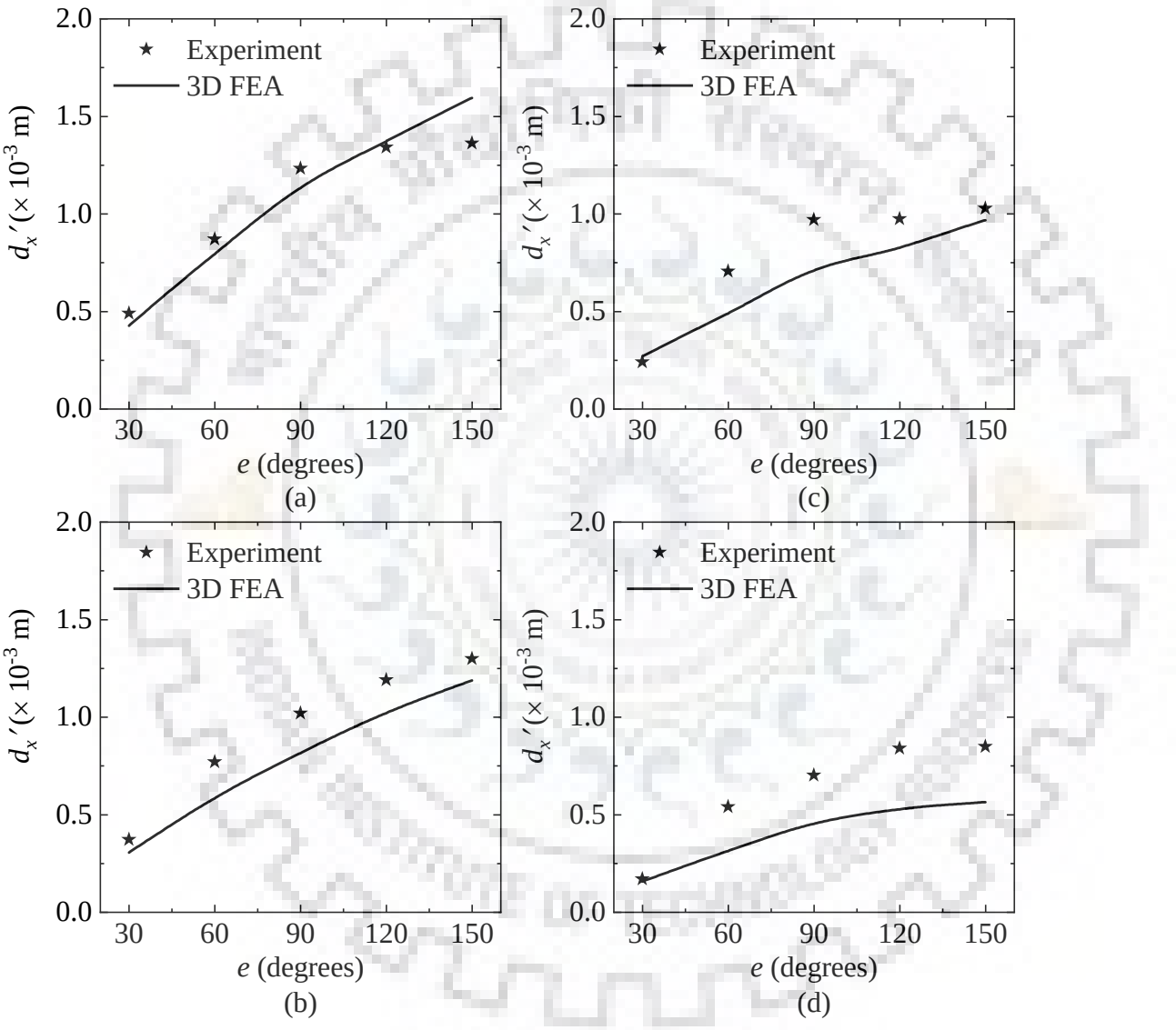

Fig. 4.23 Comparison of experimental and 3D FEA results for: (a) 3VG; (b) 4VG; (c) 3BG; and (d) 4BG excited in X direction

4.4 SUMMARY

An extensive numerical study has been performed on RC single piles and pile groups with the pile cap supported on similar soil conditions and subjected to dynamic loading. The variation of peak displacement as well as the bending moment has been explored through the developed 3D hybrid FE model. The response obtained from 3D FE models for both single vertical and batter piles and pile groups are in good agreement with their corresponding experimental results obtained through field tests. The dynamic response of pile is highly influenced by the material model used in FEA Linear and Non-linear (Mohr-Coulomb yield criterion). In linear case, as the E_p/E_s ratio decreases the displacement response of the piles increases. The batter piles attract more bending moment when compared to vertical piles at all force levels as much as three times in X direction.

Chapter 5

DYNAMIC PILE GROUP TEST INDUCED BUILDING VIBRATION

5.1 INTRODUCTION

The rapid increase in urban population and infrastructure development requires an optimized use of available land for construction. With the futuristic plan for conversion of old cities into smart cities, the construction fraternity has to face a lot of challenges throughout the project. One of the major challenges is the vibration experienced by the occupants of the existing building in the locality. These vibrations might be due to different sources, including construction, industrial and transportation activities. The vibration energy gets transmitted from the source through the supporting soil mass underneath the buildings/ structures and are felt by the occupants. In addition, excessive vibrations transmitted into the buildings, hinder the performance of vibration sensitive equipment, causing adverse effect on the living quality of the occupants and lead to micro-cracks, minor/ architectural damage or major/ structural damage to the structures Xia et al. (2009).

In the past, several researchers have reported the vibration measurements in the buildings, imparted from the underground/ overhead railway tracks and studied the influence of governing factors, including train speed, track distance and relative track height (Xia et al. 2005; Degrande et al. 2006; Sanayei et al. 2014; Zou et al. 2017). The vibrations developed due to passage of metro trains in different existing routes of Delhi Metro Rail Corporation (DMRC) were measured both on the ground level and on the buildings as reported in EQ:2017-16 (2017). With the advancement in high computational facilities, various numerical studies were performed on simulations of vibration aspects and its effects on associated/ adjacent structures. For greater insights 2D, 2.5D and 3D numerical models were developed by various researchers to understand the train-induced ground vibrations dealing with different aspects (Hall 2003; Ju 2009; Galvín et al. 2010; Mhanna et al. 2012; El Kacimi et al. 2013; Hung et al. 2013; Kouroussis et al. 2014; Lopes et al. 2014; Bian et al. 2015; Real et al. 2015; Hesami et al. 2016; Shih et al. 2016; Yang et al. 2017).

Apart from the train vibrations, Crispino and D'Apuzzo (2001) measured the vibration induced from various types of vehicles in the heritage building (in Naples) and observed that all the records exceeded the threshold values suggested by ISO (2003). In addition, Bertero et al. (2013) examined the building vibrations due to rock concerts in stadiums and concluded that ground and building accelerations are directly proportional to the number of spectators jumping simultaneously to the rhythm of the music.

In urban areas, the rapid growth in population have led to construction in the vicinity of existing structures. In majority of construction sites, pile driving is a common practice adopted for pile installation. The vibrations produced by pile driving, either transient or continuous depending upon the driving technique (impact or vibratory), is usually experienced by the occupants in the buildings nearby. However, the vibrations produced might cause significant damage to the structures in the surrounding (Athanasopoulos and Pelekis 2000; Thandavamoorthy 2004; Svinkin 2006; Zhang et al. 2013; Grizi et al. 2016). These vibrations generated during pile driving have been quantified through field experiments (Hwang et al. 2001; Grizi et al. 2016) and numerical simulation (Zhang and Tao 2011; Ekanayake et al. 2013; Rezaei et al. 2016; Rooz and Hamidi 2017; Hamidi et al. 2018). In addition, its effect on adjacent structure has also been explored (Athanasopoulos and Pelekis 2000; Henke 2010). When these vibrations propagate through the structures, the parameters, including structural material, building configuration, potential degradation due to structural age, soil supporting the structure, soil structure interaction etc., influence the vibration response. In literature, the vibration induced from the pile driving was mostly measured at the ground surface only and no studies could be found dealing with its effect/ vibration measurement on an adjacent building. However, wave propagation in structures using ambient vibrations and earthquake recordings has also been explored in detail using deconvolution approach (Picozzi et al. 2011; Newton and Snieder 2012; Nakata and Snieder 2013; Rahmani and Todorovska 2013; Cheng et al. 2014; Bindi et al. 2015; Petrovic and Parolai 2016; Wen and Kalkan 2017; Petrovic et al. 2018; Pianese et al. 2018).

In this chapter, vibrations induced in an adjacent building during the dynamic tests conducted on pile groups have been reported. When the dynamic lateral load tests were conducted on two different pile groups constructed at the site adjacent to the Department of Earthquake Engineering (DEQ) Building, Indian Institute of Technology Roorkee (IITR), India, occupants of the building experienced annoying vibrations, crackling of window panes, etc. To quantify the vibration level, sensors (accelerometers and seismometers) were placed on each floor of the DEQ building and the vibrations were measured in real time. In addition, 2D plane-

strain FE model was also developed to study the effect of the vibration caused by the dynamic tests of the pile group on the adjacent building. The vibration produced during pile driving in the field is either continuous or transient, which is similar to the loading pattern considered in this study. The vibration parameters obtained from experiment and FE analyses were checked with the permissible limits suggested by various standards, to examine its validity, and finally a comparative study is also presented herein.

5.2 PERMISSIBLE LIMITS IN DESIGN CODES AND STANDARDS

Most of the available guidelines in design codes and standards deal either with the vibration caused due to traffic, transportation and construction activities. The guidelines thus provided on vibration assessment and its impacts from various standards available are summarized in the following sections.

5.2.1 International Standards Organization

ISO (1997) and BIS (2000a) states "*Experience in many countries has shown that occupants of residential buildings are likely to complain if the vibration magnitudes are only slightly above the perception threshold*". BIS (1992) and ISO (2003) also mentions "*In some cases complaints arise due to secondary effects associated with vibration, e.g. reradiated noise*". It also provides the following approximate indications on likely reaction of passengers experiencing overall vibration in public transport as reported in Table 5.1. The frequency range considered for health, comfort and perception for human performance exposed to vibrations is 0.5 Hz to 80 Hz. According to BIS (1992) and ISO (2003), the vibration impact on humans is within the frequency range 1 Hz to 80 Hz when the posture of the occupant need not be defined. BIS (1992) and ISO (2003) classifies the source of vibration broadly as continuous or semi-continuous (e.g. industry), permanent intermittent (e.g. traffic) and limited (or non-permanent) duration activities (e.g. construction). According to BIS (2000b) and ISO (2010), most of the structural damage from man-made sources occurs in the frequency range from 1 Hz to 150 Hz whereas, natural sources, such as earthquakes and wind excitation, usually contain damage-level energy at lower frequencies, in the range from 0.1 Hz to 30 Hz. But, the suggested threshold frequency ranges as per BIS (1992) and ISO (2003) do not consider the combined effect of vibration in building and noise effect on humans. Therefore, to quantify the threshold value for combined effect (noise and

vibration), accurate physiological and behavioural analysis of humans is also required (Schiavi and Rossi 2015).

Table 5.1 Vibration magnitude and comfort reactions (ISO 1997; BIS 2000a)

Vibration magnitude (m/s^2)	Comfort reactions
< 0.315	Not uncomfortable
0.315 to 0.63	A little uncomfortable
0.5 to 1	Fairly uncomfortable
0.8 to 1.6	Uncomfortable
1.25 to 2.5	Very uncomfortable
> 2	Extremely uncomfortable

The response of structures subjected to vibration from various sources in terms of frequency, particle velocity and particle acceleration has been presented in Table 5.2. Other details regarding the measurement distance and location are elaborated in Table 5.3.

Table 5.2 Structural response range for various sources (BIS 2000b; ISO 2010)

Source of vibration	Frequency (Hz)	Particle velocity range (mm/s)	Particle acceleration range (m/s^2)
Road, rail and ground borne traffic	1 - 100	0.2 - 50	0.02 - 1
Blasting vibration ground borne	1 - 300	0.2 - 100	0.02 - 50
Air over pressure	1 - 40	0.2 - 3	0.02 - 0.5
Pile driving ground borne	1 - 100	0.2 - 100	0.02 - 2
Machinery outside ground borne	1 - 100	0.2 - 100	0.02 - 1
Machine inside	1 - 300	0.2 - 30	0.02 - 1
Human activities inside	0.1 - 30	0.2 - 20	0.02 - 0.2
Earthquakes	0.1 - 30	0.2 - 400	0.02 - 20
Wind	0.1 - 10	--	--
Acoustic (inside)	5 - 500	--	--

Table 5.3 Structural response range for various sources (according to French experiences) (BIS 2000b; ISO 2010)

Vibration source	Measuring location	Frequency (Hz)	Amplitude (mm/s)	Distance (m)
Mass pile driving	Foundation	10 to 20	1.6	14
	Flooring tile		2.0	14
Vibrating pile driving	Foundation	20	2.6	14
	Flooring tile		4.3	14
Concrete cruncher	5^{th} floor	3	7.5	10
Rock breaker	5^{th} floor	35	9.9	15
Petroleum vibrators	Main structure foundation	26	6.1	6.5
Forging hammers	Main structure foundation	10 to 25	0.8	30
		6 to 20	0.2	
		8 to 10	2.5	
Quarry blasting	Main structure foundation	28	3.3	200
		36	3.7	
		27	1.8	
Road traffic	Main structure foundation	10 to 15	0.2 to 1.0	5 to 10
		12 to 15	2.0 to 2.5	
		10	1.0 to 1.3	
		3 to 4	1.0 to 1.4	
		9 to 12	0.5 to 1.2	
		10 to 15	1.2 to 1.7	
		10 to 45	0.5 to 1.5	
	Floor	10 to 20	0.2	
		12 to 20	0.4 to 0.6	
		12 to 15	2.5 to 3.5	
		17	3.5 to 5.3	
		11 to 13	1.0	
	Centre of paving stone	3 to 4	1.5 to 2.1	
		9 to 12	0.5 to 1.2	
		10 to 20	0.4 to 2.0	
		35	1.5 to 2.0	
		8 to 50	2.0 to 3.0	
Railway traffic	Main structure foundation	60	2.0	10 to 20
		10	0.5	
		51	1.9	
		20	2.2	
		90 to 110	2.5	

5.2.2 British Standards

According to BSI (2014), when the threshold of vibration in terms of (Peak Particle Velocity) PPV exceed the range of 0.14 mm/s to 0.3 mm/s human beings tend to get disturbed, frighten, cause annoyance or interfere with work activities. Exposure to these vibrations at higher levels

could be unpleasant or even painful. They also promote anxiety lest some structural mishap might occur. In this line the effect of exposure to vibration level is summarized in Table 5.4. When the buildings are exposed to continuous vibrations, dynamic magnification occurs due to resonance especially at lower frequencies. In that case, the limits prescribed in Table 5.5 for transient vibrations might be reduced by 50%. In addition, vibration levels measured during impact pile driving, driven cast-in place piling, dynamic consolidation, vibroflotation or vibroreplacement, use of casing vibrators, rotary bored piling, tripod bored piling, driven sheet steel piling, driving of bearing piles and vibratory pile drivers are summarized in detail in BSI (2014) based on historic case history data.

Table 5.4 Guidance on effect of vibration levels (BSI 2014)

Vibration level	**Effect on human beings**
0.14 mm/s	Vibration might be just perceptible in the most sensitive situations for most vibration frequencies associated with construction. At lower frequencies, people are less sensitive to vibration
0.3 mm/s	Vibration might be just perceptible in residential environments.
1.0 mm/s	It is likely that vibration of this level in residential environments will cause complaint, but can be tolerated if prior warning and explanation has been given to residents.
10 mm/s	Vibration is likely to be intolerable for any more than a very brief exposure to this level in most building environments

Table 5.5 Guidance for cosmetic damage due to transient vibrations (BSI 1993; BSI 2014)

Building type	**Peak component particle velocity at the base of the building for transient vibrations in frequency range of predominant pulse**	
	4 to 15 Hz	**15 Hz and above**
Reinforced or framed structures, Industrial and heavy commercial buildings	50 mm/s at 4 Hz and above	
Unreinforced or light framed structures, Residential or light commercial type buildings	15 mm/s at 4 Hz increasing to 20 mm/s at 15 Hz. At frequencies below 4 Hz a maximum displacement of 0.6 mm should not be exceeded.	20 mm/s at 15 Hz increasing to 50 mm/s at 40 Hz and above

5.2.3 Swedish Standards

According to the Swedish standard (SIS 1999) the dominant frequency of vibration generated from pile driving and soil compaction usually varies between 5 to 30 Hz. The limiting vibration values are independent of vibration frequency. The maximum allowable PPV value for transient vibration, V is a product of vertical component of uncorrected vibration velocity at the base of the building, V_0; building factor, F_b; material factor, F_m and foundation factor, F_g can be estimated based on the details in the following table (Table 5.6).

Table 5.6 Factors for estimation of vertical vibration velocity (SIS 1999)

Factor	Condition	Value (mm/s)
V_0	Bedrock	15
	Glacial Till	12
	Clay, silt, sand or gravel	9
F_b	Heavy structures, such as bridges, quay walls, defense structures etc.	1.7
	Industrial or office buildings	1.2
	Normal residential buildings	1
	Especially susceptible buildings and buildings with high value or structural elements with spans e.g. church or museum	0.65
	Historic buildings in a sensitive state as well as certain sensitive ruins	0.5
F_m	Reinforced concrete, steel or wood	1.2
	Unreinforced concrete, bricks, concrete blocks with voids, light weight concrete elements, masonry	1
	Light concrete blocks and plaster	0.75
	Limestone	0.65
F_g	Buildings founded on toe-bearing piles	1
	Buildings founded on shaft-bearing piles	0.8
	Spread footings, raft foundations	0.6

5.2.4 German Standards

The guidelines provided by German standard (DIN 1999) to evaluate the effect on short and long term vibrations on structures have been summarized in Table 5.7. The vibration limits exceeding the values in Table 5.7 does not necessarily lead to damage, but when they are exceeded by significant amount further investigations are necessary. However, the maximum velocity at the centre of floor should not be greater than 20 mm/s for short-term vibrations. Similarly, the guidelines used to evaluate the effect of short and long term vibrations on buried pipework are reported in Table 5.8.

Table 5.7 Guidelines to evaluate the effect of short and long term vibrations on structures (DIN 1999)

Vibration source type	Short term				Long term
	At the foundation (mm/s)			Horizontal plane of highest floor (mm/s)	Horizontal plane of highest floor (mm/s)
Location	1 to 10 Hz	10 to 50 Hz	50 to 100 Hz*		
Buildings used for commercial purposes, industrial buildings and building of similar design	20	20 to 40	40 to 50	40	10
Dwellings and buildings of similar design and/or occupancy	5	5 to 15	15 to 20	15	5
Structures that, because of their particular sensitivity to vibration, cannot be classified as above and are of great intrinsic value (e.g. Listed under preservation order)	3	3 to 8	8 to 10	8	2.5

*At frequencies beyond 100 Hz, the values of this column may be used a minimum value

Table 5.8 Guidelines to evaluate the effect of short and long term vibrations on buried pipework (DIN 1999)

Pipe material	Velocity of short-term vibration measured on the pipe (mm/s)	Velocity of long-term vibration measured on the pipe (mm/s)
Steel including welded pipes	100	50
Clay, concrete, reinforced concrete, prestressed concrete, metal (with or without flange)	80	40
Masonry, plastic	50	25

5.2.5 U.S. Department of Transportation

The guidance manual (FRA 2012) by U.S. Department of Transportation, Federal Railroad Administration sets guidelines for noise and vibration assessment due to high-speed ground transportation. The details regarding the screening distance, vibration source levels from construction equipment and vibration damage criteria are summarized below in Tables 5.9 - 5.11 respectively.

Table 5.9 Screening distance for vibration assessment (FRA 2012)

Land use	Train frequency	Screening distance (ft) for train speed		
		Less than 100 mph	100 to 200 mph	200 to 300 mph
Residential	Frequent or Occasional	120	220	275
	Infrequent	60	100	140
Institutional	Frequent or Occasional	100	160	220
	Infrequent	20	70	100

Note: Applicable to steel-wheel/ steel-rail high-speed rail systems. Frequent > 70 passbys per day; Infrequent < 70 passbys per day

Table 5.10 Construction vibration damage criteria (FRA 2012)

Building type	PPV (in/s)
Reinforced-concrete, steel or timber (no plaster)	0.5
Engineered concrete and masonry (no plaster)	0.3
Non-engineered timber and masonry buildings	0.2
Buildings extremely susceptible to vibration damage	0.12

Table 5.11 Vibration source levels from construction equipment (FRA 2012)

Equipment		PPV at 25 ft (in/s)
Pile driver (impact)	Upper range	1.518
	Typical	0.644
Pile driver (vibratory)	Upper range	0.734
	Typical	0.170
Calm shovel drop (slurry wall)		0.202
Hydromill (slurry wall)	In soil	0.008
	In rock	0.017
Vibratory roller		0.210
Hoe ram, Large bulldozer and Caisson drilling		0.089
Loaded trucks		0.076
Jackhammer		0.035
Small bulldozer		0.003

In addition, to evaluate the architectural damage, PPV in the range of 0.10 mm/s to 0.75 mm/s is recommended by Chinese Standard, GB/T (2008). Italian Standard, UNI (1991) also follows the same limit as BSI (1993) and (DIN 1999).

5.2.6 Department of Environment and Conservation (NSW), Australia

Vibration assessment guideline (NSW 2006) by Department of Environment and Conservation (NSW), Australia provides both preferred and maximum of root mean square (rms) acceleration and peak velocity values for continuous, impulsive and intermittent vibrations among which the maximum values are reported in Table 5.12.

Table 5.12 Acceptable vibration criteria (NSW 2006)

Location	Assessment period	RMS acceleration (Max.)					Peak velocity (Max.)	
		Continuous (m/s^2)		Impulsive (m/s^2)		Intermittent ($m/s^{1.75}$)	Continuous (mm/s)	Impulsive (mm/s)
		Z axis	X and Y axes	Z axis	X and Y axes			
Critical areas	Day or night time	0.010	0.0072	0.010	0.0072	0.20	0.28	0.28
Residences	Daytime	0.020	0.014	0.60	0.42	0.40	0.56	17
	Night-time	0.014	0.010	0.20	0.14	0.26	0.40	5.6
Offices, schools, educational institutions and places of worship	Day or night time	0.040	0.028	1.28	0.92	0.80	1.1	36
Workshops	Day or night time	0.080	0.058	1.28	0.92	1.60	2.2	36

Note: Daytime is 7.00 am to 10.00 pm and night time is 10.00 pm to 7.00 am

5.3 SITE CHARACTERISTICS

The test site considered in this study is located near the building of Department of Earthquake Engineering (DEQ), Indian Institute of technology Roorkee (IITR), India. The effect of vibration induced by the dynamic lateral load tests conducted on two different pile groups on the adjacent building (i.e. DEQ building) has been examined. The location of vertical pile group with four piles (termed as 4VG), batter pile group with four piles inclined at 20° to the vertical axis (termed as 4BG), building adjacent to the pile groups and soil profile corresponds to test site 2 reported earlier in Chapter 3.

5.4 EXPERIMENTAL STUDY

In the experimental study, the dynamic lateral vibration tests have been conducted on two pile groups for varying excitation levels and the vibrations induced in the adjacent building from these dynamic tests were measured simultaneously in real time. The following sections explain the details of all experimental investigations carried out on both the pile groups and thus induced vibrations measured in the adjacent building.

5.4.1 Measurements on the Pile Groups and Discussion

Each pile group was subjected to two different force levels generated at varying frequencies. The dynamic (sinusoidal) load was generated from the in-house mechanical oscillator-motor assembly, which operates up to 3000 rpm. The oscillator consists of two eccentric masses, each of 8.2 kg. The oscillator was firmly mounted on the pile group cap with the help of four hardened steel (HS) bolts, which were already welded to pile cap reinforcement cage before casting. A 3 Horse Power (HP) motor with the maximum operating frequency of 45 Hz was mounted on the top of the oscillator. The operating frequency of the oscillator motor assembly was controlled with the help of a speed control unit. The force level was adjusted by varying the eccentricity setting of the oscillator motor assembly. The oscillator motor assembly generated the dynamic load in the form of sinusoidal waves represented using Eq. (3.1).

The response of the pile groups has been recorded with the help of three uniaxial accelerometers placed along the depth of the pile cap. A tachometer is used to measure the operating frequency of the system. The recorded response in terms of acceleration time history

is converted to displacement. The dynamic response thus obtained is presented as frequency versus displacement amplitude as shown in Fig. 5.1.

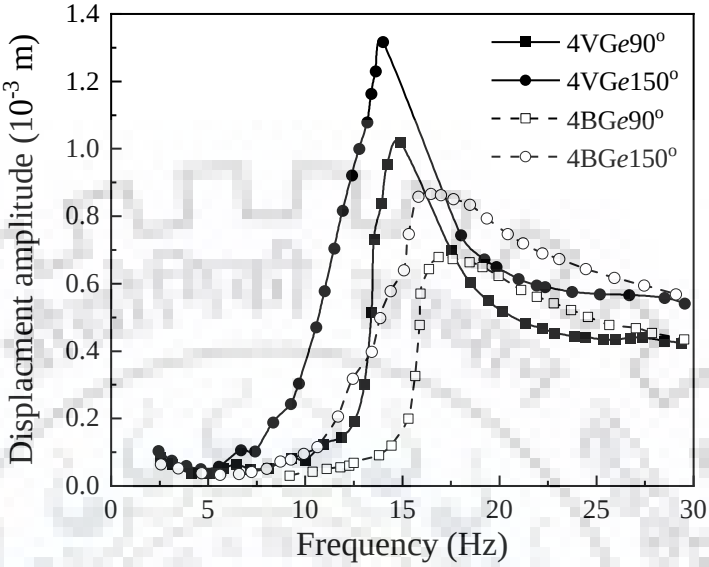

Fig. 5.1 Measurements of displacement response pile group

While conducting dynamic tests on pile groups especially at higher eccentricities (i.e. e = 90° onwards), the occupants of the DEQ building experienced annoying vibrations. Hence, to measure the induced vibrations in the building, four different tests have been conducted once again, on two different pile groups 4VG and 4BG nearer to the DEQ building which influenced the reported vibrations. A clear peak at resonant frequency was observed in all the four tests. It is clear from Fig. 5.1 that there is a significant difference in both resonant frequency and displacement amplitudes between two pile groups. At force level, e = 90° resonance occurred at 14.93 Hz in 4VG with a displacement amplitude of 1.02×10^{-3} m whereas in 4BG, the resonance occurred at 16.87 Hz with 0.68×10^{-3} m displacement. Whereas, at force level e = 150°, the resonance occurred at 14.02 Hz and 16.48 Hz with peak displacement amplitudes of 1.32×10^{-3} m and 0.86×10^{-3} m in pile groups 4VG and 4BG, respectively. From these test results, it is clear that 4BG provides a lower lateral displacement when compared to 4VG under horizontal dynamic (i.e. sinusoidal) loading. The maximum lateral displacement measured among the pile groups during the dynamic excitation is 1.32×10^{-3} m. However, the generated dynamic load on the pile head was adequate to induce vibrations causing inconvenience to the occupants of the adjacent building.

5.4.2 Measurements at Different Levels of the Building and Discussion

The occupants of the adjacent building experienced irritating vibrations, and crackling of window panes when the dynamic load tests on pile groups were in progress. In order to quantify these vibrations, the sensors were placed at various floor levels of the building to measure the induced vibrations in terms of acceleration and velocity time histories. From the recorded time histories, the vibration parameters i.e. peak ground acceleration (PGA), peak ground velocity (PGV), pseudo-spectral acceleration (PSA) and predominant frequencies (*f*) have been obtained. The plan dimensions of the considered building are represented in Fig. 5.2. The height of each floor in the building is 3.80 m. The distances between the pile groups, 4VG and 4BG from the nearest face of the building are 9.80 m and 15.20 m, respectively and their locations are illustrated in Fig. 5.3 (a). Two triaxial accelerometers (Kinemetrics EpiSensor FBA ES-T), A1 and A2 were placed on the ground level and on the roof of the building. Further, three uniaxial seismometers (Kinemetrics SS-1 Ranger Seismometer), S1, S2, and S3 were also placed on the 1st and 2nd floor levels and on the roof of the building as shown in Fig. 5.3 (b). These five sensors were connected to a multi-channel data acquisition (Kinemetrics Granite 12). The accelerometer, seismometer and the data acquisition system used in this study are shown in Fig. 5.4 (a-b).

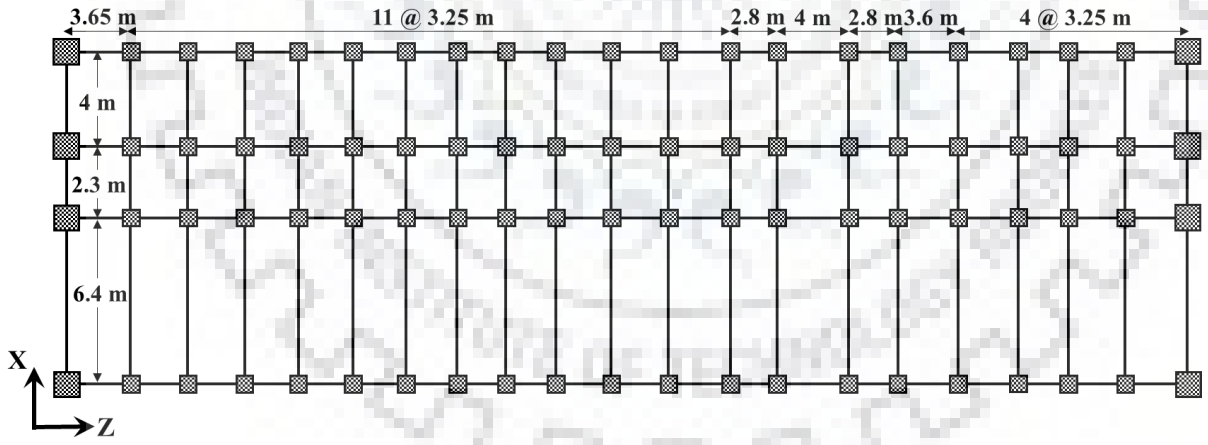

Fig. 5.2 Building dimensions in plan

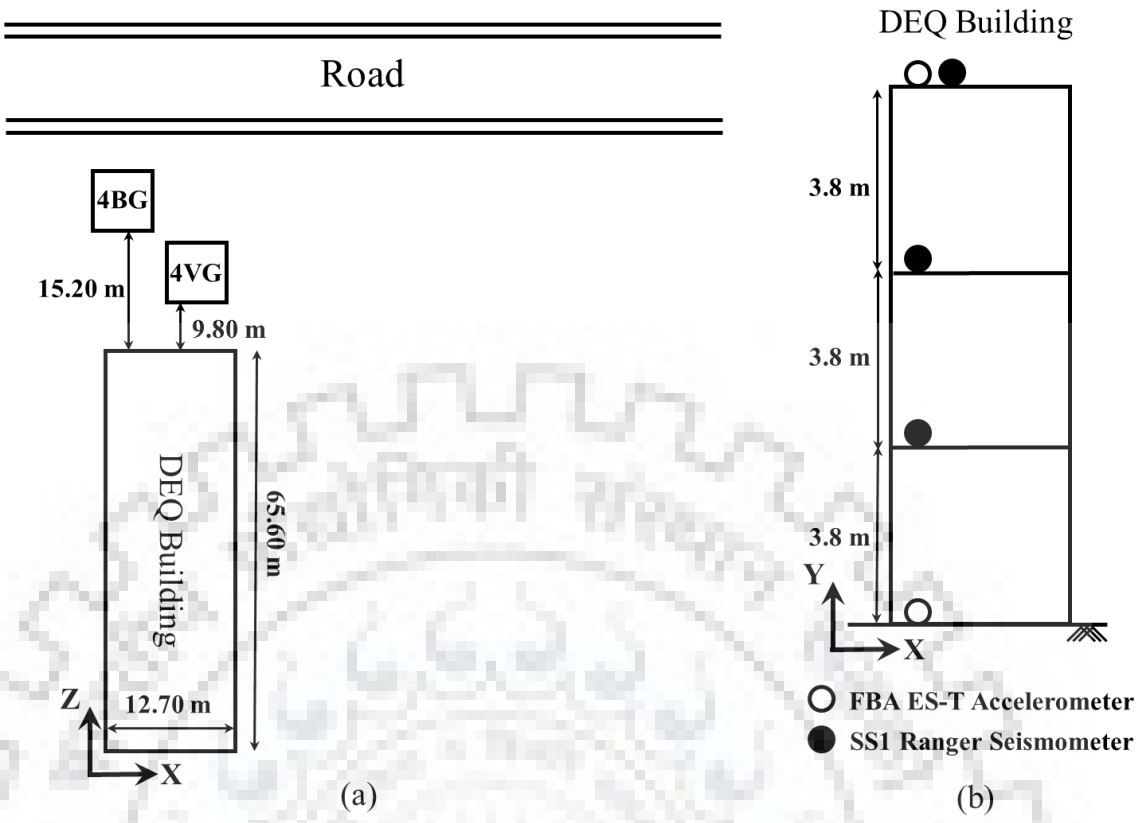

Fig. 5.3 Details of the DEQ building: (a) location; and (b) sensor arrangement

The total duration of dynamic tests on pile groups was between fifteen to twenty minutes approximately. Vibration record capturing the response of the building for a duration of twenty minutes at a stretch was not feasible. An attempt was made to obtain multiple records with each record consisting of five minutes duration, capturing the entire test. But, only eight vibration records of five minutes duration were obtained while conducting dynamic lateral vibration tests on both the pile groups (each excited at two different force levels). Among the eight records, first three records correspond to the excitation on 4VG at e = 90° whereas 4th and 5th records represent excitations on 4VG at e = 150°. When 4BG was excited at e = 90°, only one record (6th) was obtained. The last two records (7th and 8th) correspond to excitation of 4BG at e = 150°.

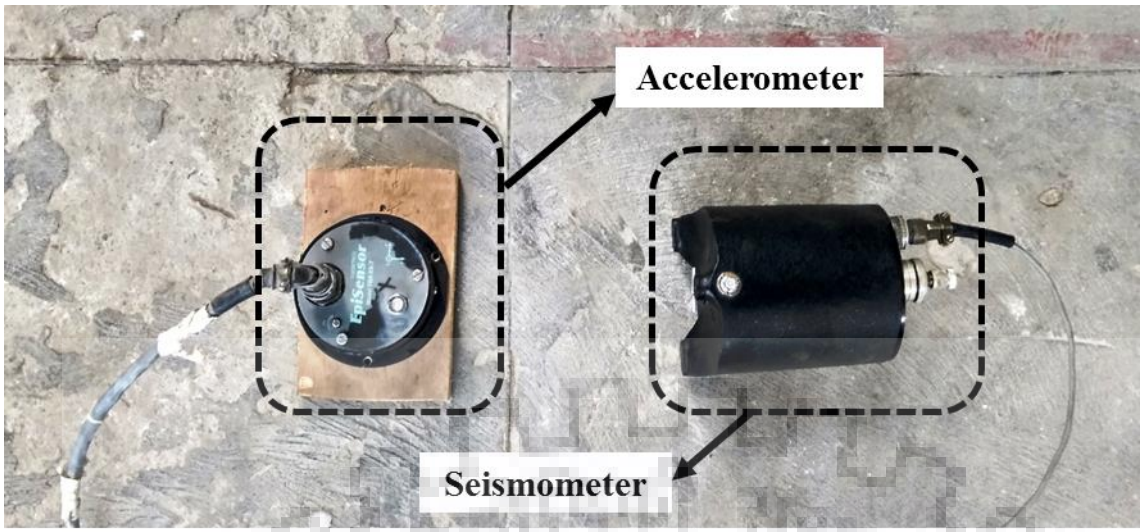

(a)

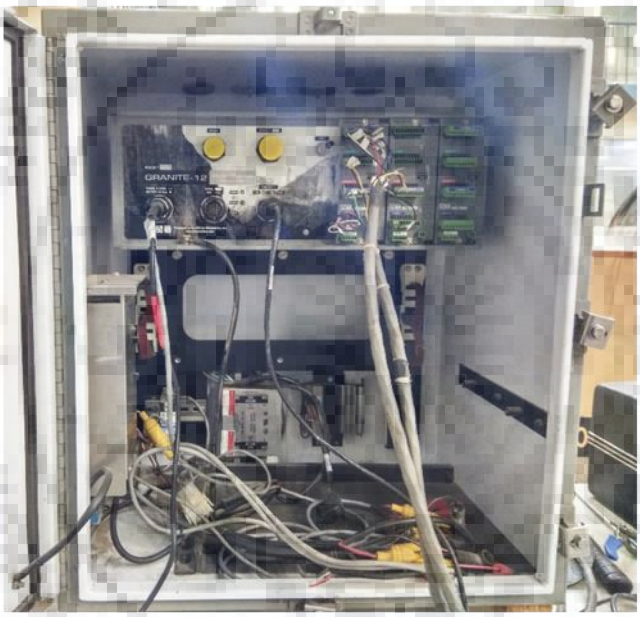

(b)

Fig. 5.4 Measurements on building: (a) sensors; and (b) multi-channel data acquisition system

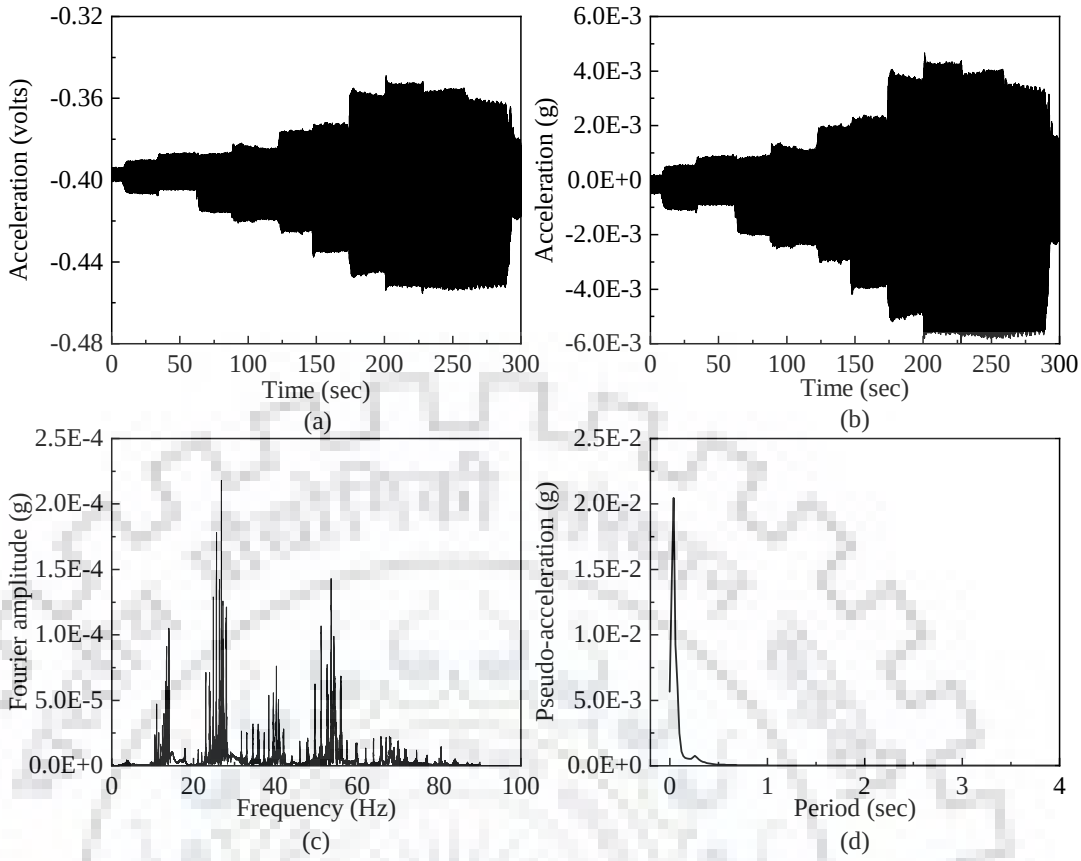

Fig. 5.5 Processing of typical vibration record: (a) acceleration time history (in volts); (b) acceleration time history (in 'g'); (c) Fourier spectrum; and (d) 5% damped elastic response spectrum

The vibrations recorded for a duration of five minutes at a sampling rate of 200 samples per second in the form of acceleration and velocity time histories have been processed to obtain the vibration parameters. A sample raw data thus obtained with the help of an accelerometer is shown in Fig. 5.5 (a). Both acceleration (using A1 and A2) and velocity (using S1, S2, and S3) time histories recorded in the terms of volts have been converted into 'g' and 'm/s' units, respectively using the sensitivity of the corresponding sensors. Linear baseline correction and Butterworth bandpass filter of the fourth order, for a frequency range of 0.07 Hz to 80 Hz, was applied to the raw data (Fig. 5.5 (a)) and has been plotted as shown in Fig. 5.5 (b). Thus, the processed records have been used to obtain the vibration parameters namely PGA, PSA, PGV, and *f*. Fast Fourier Transform (FFT) of a vibration record depicting the frequency content was also obtained as presented in Fig. 5.5 (c). Similarly, the elastic response spectrum (for 5% damping) has also been obtained and plotted as shown in Fig. 5.5 (d).

Figure 5.6 depicts the integrated building foundation system with 4BG representing vibration measurements obtained simultaneously on both 4BG and different floor levels of the adjacent building. From the vibration records, the PGA values in X, Y and Z directions are obtained and presented in Figs. 5.7 (a-c), respectively. The minimum permissible limit for acceleration is 2.0 cm/s^2 according to BIS (2000b), which is represented by a horizontal dotted line in Fig. 5.7. It can be observed from Figs. 5.7 (a-b) that the PGA values vary between 0.66 cm/s^2 to 6.73 cm/s^2 in X and Z directions whereas in Y direction, the variation extends to wider range between 5.95 cm/s^2 and 34.37 cm/s^2. The mode corresponding to the excitation force, site effect, damping of the building and soil material and impedance contrast might have resulted in much larger PGA in the Y direction.

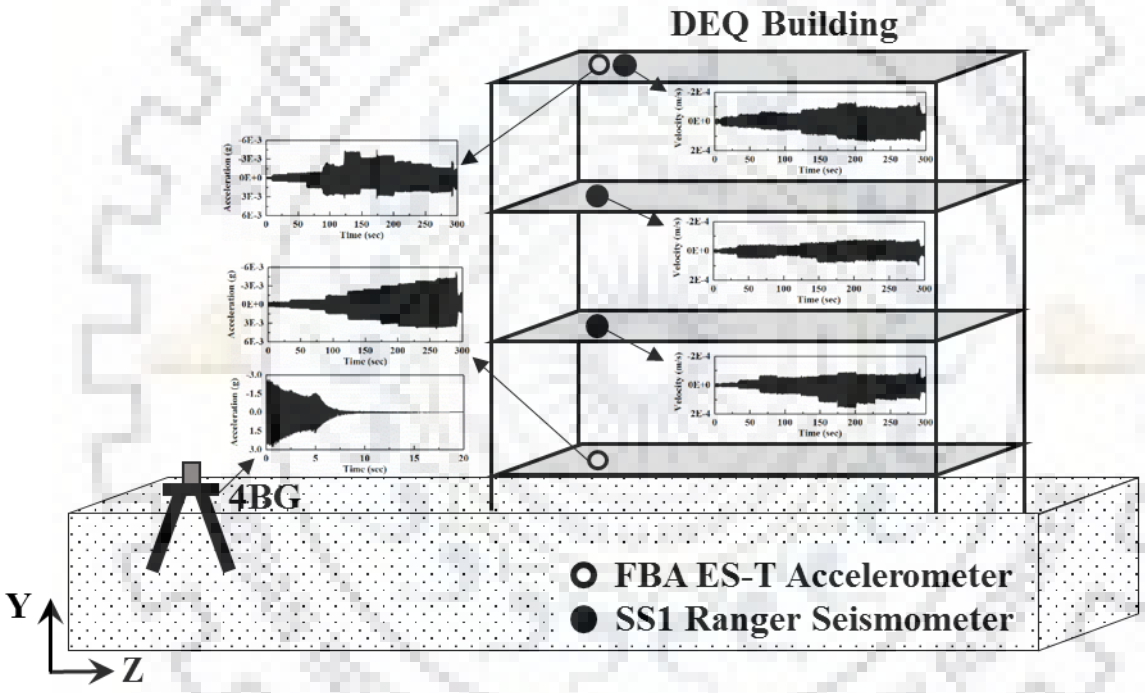

Fig. 5.6 2D integrated FE model with 4BG showing typical records

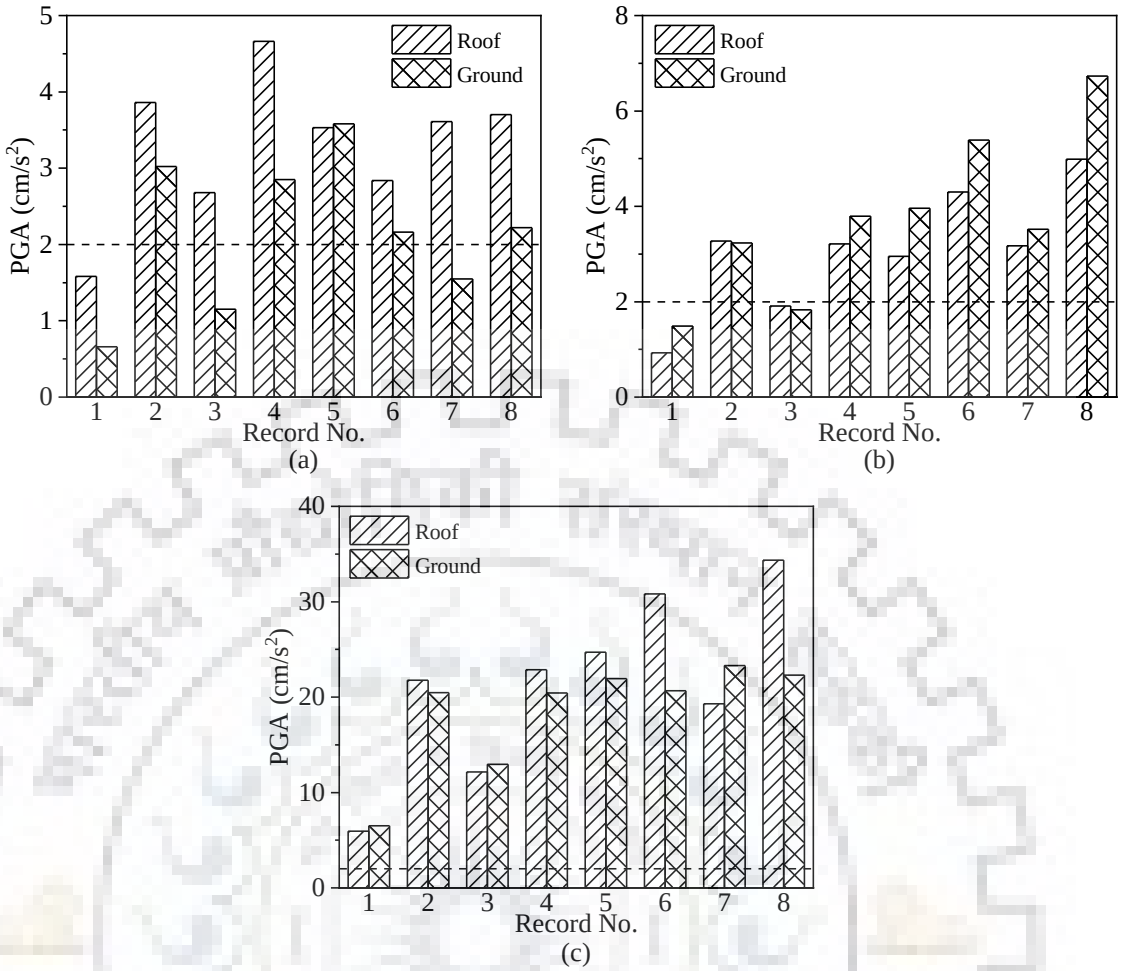

Fig. 5.7 PGA along: (a) X; (b) Z; and (c) Y directions from experimental observation

The variation in terms of PSA and *f* has been summarized in Tables 5.13 and 5.14, respectively. It can be observed from Table 5.13 that the minimum and maximum values of PSA in horizontal (X, Z) and vertical (Y) directions vary between 1.96 cm/s^2 to 47.09 cm/s^2 and 18.25 cm/s^2 to 94.47 cm/s^2, respectively. For a particular record, PSA in the horizontal direction is 2 to 10 times the PGA whereas the PSA in the Y direction has increased only from 2 to 5 times. Generally, for a ground motion record, the PSA is approximately 2.5 times the PGA whereas, in this case, PSA is much larger than PGA which might be due to the machine induced vibration source. Table 5.14 summarizes the variation in the predominant frequency from the acceleration and velocity measurements. The predominant frequency obtained from the acceleration time histories varies between 13.07 Hz to 53.67 Hz in horizontal directions whereas, in Y direction it varies in the range of 26.12 Hz and 53.67 Hz. This range is in agreement with the typical frequency range specified by BIS (2000b) for a structural response which is between 1 Hz to 300

Hz for ground-borne vibrations from machinery outside the building with either continuous or transient source.

Table 5.13 Summary of acceleration measurement in terms of PSA (g)

Record No.	Roof			Ground		
	X	Z	Y	X	Z	Y
1	0.0060	0.0047	0.0213	0.0020	0.0049	0.0186
2	0.0131	0.0136	0.0542	0.0062	0.0106	0.0429
3	0.0119	0.0141	0.0618	0.0058	0.0151	0.0542
4	0.0204	0.0287	0.0729	0.0057	0.0192	0.0743
5	0.0144	0.0192	0.0670	0.0081	0.0147	0.0588
6	0.0163	0.0444	0.0797	0.0046	0.0259	0.0865
7	0.0123	0.0166	0.0825	0.0038	0.0140	0.0706
8	0.0167	0.0480	0.0877	0.0055	0.0281	0.0963

Table 5.14 Summary of predominant frequencies, *f* (Hz)

Record No.	From Accelerometers						From Seismometers			
	Roof			Ground			Roof	2nd	1st	Ground
	X	Z	Y	X	Z	Y	X	X	X	X
1	26.12	26.12	26.12	13.07	39.16	26.12	3.84	3.84	13.07	13.07
2	28.58	26.40	30.09	30.08	28.58	30.08	14.30	28.58	14.30	30.08
3	53.67	26.82	53.67	22.25	25.99	47.85	23.93	51.99	22.25	22.25
4	26.83	24.85	26.83	26.83	26.83	26.83	26.83	26.83	13.42	26.83
5	29.56	47.59	29.55	29.56	29.55	29.56	29.56	29.55	22.40	29.56
6	27.88	24.62	29.54	29.54	24.62	29.54	24.62	27.88	27.88	29.54
7	30.75	15.87	30.75	14.41	31.73	30.75	14.41	15.06	14.41	14.41
8	29.11	24.49	29.11	29.11	24.49	29.11	25.98	29.11	27.51	29.11

As it is obvious from the plan/ top view dimension of the considered building that the building is stiffer in the Z direction, and the seismometers used for vibration measurements are uniaxial, thus, the velocity measurements were made only in the X direction. Due to limited availability of sensors, the velocity measurements were obtained only for the first floor, second

floor and roof of the building. From the acceleration measurements at the ground floor, the velocity time histories have been obtained and reported herein. The ground and roof of the building are represented as 0 and 3rd floor level, respectively. Figure 5.8 shows the variation in the peak ground velocity (PGV) along different levels of the building in the X direction. The minimum permissible value of PGV is 0.01 cm/s suggested by GB/T (2008), which is indicated by a horizontal dotted line in Fig. 5.8 (a). From the records obtained, a variation of PGV between 0.004 cm/s to 0.016 cm/s could be observed which is slightly higher than the minimum permissible value but well within the maximum permissible limit of 5 cm/s suggested by BIS (2000b). PGV values thus reported are also presented in terms of minimum (Min), maximum (Max) and average (Mean) in Fig. 5.8 (b). The predominant frequencies obtained from the velocity time histories are in the range of 3.84 Hz to 51.99 Hz as reported in Table 5.14.

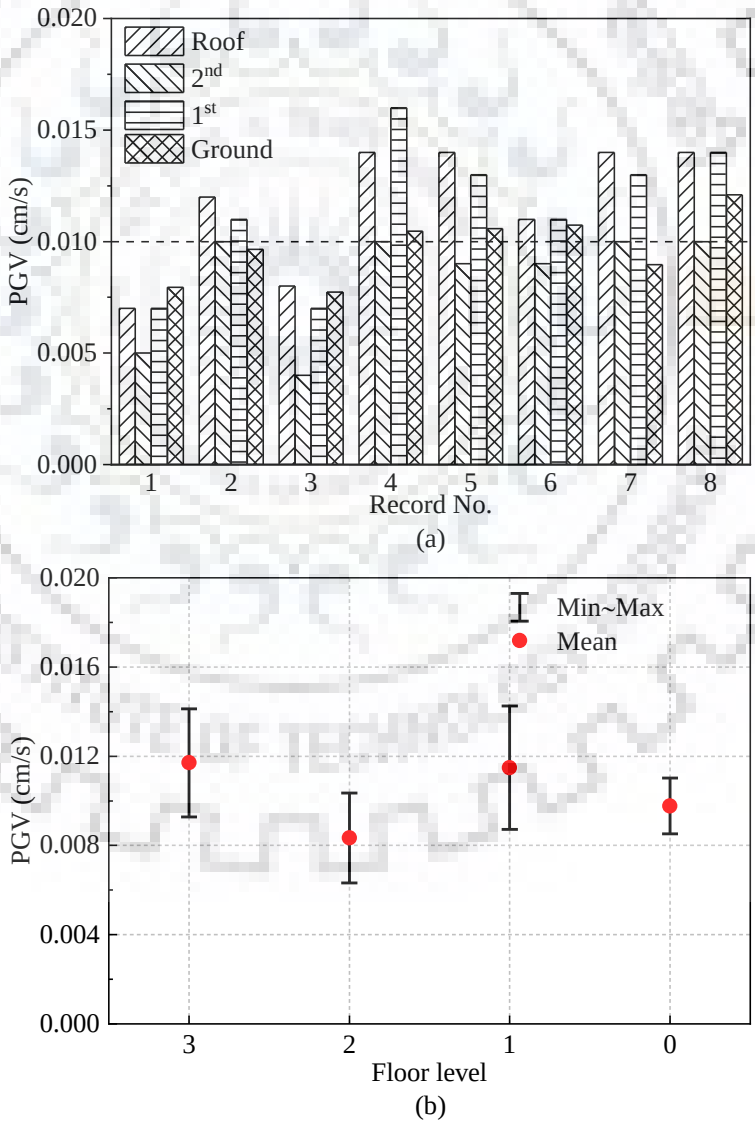

Fig. 5.8 PGV along floor level in X direction from experimental observation (a) variation; and (b) summary

5.5 INTEGRATED 2D FE MODELLING

In this study, a 2D FE integrated model of the building with foundation, pile group with pile cap and supporting soil mass has been developed in commercially available FE package (Abaqus/CAE 2016). The integrated 2D FE models with 4VG or 4BG (Figs. 5.9 (a-b)) has been analyzed for the combined effect of gravity and dynamic loading. A huge storage and computational effort are required to analyze an integrated 3D FE model of building foundation soil system. In order to obtain stability in the 3D integrated models, various computational parameters have to be carefully selected. Thus, integrated 3D FE models are generally developed for projects with high sensitivity (e.g. Nuclear power plants), and are still not feasible for day to day design or evaluation projects. The 3D numerical analyses predicted the vibration response much closer to actual measurements, but they consumed relatively large time and computational effort which in turn makes the 2D analysis an interesting choice (Hall 2003; Real et al. 2015).

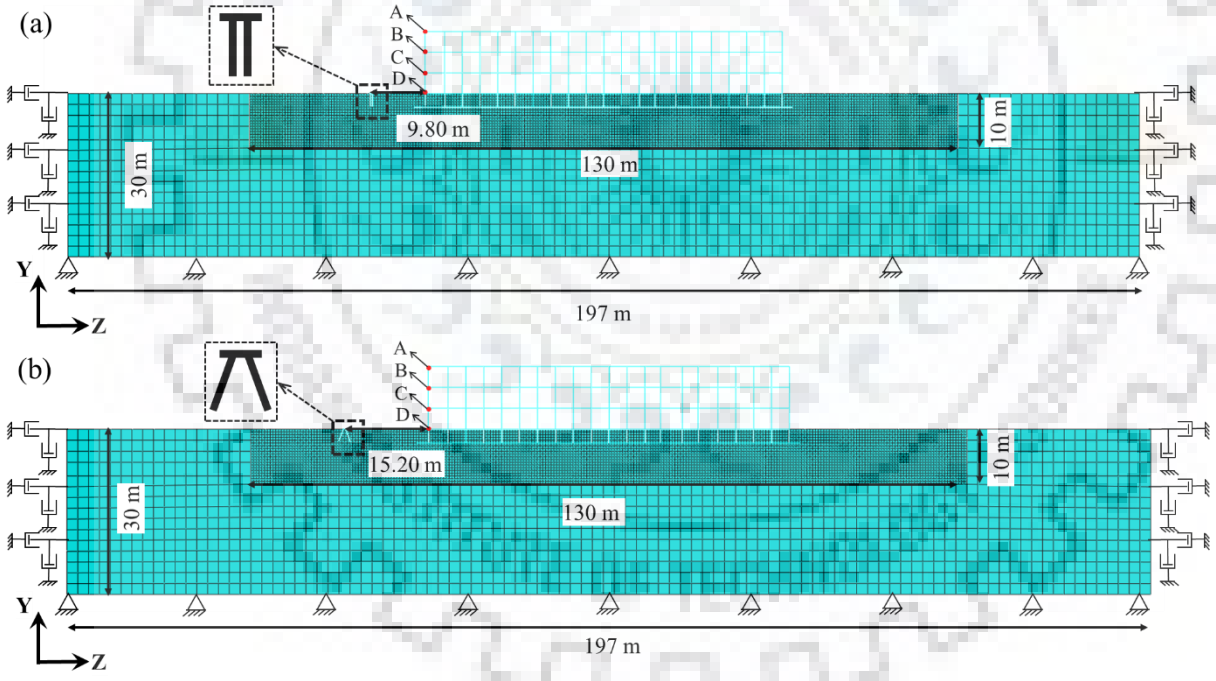

Fig. 5.9 2D integrated FE model with (a) 4VG; and (b) 4BG

5.5.1 General Assumptions

To develop an integrated 2D FE model, a raft foundation, with a uniform thickness of 1.0 m throughout placed at a depth of 2.50 m below the ground level is considered to support the

building. The dimension of the beam was considered to be 0.23 m × 0.40 m, all interior columns were of the size 0.40 m × 0.40 m and exterior columns are 1 m × 1 m (Fig. 5.1). The dimensions of pile group, plan dimensions of the building and its location from the pile groups have been kept similar to the existing condition. The soil mass was assumed to be homogenous within each horizontal layer.

5.5.2 Constitutive Model

Most commercial finite element packages have in-built basic constitutive laws with adequate properties to simulate the material behavior. The basic material model is the one which consists of an initial elastic part along with plastic part to monitor the failure of the material when it begins to yield. Combination of both these parts gives a complete constitutive model. In most of the cases, linear elastic constitutive model results in good prediction where the materials are subjected to very low strain (of order 10^{-3} %) (Ishihara 1996). The difference in results obtained using linear elastic and other complex constitutive models are insignificant prior to yielding of materials.

In this study, viscoelastic material behavior has been used in form of elastic modulus and viscous material damping for both soil and reinforced cement concrete. Properties of the M25 grade of concrete (γ_c = 25 kN/m^3; v_c = 0.20 and E_c = 25 GPa) has been assigned to the pile group, raft foundation and the building. The material properties of soil obtained from field tests for test site 2 have been used for FE model. Rayleigh damping, specified in terms of coefficients, α_{rd}, and β_{rd}, has been used in the present study. Rayleigh damping parameters have been estimated for soil and structural components using Eqs. 4.1 and 4.2 assuming the damping ratio of 2% and 5%, respectively. The ω_1 and ω_2 values for soil mass were estimated as 8.45 rad/s and 42.25 rad/s corresponding to the 1st mode and 2nd mode of vibration, respectively. Similarly, ω_1 and ω_2 values for the structural components are 5.97 rad/s and 17.20 rad/s, respectively (Fig. 5.10). Rayleigh damping parameters for the soil mass and structural components were estimated as α_{rd} = 0.2816, β_{rd} = 0.0008 and α_{rd} = 0.1773, β_{rd} = 0.0017, respectively. For the frequency range of interest, the estimated average damping ratio for soil mass and structural components are 1.67% and 4.59%, respectively which is in good agreement with the assumed values.

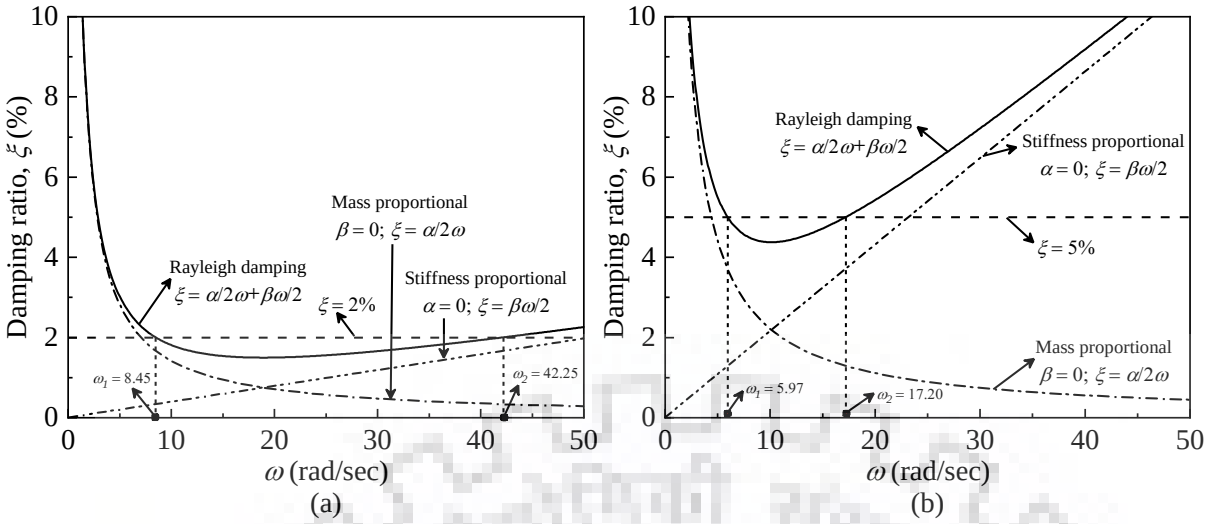

Fig. 5.10 Damping ratio curves for: (a) soil; and (b) structural components

5.5.3 Lateral Boundary Condition

Although the soil mass is an infinite media, for the FE simulation, the extent of the soil models has been considered through a sensitivity analysis so that the effect of boundary conditions is minimal on the domain of interest. All movements are restraint at the base (i.e. both Z and Y displacements are zero). However, in static case (i.e. under gravity loading), the left and right lateral boundaries have been restrained in horizontal direction (i.e. Z displacement is zero) and in case of dynamic analysis, restraint in horizontal direction has been replaced by the equivalent earth pressure required to keep the soil mass in equilibrium and in addition viscous boundary has also been assigned to absorb the reflected waves (Lysmer and Kuhlemeyer 1969).

5.5.4 Mesh Size and Element Type

For simulation of wave propagation problems, the maximum size of the element has been restricted to $1/8^{th}$ to $1/12^{th}$ of the wavelength of the propagating wave (Lysmer and Drake 1972; Kuhlemeyer and Lysmer 1973), whereas, the suggested element size was in the range of $1/10^{th}$ to $1/20^{th}$ of the wavelength of the propagating waves for large propagating distances (Semblat and Brioist 2000). In the present study, smaller mesh size of the order of $1/12^{th}$ of the desired wavelength (50 Hz) has been used for soil mass near the building base, whereas mesh size has been increased near the boundaries. Discretizing the soil mass into smaller and larger element sizes gave the advantage in predicting the vibration response with comparatively less computational efforts.

Soil mass has been modeled using 8-node biquadratic plane strain quadrilateral element with reduced integration (CPE8R). In FE modeling, piles are often modelled as linear elastic elements with either 2-node or 3-node beam elements. This method offers a major advantage in capturing the response of piles in terms of bending moment and shear forces just with 2 or 3 nodes but, the interaction between the pile and the soil mass and the effect of pile volume are not being taken into account (Zhang et al. 2017). 3-noded quadratic beam element in a plane (B22) has been used to model the beams, columns and raft foundation of the building and the pile group along with its cap. Rigid diaphragm action of floor slabs has been simulated at each floor level by assigning multipoint constraint (which restrict the relative movement of the beam-column joint at a particular floor level).

5.5.5 Time Step Increment

The dynamic implicit method has been used for time history analyses of the FE model. In implicit method, the solution is predicted at the current time step based on the result at an incremental time step prior to the current step. The time step, Δt should be $\leq \left(h/V_s\sqrt{6}\right)$ for a quadratic element based on Simpson's rule with lumped mass matrix formulation of mass matrix, where h is the element size and V_s is the shear wave velocity (Hughes 2000). However, the maximum time step can be obtained using Hilber-Hughes-Taylor operator given by $\Delta t \leq \overline{T}/10$ based on direct integration scheme, where $\overline{T}$ is the typical period of vibration (Abaqus/CAE 2016).

5.5.6 Foundation Soil Interface

Both pile and raft foundations have been kept embedded inside the soil mass, where the soil-foundation interaction has been considered by assigning embedded constraint between the foundation and the surrounding soil mass. In embedded constraint, the soil mass has been considered as surrounding host element, whereas the pile group and the raft foundation have been considered as an embedded element. In Abaqus software, the nodes of the embedded element are automatically constrained (to follow geometric relationship) to the nearest nodes of surrounding host element that contains embedded nodes. The embedded nodes are then constrained by the response of these host soil elements by the default geometric tolerance values ($\times 10^{-6}$ unit).

5.5.7 Loading

In the representative 2D FE model, the building loads have been applied as a concentrated point mass at the columns and mass per length (UDL) on the beams. Concentrated loads of magnitude 86 kN and 29 kN have been applied to the exterior column at each floor level and roof, respectively, whereas, concentrated loads of magnitude 171 kN and 56 kN have been applied to the interior column at each floor level and roof, respectively. The tributary loads from slabs have been applied as UDL of intensity 26 kN/m and 11 kN/m at each floor level and roof, respectively. The mass of the oscillator motor assembly mounted on the top of the pile cap, (≈ 367 kg) has been assigned to the node representing the center of gravity of the pile cap. At the same node, the dynamic lateral load generated during the experiment has been applied in the form of sweep load for two different force levels. Figures 5.11 (a) and (b) show the force-time history similar to the one generated by the oscillator motor assembly using Eq. (3.1), at e = 90º and 150º, respectively.

5.5.8 Response

The response of the 2D integrated FE model was obtained in terms of acceleration and velocity time histories at the points A, B, C, and D, as shown in Figs. 5.9 (a-b) for all considered cases and presented in form of PGA and PGV (Figs. 5.12 and 5.13). It can be observed from Figs. 5.12 (a-b) that, at a particular force level applied on 4VG and 4BG, PGA in both Z and Y directions at a particular floor level is always higher for 4VG. This may partially attribute to the fact that 4BG is at a relatively far distance from the building as compared to 4VG, apart from the variations in amplification/ de-amplification scenario. It can be observed that the PGA values vary from 1.89 cm/s^2 to 6.96 cm/s^2 in Z direction and from 0.32 cm/s^2 to 2.29 cm/s^2, in Y direction. It can be observed that in Z direction almost all the PGA values exceed the minimum permissible value of 2 cm/s^2 suggested by BIS (2000b).

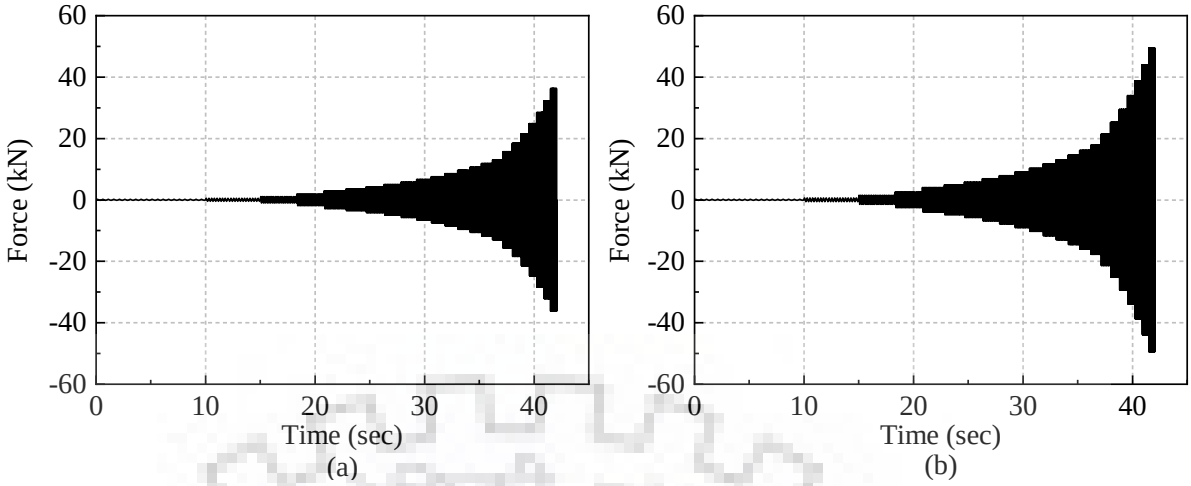

Fig. 5.11 Force time history at: (a) *e* = 90°; and (b) *e* =150°

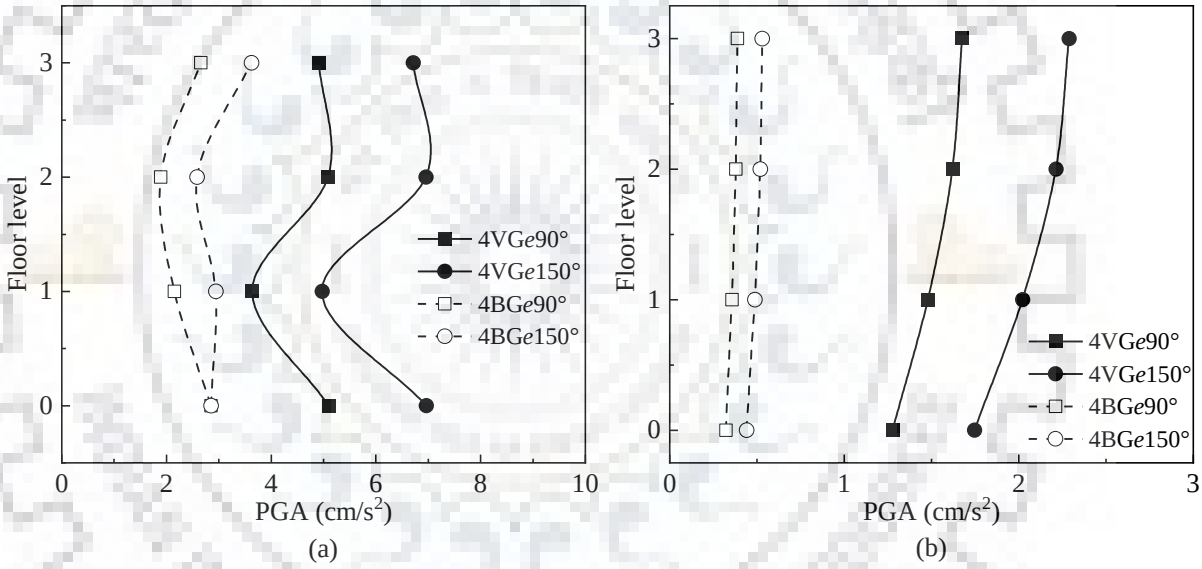

Fig. 5.12 PGA along floor level from 2D FE model in: (a) Z; and (b) Y direction

The results obtained in terms of PGA from experiments and 2D integrated FE model have been compared in terms of minimum, maximum and mean values Fig. 5.13 (a-c). It can be observed that the PGA values obtained by experiment and 2D integrated FE analysis are in good agreement, except in Y direction. This can be attributed to the fact that the site effect or impedance contrast is affecting the Y component significantly when compared with X or Z component. Except for a few cases, the average value is higher than the minimum permissible value of 2 cm/s^2 as per BIS (2000b).

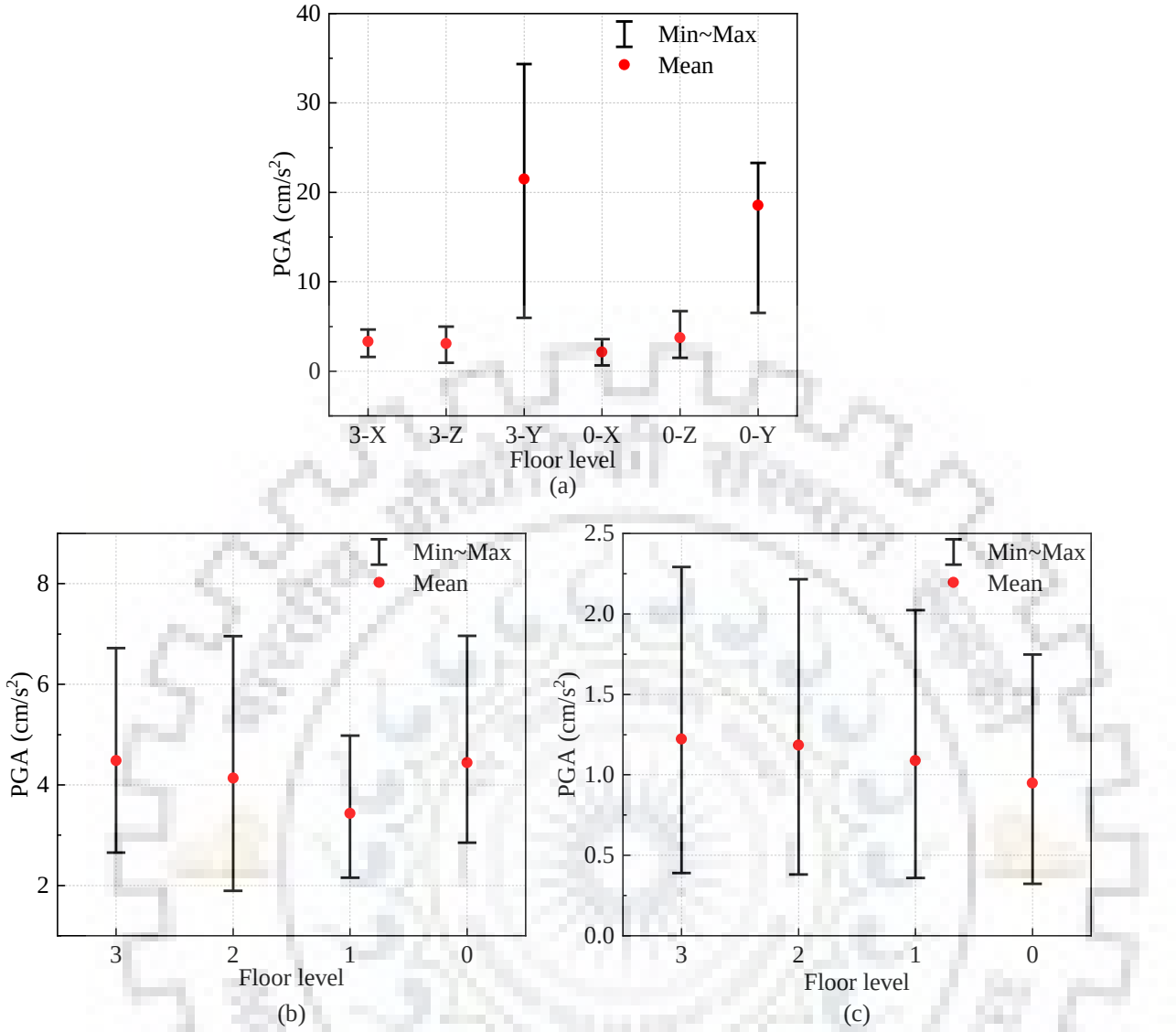

Fig. 5.13 Summary of PGA along floor level in: (a) all directions from experimental observations; (b) Z direction from 2D FE model; and (c) Y direction from 2D FE model

Figures 5.14 (a-b) show the variation in PGV values at different floor levels in Z and Y direction, respectively. In Z direction, the PGV values vary in the range of 0.016 cm/s to 0.046 cm/s, however, this variation is insignificant in the Y direction. All the observed PGV values are higher than the minimum permissible value of 0.01 cm/s suggested by GB/T (2008). It can also be observed from Figs. 5.12 and 5.14 that, with the increase in force level on a pile group, the response (both PGA and PGV) at particular floor level increased in all the cases. PGV from 2D integrated FE model is summarized in terms of Min, Max and Mean in Fig. 5.15. In all the cases the average PGV is higher than the minimum permissible value of 0.01 cm/s given by GB/T (2008).

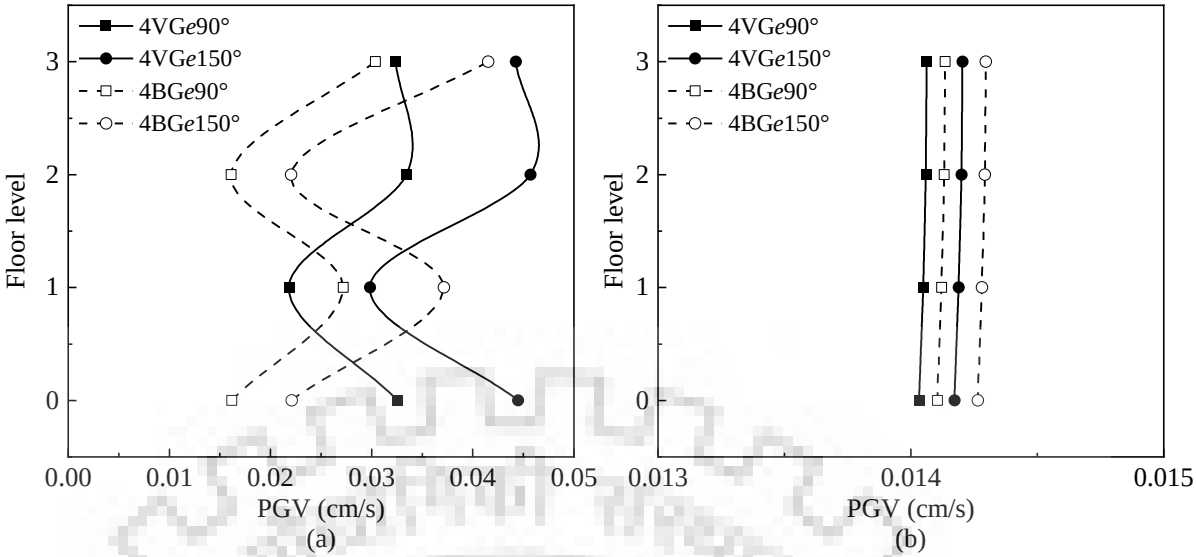

Fig. 5.14 PGV along floor level in: (a) Z; and (b) Y direction

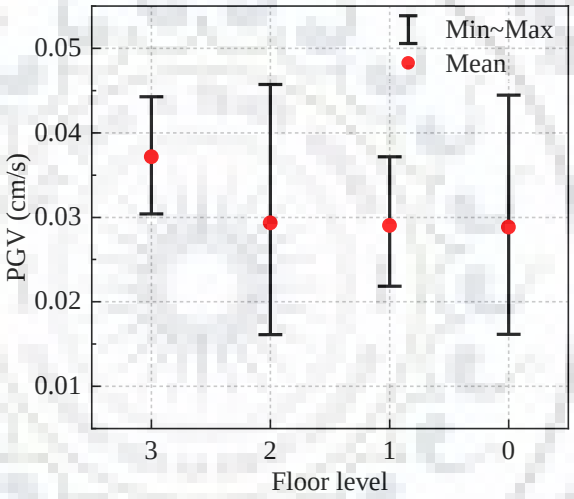

Fig. 5.15 Summary of PGV along floor level in Z direction from 2D FE model

5.5.9 Discussion

The present study estimates the response of a building subjected to vibrations induced from the adjacent site during horizontal dynamic load tests on pile groups. The vibrations were measured in terms of acceleration and velocity time histories both at the source (i.e. on the pile group) and at different floor levels of the building simultaneously. Apart from the experimental studies, the FE analyses also have been performed on 2D integrated FE model consisting of pile group and building foundation system along with the supporting soil mass. The response of the building at different floor level has been obtained for the simulated dynamic load (generated during the experiment) applied to pile group in the model.

The vibration parameters obtained from experiments and numerical simulations are reported in terms of PGA, PGV, PSA, and *f*. The intensity of vibration usually amplifies with the storey height of a multi-story building exposed to train induced vibrations (Xia et al. 2005; Xia et al. 2009) and vibrations generated from sheet pile driving (Athanasopoulos and Pelekis 2000). The fluctuating behaviour in the intensity of vibration along the floor level may be attributed to the fact that the building vibrates in higher modes (except fundamental mode) along Z direction. However, the amplification along floor level was found to satisfy the prescribed limits of ASCE (2014) where the maximum amplification of vibration at floor level is three times the ground level.

In the recent years, there has been a dramatic increase in the concern over the possible damage to the structures in the vicinity of pile driving. The observations of the present study, considering a vibration source similar to pile driving, might help to understand the importance of quantifying these vibrations in the nearby structures in order to adopt suitable techniques to minimize such vibrations further to avoid the inconvenience to its occupants and possible non-structural damage.

5.6 SUMMARY

The vibrations reported in terms of PGA in Y direction from experiments differ largely with the results obtained from 2D numerical simulation. The contribution of a higher mode of excitation, spatial site effect, damping of the building and soil materials and abrupt variation in impedance have resulted in much larger PGA values in the Y direction. These effects are not significant in the developed 2D FE model thus resulting in much less value of PGA in the Y direction. The PSA values were in the range of 2 to 10 times the PGA values of a record. This enormous increase in PSA is due to the frequency content of the vibration source which is sinusoidal in nature. The predominant frequencies of these vibrations are within the permissible limits (1 Hz to 80 Hz) specified in ISO (2003). It is interesting to note that there is no variation in PGV in Y direction, whereas the maximum values of PGV in Z direction is 2.3 times that of X direction. A 3D integrated FE analysis is expected to get a closer response as obtained from experiments. Moreover, the vibrations levels reported are higher than the minimum permissible limit but still within the maximum permissible limits specified in most of the cases. The experienced vibrations may not induce any major damage to the building but, they may have a huge impact on the occupants due to the annoying physical sensations in the human body and psychological fear of damage to the building and/ or its contents. If the building already had any pre-existing damage

due to various other reasons, it can also be exposed by these continuous vibrations. Quantifying these vibrations induced in the buildings will help the construction fraternity to suggest suitable remedial measures to minimize the vibrations, avoid discomfort to occupants and safeguard the structure from any possible major damage in future.

Chapter 6

CONCLUSIONS AND SCOPE FOR FUTURE WORK

6.1 CONCLUSIONS

The most important objective of this thesis was to understand the behaviour of cast in-situ RC batter piles subjected to dynamic loads. Initially, the dynamic behaviour of single piles and pile groups has been explored through field tests. In continuation, 3D FE analysis has been performed corresponding to the set of experimental configuration of single piles and pile groups were developed. Finally, the dynamic pile load test induced vibration in an adjacent building was also measured experimentally and numerically by developing 2D FE models. The major conclusions drawn from the present study are described below.

6.1.1 Dynamic Behaviour of Single Piles: Experimental Observations

Experimental investigations have been carried out to understand the dynamic behaviour of single vertical and batter piles with and without under-ream subjected to lateral and vertical vibrations. The major conclusions based on the experimental study are as follows:

i. Resonant frequency of the soil-pile system decreases with an increase in the force level in both lateral (X and Z) and vertical (Y) directions. With the increase in force level, the degradation in stiffness of soil mass also increases. Thus, at the particular force level, when the mass participation increases, the resonant frequency of the system automatically decreases.

ii. The highest resonant frequency was observed for 20° batter pile (B20), regardless of the force level and direction of excitation, and this signifies the importance of batter pile subjected to dynamic lateral load over the vertical pile. The peak displacement and shear/ axial strain increase linearly with the increase in the force level.

iii. The decrease in peak lateral displacement amplitude is higher in case of B10U1 than in B20U1 in X direction, whereas the decrease in the peak lateral displacement is higher in B20U1 than in B10U1 in Z direction.

iv. The rotational stiffness of the system decreases and the damping ratio increases nonlinearly with an increase in shear strain. This, on the other hand, means that with increasing force level, rotational stiffness decreases and damping ratio increases nonlinearly.

v. The variation of rotational stiffness and damping ratio of all the soil-pile system along with the force level excited both in X and Z directions does not seem to have a significant role in determining the lateral behaviour of combined batter and under-reamed pile. This may be attributed to the soil mass participation above and below the under-reamed bulb and the pressure distribution on both the lateral sides of the piles along the direction of loading.

vi. The direction of loading (X or Z) has a significant influence on the dynamic performance of single piles. This may be attributed to the soil mass participation, stiffness degradation and the pressure distribution on the two directions of loading in the horizontal plane.

6.1.2 Dynamic Behaviour of Pile Groups: Experimental Observations

The dynamic lateral and vertical behaviour of vertical and batter pile groups are also examined through field tests. Based on the results obtained and discussion presented, the following general conclusions can be made:

i. The resonant frequency decreases and the peak displacement increases with the increase in the exciting force level in all the excitation directions.

ii. With the increase in force level, there is a significant reduction in resonant frequency in all directions. In the lateral direction, with the increase in force level maximum reduction in peak displacement of about 38% (for 3BG) was observed, whereas in vertical direction maximum reduction was about 30% (for 4VG).

iii. The peak displacement of batter pile groups was always lower than the vertical pile groups. In lateral and vertical directions, a maximum reductions of 54% for 4BG and 40% for 3BG in peak displacement were observed when compared to their respective vertical pile group.

iv. A minimum reduction of 56% in peak displacement was observed in the pile groups when compared to a single pile.

v. In comparison to single piles, the reduction in peak displacement was higher by 8 to 14% in the batter pile groups compared to the vertical pile groups.

6.1.3 Dynamic Behaviour of Single Piles and Pile Groups: 3D Finite Element Simulations

A numerical study has been performed to understand the dynamic behaviour of single piles and pile groups considered in the experimental investigation through 3D FE models. The dynamic behaviour of the developed models have been compared with their corresponding experimental results. The major findings of this numerical study are summarized below:

i. The response obtained from 3D FE models for both single vertical and batter piles and pile groups are in good agreement with the corresponding experimental results obtained through field tests.
ii. The dynamic response of pile is highly influenced by the material model used in FEA Linear and Non-linear (Mohr-Coulomb yield criterion).
iii. In linear case, as the E_p/E_s ratio decreases the displacement response of the piles increases.
iv. The batter piles attract more bending moment when compared to vertical piles at all force levels as much as three times in X direction.

6.1.4 Dynamic Pile Load Test Induced Vibration in Adjacent Buildings

The vibrations generated from the dynamic load tests propagated through the soil mass and induced vibrations in an adjacent building. The vibrations thus induced in the adjacent building were measured experimentally and a 2D FE model was also developed to simulate the coupled building pile group soil system. The key findings of this study are as follows:

i. The vibrations reported in terms of PGA in Y direction from experiments differ largely with the results obtained from numerical simulations. The contribution of a higher mode of excitation, spatial site effect, damping of the building and soil materials and abrupt variation in impedance have resulted in much larger PGA values in the Y direction. These effects are not significant in the developed 2D FE model thus resulting in much less value of PGA in the Y direction.
ii. The PSA values were in the range of 2 to 10 times the PGA values of a record. This enormous increase in PSA is due to the frequency content of the vibration source. The predominant frequencies of these vibrations are within the permissible limits (1 Hz to 80 Hz) specified in ISO (2003). There is no variation in PGV in Y direction, whereas the maximum values of PGV in Z direction is 2.3 times that of X direction.

iii. The vibrations levels measured are within the permissible limits specified in most of the cases. The induced vibrations may not cause any major damage to the building but, they may have a huge impact on the occupants due to the annoying physical sensations in the human body and psychological fear of damage to the building and/ or its contents. If the building already had any pre-existing damage due to various other reasons, it can also be exposed by these continuous vibrations.

iv. Quantifying these vibrations induced in the buildings will help the construction fraternity to suggest suitable remedial measures to minimize the vibrations, avoid discomfort to occupants and safeguard the structure from any possible major damage in future.

6.2 RECOMMENDATIONS FOR FUTURE WORK

The research work presented in this thesis has certain limitations which should be addressed through additional research in the following areas:

i. The present study has been conducted in dry field conditions both experimentally and numerically. Additional numerical simulations considering the effect of moisture content of soil is recommended.

ii. The present study adapts soil material model based on Mohr-Coulomb yield criteria and concrete model based on linear elastic behaviour. Further, advanced nonlinear material models might be used for both soil and concrete to enhance the observed results.

iii. The present numerical study has been conducted only for lateral excitation. An extension of 3D simulations for vertical excitation is recommended.

iv. Parametric study considering other feasible batter angles, varying length and diameter of pile, varying spacing between piles in a group, varying soil and pile material should also be explored for better understanding.

v. Pile groups used in the field are subjected to huge vertical load from superstructure. The effect of varying vertical load intensity on dynamic behaviour of batter pile groups can also be explored.

vi. Future research should aim at understanding the seismic behaviour of batter pile groups supporting structures like offshore platform, wharfs, communication and transmission line towers etc.

vii. Batter piles are often used in offshore environment where they also experience impact from ships. Further studies are recommended for batter piles subjected to impact loads.

REFERENCES

1. AASHTO (2014). "LRFD bridge design specifications." American Association of State Highway and Transportation Officials, Washington, D.C.
2. Abaqus/CAE (2016). "ABAQUS documentation." *Dassault Systèmes*, Providence, RI, USA.
3. Abu-Farsakh, M. Y., Yu, X., Pathak, B., Alshibli, K., and Zhang, Z. (2011). "Field testing and analyses of a batter pile group foundation under lateral loading." *Transportation Research Record*, 2212(1), 42-55.
4. Adhikari, S., and Bhattacharya, S. (2008). "Dynamic instability of pile-supported structures in liquefiable soils during earthquakes." *Shock and Vibration*, 15(6), 665-685.
5. AFPS (1990). *Association française du génie parasismique, Presses des Ponts et Chaussees [French Association for Earthquake Engineering, Presses of Bridges and Engineering]*.
6. Ai, Z. Y., Liu, C. L., Wang, L. J., and Wang, L. H. (2016). "Vertical vibration of a partially embedded pile group in transversely isotropic soils." *Computers and Geotechnics*, 80, 107-114.
7. Alielahi, H., Mardani, Z., and Daneshvar, S. (2014). "Influence of under-reamed pile groups arrangement on tensile bearing capacity using FE method." *Electronic Journal of Geotechnical Engineering*, 19, 1395-1410.
8. Allotey, N., and El Naggar, M. H. (2008). "A numerical study into lateral cyclic nonlinear soil–pile response." *Canadian Geotechnical Journal*, 45(9), 1268-1281.
9. API (2000). *Recommended Practice for Planning, Designing and Constructing Fixed Offshore Platforms - Working Stress Design*. American Petroleum Institute. NW, Washington, D.C.
10. ASCE (2014). *Seismic evaluation and retrofit of existing buildings*. SEI 41-13. American Society of Civil Engineers. Reston, Virginia.
11. ATC (1996). *Seismic evaluation and retrofit of concrete buildings*. ATC 40. Applied Technology Council. Redwood City, California, United States.
12. Athanasopoulos, G. A., and Pelekis, P. C. (2000). "Ground vibrations from sheet pile driving in urban environment: measurements, analysis and effects on buildings and occupants." *Soil Dynamics and Earthquake Engineering*, 19(5), 371-387.

13. Ayothiraman, R., and Boominathan, A. (2013). "Depth of fixity of piles in clay under dynamic lateral load." *Geotechnical and Geological Engineering*, 31(2), 447-461.
14. Banerjee, S. (2009). "Centrifuge and numerical modelling of soft clay-pile-raft foundations subjected to seismic shaking." Doctoral dissertation, National University of Singapore, Singapore.
15. Banerjee, S., Goh, S. H., and Lee, F. H. (2014). "Earthquake-induced bending moment in fixed-head piles in soft clay." *Géotechnique*, 64(6), 431-446.
16. Banerjee, S., Joy, M., and Sarkar, D. (2016). "Parametric study and centrifuge-test verification for amplification and bending moment of clay–pile system subject to earthquakes." *Geotechnical and Geological Engineering*, 34(6), 1899-1908.
17. Banerjee, S., and Lee, F. H. (2013). "Centrifuge shaking table tests on a single pile embedded in clay subjected to earthquake excitation." *International Journal of Geotechnical Engineering*, 7(2), 117-123.
18. Banerjee, S., and Shirole, O. N. (2014). "Numerical analysis of piles under cyclic lateral load." *Indian Geotechnical Journal*, 44(4), 436-448.
19. Basack, S., and Nimbalkar, S. (2017). "Numerical solution of single pile subjected to torsional cyclic load." *International Journal of Geomechanics*, 17(8).
20. Basack, S., and Nimbalkar, S. (2018). "Measured and predicted response of pile groups in soft clay subjected to cyclic lateral loading." *International Journal of Geomechanics*, 18(7).
21. Berrill, J. B., Christensen, S. A., Keenan, R. P., Okada, W., and Pettinga, J. R. (1997). "Lateral spreading loads on a piled bridge foundation." *International Conference on Soil Mechanics and Geotechnical Engineering, Seismic Behavior of Ground and Geotechnical Structures*, Balkema Publisher, Rotterdam, Netherlands, 173-183.
22. Bertero, R. D., Lehmann, A., Mussat, J., and Vaquero, S. (2013). "Vibrations in neighborhood buildings due to rock concerts in stadiums." *Journal of Structural Engineering*, 139(11), 1981-1991.
23. Bhardwaj, S., and Singh, S. K. (2015). "Ultimate capacity of battered micropiles under oblique pullout loads." *International Journal of Geotechnical Engineering*, 9(2), 190-200.
24. Bhattacharya, S., Orense, R. P., and Lombardi, D. (2019). *Seismic design of foundations*, ICE Publishing, Westminster, London.

25. Bhattacharya, S., Tazoh, T., Jang, J., and Sato, M. (2009). "A study on the behavior of raked piles in seismically liquefiable soils." *Proc., 3rd Greece–Japan Workshop: Seismic Design, Observation, and Retrofit of Foundations*, Santorini, Greece.
26. Bhowmik, D., Baidya, D. K., and Dasgupta, S. P. (2013). "A numerical and experimental study of hollow steel pile in layered soil subjected to lateral dynamic loading." *Soil Dynamics and Earthquake Engineering*, 53, 119-129.
27. Bian, X., Jiang, H., Chang, C., Hu, J., and Chen, Y. (2015). "Track and ground vibrations generated by high-speed train running on ballastless railway with excitation of vertical track irregularities." *Soil Dynamics and Earthquake Engineering*, 76, 29-43.
28. Bindi, D., Petrovic, B., Karapetrou, S., Manakou, M., Boxberger, T., Raptakis, D., Pitilakis, K. D., and Parolai, S. (2015). "Seismic response of an 8-story RC-building from ambient vibration analysis." *Bulletin of Earthquake Engineering*, 13(7), 2095-2120.
29. BIS (1970). *Classification and identification of soils for general engineering purposes*. IS 1498. Bureau of Indian Standards. New Delhi, India.
30. BIS (1973). *Methods of test for soils: Determination of water content*. IS 2720 (Part 2). Bureau of Indian Standards. New Delhi, India.
31. BIS (1981a). *Code of practice for determination of bearing capacity of shallow foundations*. IS 6403. Bureau of Indian Standards. New Delhi, India.
32. BIS (1981b). *Guide for lateral dynamic load test on piles*. IS 9716. Bureau of Indian Standards. New Delhi, India.
33. BIS (1985a). *Methods of test for soils: Grain size analysis*. IS 2720 (Part 4). Bureau of Indian Standards. New Delhi, India.
34. BIS (1985b). *Methods of test for soils: Determination of liquid and plastic limit*. IS 2720 (Part 5). Bureau of Indian Standards. New Delhi, India.
35. BIS (1992). *Mechanical vibration and shock - evaluation of human exposure to whole body vibration - Part 2: Vibration in buildings (1 Hz to 80 Hz)*. IS 13276 (Part 2). Bureau of Indian Standards. New Delhi, India.
36. BIS (2000a). *Mechanical vibration and shock - evaluation of human exposure to whole body vibration - Part 1: General requirements*. IS 13276 (Part 1). Bureau of Indian Standards. New Delhi, India.
37. BIS (2000b). *Mechanical vibration and shock - Vibration of buildings - Guidelines for the measurement of vibrations and evaluation of their effects on buildings*. IS 14884. Bureau of Indian Standards. New Delhi, India.

38. BIS (2010). *Design and construction of pile foundations, Cocrete piles, Bored cast in-situ concrete piles*. IS 2911 (Part1/Sec2). Bureau of Indian Standards. New Delhi, India.
39. Boominathan, A., and Ayothiraman, R. (2005). "Dynamic behaviour of laterally loaded model piles in clay." *Proceedings of the Institution of Civil Engineers - Geotechnical Engineering*, 158(4), 207-215.
40. Boominathan, A., and Ayothiraman, R. (2006a). "Dynamic response of laterally loaded piles in clay." *Proceedings of the Institution of Civil Engineers - Geotechnical Engineering*, 159(3), 233-241.
41. Boominathan, A., and Ayothiraman, R. (2006b). "An experimental study on static and dynamic bending behaviour of piles in soft clay." *Geotechnical and Geological Engineering*, 25(2), 177-189.
42. Boominathan, A., and Ayothiraman, R. (2007). "Measurement and analysis of horizontal vibration response of pile foundations." *Shock and Vibration*, 14(2), 89-106.
43. Boominathan, A., Krishna Kumar, S., and Subramanian, R. (2015). "Lateral dynamic response and effect of weakzone on the stiffness of full scale single piles." *Indian Geotechnical Journal*, 45(1), 43-50.
44. BSI (1993). *Evaluation and measurement for vibration in buildings. Part 2: Guide to damage levels from ground borne vibration*. BS 7385-2. British Standards Institution. London, United Kingdom.
45. BSI (2014). *Code of practice for noise and vibration control on construction and open sites - Part 2: Vibration*. BS 5228-2. British Standards Institution. London, United Kingdom.
46. Burr, J. P., Pender, M. J., and Larkin, T. J. (1997). "Dynamic response of laterally excited pile groups." *Journal of Geotechnical and Geoenvironmental Engineering*, 123(1), 1-8.
47. Cairo, R., Conte, E., and Dente, G. (2005). "Interaction factors for the analysis of pile groups in layered soils." *Journal of Geotechnical and Geoenvironmental Engineering*, 131(4), 525-528.
48. Carbonari, S., Morici, M., Dezi, F., Gara, F., and Leoni, G. (2017). "Soil-structure interaction effects in single bridge piers founded on inclined pile groups." *Soil Dynamics and Earthquake Engineering*, 92, 52-67.
49. Chandrasekaran, S. S., Boominathan, A., and Dodagoudar, G. R. (2013). "Dynamic response of laterally loaded pile groups in clay." *Journal of Earthquake Engineering*, 17(1), 33-53.

50. Chatterjee, K., and Choudhury, D. (2016). "Analytical and numerical approaches to compute the influence of vertical load on lateral response of single pile." *Japanese Geotechnical Society Special Publication*, 2(36), 1319-1322.

51. Chatterjee, K., Choudhury, D., and Poulos, H. G. (2015a). "Seismic analysis of laterally loaded pile under influence of vertical loading using finite element method." *Computers and Geotechnics*, 67, 172-186.

52. Chatterjee, K., Choudhury, D., Rao, V. D., and Mukherjee, S. P. (2015b). "Dynamic analyses and field observations on piles in Kolkata city." *Geomechanics and Engineering, An Int'l Journal*, 8(3), 415-440.

53. Cheng, M. H., Kohler, M. D., and Heaton, T. H. (2014). "Prediction of wave propagation in buildings using data from a single seismometer." *Bulletin of the Seismological Society of America*, 105(1), 107-119.

54. Crispino, M., and D'Apuzzo, M. (2001). "Measurement and prediction of traffic-induced vibrations in a heritage building." *Journal of Sound and Vibration*, 246(2), 319-335.

55. Degrande, G., Schevenels, M., Chatterjee, P., Van de Velde, W., Hölscher, P., Hopman, V., Wang, A., and Dadkah, N. (2006). "Vibrations due to a test train at variable speeds in a deep bored tunnel embedded in London clay." *Journal of Sound and Vibration*, 293(3), 626-644.

56. Deng, N., Kulesza, R., and Ostadan, F. (2007). "Seismic soil-pile group interaction analysis of a battered pile group." *Proc., 4th International Conference on Earthquake Geotechnical Engineering*, Thessaloniki, Greece.

57. Dezi, F., Carbonari, S., and Morici, M. (2016). "A numerical model for the dynamic analysis of inclined pile groups." *Earthquake Engineering and Structural Dynamics*, 45(1), 45-68.

58. Dickin, E. A., and Leung, C. F. (1990). "Performance of piles with enlarged bases subject to uplift forces." *Canadian Geotechnical Journal*, 27(5), 546-556.

59. Dickin, E. A., and Leung, C. F. (1992). "The influence of foundation geometry on the uplift behaviour of piles with enlarged bases." *Canadian Geotechnical Journal*, 29(3), 498-505.

60. DIN (1999). *Vibrations in buildings - Part 3: Effects on structure*. DIN 4150-3. German Institute for Standardisation (Deutsches Institut für Normung). Berlin.

61. EC8 (2003). *Eurocode 8: Design provisions for earthquake resistance of structures, Part 5. Foundations, retaining structures, and geotechnical aspects*. British Standards Institution. London.

62. Ekanayake, S. D., Liyanapathirana, D. S., and Leo, C. J. (2013). "Influence zone around a closed-ended pile during vibratory driving." *Soil Dynamics and Earthquake Engineering*, 53, 26-36.
63. El Kacimi, A., Woodward, P. K., Laghrouche, O., and Medero, G. (2013). "Time domain 3D finite element modelling of train-induced vibration at high speed." *Computers & Structures*, 118 (Supplement C), 66-73.
64. El Sharnouby, B., and Novak, M. (1984). "Dynamic experiments with group of piles." *Journal of Geotechnical and Geoenvironmental Engineering*, 110(6), 719-737.
65. El-Marsafawi, H., Han, Y. C., and Novak, M. (1992). "Dynamic experiments on two pile groups." *Journal of Geotechnical Engineering*, 118(4), 576-592.
66. Emani, P. K., and Maheshwari, B. K. (2009). "Dynamic impedances of pile groups with embedded caps in homogeneous elastic soils using CIFECM." *Soil Dynamics and Earthquake Engineering*, 29(6), 963-973.
67. EQ: 2017-16 (2017). "Delhi metro induced vibration measurement on various buildings." Department of Earthquake Engineering, Indian Institute of Technology Roorkee, Roorkee, India.
68. Escoffier, S. (2012). "Experimental study of the effect of inclined pile on the seismic behavior of pile group." *Soil Dynamics and Earthquake Engineering*, 42, 275-291.
69. Escoffier, S., Chazelas, J.-L., and Garnier, J. (2008). "Centrifuge modelling of raked piles." *Bulletin of Earthquake Engineering*, 6(4), 689-704.
70. ETABS. 2018. V16.2.1, Computers and Structures Inc., Berkeley.
71. Farokhi, A. S., Alielahi, H., and Mardani, Z. (2014). "Optimizing the performance of underreamed piles in clay using numerical method." *Electronic Journal of Geotechnical Engineering*, 19, 1507-1520.
72. Fatahi, B., Basack, S., Ryan, P., Zhou, W.-H., and Khabbaz, H. (2014). "Performance of laterally loaded piles considering soil and interface parameters." *Geomechanics and Engineering, An Int'l Journal*, 7(5), 495-524.
73. Fattah, M. Y., Zbar, B. S., and Mustafa, F. S. (2017). "Vertical vibration capacity of a single pile in dry sand." *Marine Georesources & Geotechnology*, 35(8), 1-10.
74. Feagin, L. B. (1937). "Lateral pile loading tests." *Transaction, ASCE*, 102, 236-254.
75. FEMA (2000). *Prestandard and commentary for the seismic rehabilitation of buildings*. FEMA 356. Federal Emergency Management Agency. Washington, D.C., United States.

76. FRA (2012). *High-speed ground transportation noise and vibration impact assessment*. DOT/FRA/ORD-12/15. Federal Railroad Administration, U.S. Department of Transportation. Washington, DC.

77. Galvín, P., Romero, A., and Domínguez, J. (2010). "Fully three-dimensional analysis of high-speed train–track–soil-structure dynamic interaction." *Journal of Sound and Vibration*, 329(24), 5147-5163.

78. Gazetas, G., and Mylonakis, G. (1998). "Seismic soil–structure interaction: new evidence and emerging issues." *Geotechnical Special Publication II, Geotechnical Earthquake Engineering and Soil Dynamics III*, ASCE, ed., 1119-1174.

79. GB/T (2008). *Technical specifications for protection of historic buildings against man-made vibration*. GB/T 50452. China Building Industry Press (in Chinese). Beijing.

80. Gerolymos, N., Giannakou, A., Anastasopoulos, I., and Gazetas, G. (2008). "Evidence of beneficial role of inclined piles: observations and summary of numerical analyses." *Bulletin of Earthquake Engineering*, 6(4), 705-722.

81. Ghasemzadeh, H., and Alibeikloo, M. (2011). "Pile–soil–pile interaction in pile groups with batter piles under dynamic loads." *Soil Dynamics and Earthquake Engineering*, 31(8), 1159-1170.

82. Ghazavi, M., Ravanshenas, P., and El Naggar, M. H. (2013). "Interaction between inclined pile groups subjected to harmonic vibrations." *Soils and Foundations*, 53(6), 789-803.

83. Giannakou, A., Gerolymos, N., Gazetas, G., Tazoh, T., and Anastasopoulos, I. (2010). "Seismic behavior of batter piles: Elastic response." *Journal of Geotechnical and Geoenvironmental Engineering*, 136(9), 1187-1199.

84. Goit, C. S., and Saitoh, M. (2013). "Model tests and numerical analyses on horizontal impedance functions of inclined single piles embedded in cohesionless soil." *Earthquake Engineering and Engineering Vibration*, 12(1), 143-154.

85. Goit, C. S., and Saitoh, M. (2014). "Model tests on horizontal impedance functions of fixed-head inclined pile groups under soil nonlinearity." *Journal of Geotechnical and Geoenvironmental Engineering*, 140(6).

86. Google Maps (2019). "Department of Earthquake Engineering, IIT Roorkee. 29°51'57.0"N 77°54'02.0"E." (April 07, 2019).

87. Grizi, A., Athanasopoulos-Zekkos, A., and Woods, R. D. (2016). "Ground vibration measurements near impact pile driving." *Journal of Geotechnical and Geoenvironmental Engineering*, 142(8).

88. Hall, L. (2003). "Simulations and analyses of train-induced ground vibrations in finite element models." *Soil Dynamics and Earthquake Engineering*, 23(5), 403-413.
89. Hamidi, A., Rooz, A. F. H., and Pourjenabi, M. (2018). "Allowable distance from impact pile driving to prevent structural damage considering limits in different standards." *Practice Periodical on Structural Design and Construction*, 23(1).
90. Han, Y., and Novak, M. (1988). "Dynamic behaviour of single piles under strong harmonic excitation." *Canadian Geotechnical Journal*, 25(3), 523-534.
91. Han, Y., and Vaziri, H. (1992). "Dynamic response of pile groups under lateral loading." *Soil Dynamics and Earthquake Engineering*, 11(2), 87-99.
92. Hanna, A. M., and Afram, A. (1986). "Pull-out capacity of single batter piles in sand." *Canadian Geotechnical Journal*, 23(3), 387-392.
93. Harn, R. E. (2004). "Have batter piles gotten a bad rap in seismic zones? (Or everything you wanted to know about batter piles but were afraid to ask)." *Ports 2004*, 1-10.
94. Harris, D. E., and Madabhushi, G. S. P. (2015). "Uplift capacity of an under-reamed pile foundation." *Proceedings of the Institution of Civil Engineers - Geotechnical Engineering*, 168(GE6), 526-538.
95. Henke, S. (2010). "Influence of pile installation on adjacent structures." *International Journal for Numerical and Analytical Methods in Geomechanics*, 34(11), 1191-1210.
96. Hesami, S., Ahmadi, S., and Ghalesari, A. T. (2016). "Numerical modeling of train-induced vibration of nearby multi-story building: A case study." *KSCE Journal of Civil Engineering*, 20(5), 1701-1713.
97. Hokmabadi, A. S., Fakher, A., and Fatahi, B. (2012). "Full scale lateral behaviour of monopiles in granular marine soils." *Marine Structures*, 29(1), 198-210.
98. Hokmabadi, A. S., and Fatahi, B. (2016). "Influence of foundation type on seismic performance of buildings considering soil–structure interaction." *International Journal of Structural Stability and Dynamics*, 16(08).
99. Hokmabadi, A. S., Fatahi, B., and Samali, B. (2015). "Physical modeling of seismic soil-pile-structure interaction for buildings on soft soils." *International Journal of Geomechanics*, 15(2).
100. Honda, T., Hirai, Y., and Sato, E. (2011). "Uplift capacity of belled and multi-belled piles in dense sand." *Soils and Foundations*, 51(3), 483-496.
101. Hu, A.-F., Fu, P., Xia, C.-Q., and Xie, K.-H. (2017). "Lateral dynamic response of a partially embedded pile subjected to combined loads in saturated soil." *Marine Georesources & Geotechnology*, 35(6), 788-798.

102. Hughes, T. J. R. (2000). *The finite element method: Linear static and dynamic finite element analysis*, Dover Publications, New York, USA.
103. Hung, H. H., Chen, G. H., and Yang, Y. B. (2013). "Effect of railway roughness on soil vibrations due to moving trains by 2.5D finite/infinite element approach." *Engineering Structures*, 57, 254-266.
104. Hwang, J.-H., Liang, N., and Chen, C.-H. (2001). "Ground response during pile driving." *Journal of Geotechnical and Geoenvironmental Engineering*, 127(11), 939-949.
105. Ilamparuthi, K., and Dickin, E. A. (2001a). "Predictions of the uplift response of model belled piles in geogrid-cell-reinforced sand." *Geotextiles and Geomembranes*, 19(2), 89-109.
106. Ilamparuthi, K., and Dickin, E. A. (2001b). "The influence of soil reinforcement on the uplift behaviour of belled piles embedded in sand." *Geotextiles and Geomembranes*, 19(1), 1-22.
107. Ishihara, K. (1996). *Soil behaviour in earthquake geotechnics*, Oxford University Press, New York, USA.
108. ISO (1997). *Mechanical vibration and shock - Evaluation of human exposure to whole-body vibration Part 1: General Requirements*. ISO 2631-1. International Organization for Standardization. Geneva, Switzerland.
109. ISO (2003). *Mechanical vibration and shock - Evaluation of human exposure to whole-body vibration Part 2: Continuous and shock-induced vibration in buildings (1-80 Hz)*. ISO 2631-2. International Organization for Standardization. Geneva, Switzerland.
110. ISO (2010). *Mechanical vibration and shock - Vibration of fixed structures - Guidelines for the measurement of vibrations and evaluation of their effects on structures*. ISO 4866. International Organization for Standardization. Geneva, Switzerland.
111. Ju, S.-H. (2009). "Finite element investigation of traffic induced vibrations." *Journal of Sound and Vibration*, 321(3), 837-853.
112. Juneja, A. (2009). "Centrifuge modeling of penetration of partially plugged pile in soft clay." *Contemporary Topics in In Situ Testing, Analysis, and Reliability of Foundations*, American Society of Civil Engineers, Orlando, Florida, United States, 246-253.
113. Juneja, A., and Mohammed Aslam, A. K. (2016). "Strain accumulation in soils due to repeated sinusoidal loading." *Japanese Geotechnical Society Special Publication*, 2(24), 903-906.

114. Juneja, A., and Mohammed-Aslam, A. K. (2018). "Application of a cyclic degradation model for pore pressure accumulation in loose sands and silts subjected to dynamic loading." *Journal of Earthquake and Tsunami*, 12(05).

115. Juran, I., Benslimane, A., and Hanna, S. (2001). "Engineering analysis of dynamic behavior of micropile systems." *Transportation Research Record*, 1772(1), 91-106.

116. Kastranta, G., Gazetas, G., and Tazoh, T. (1998). "Performance of three quay walls in Maya Wharf: Kobe 1995." *11th European Conference on Earthquake Engineering*, Paris, France.

117. Kaynia, A. M., and Kausel, E. (1982). "Dynamic behavior of pile groups." *Proc., 2nd International Conference on Numerical Methods in Offshore Piling*, Austin, Texas.

118. Kaynia, A. M., and Kausel, E. (1991). "Dynamics of piles and pile groups in layered soil media." *Soil Dynamics and Earthquake Engineering*, 10(8), 386-401.

119. Kouroussis, G., Van Parys, L., Conti, C., and Verlinden, O. (2014). "Using three-dimensional finite element analysis in time domain to model railway-induced ground vibrations." *Advances in Engineering Software*, 70, 63-76.

120. Kuhlemeyer, R. L., and Lysmer, J. (1973). "Finite element method accuracy for wave propagation problems." *Journal of the Soil Mechanics and Foundations Division*, 99(5), 421-427.

121. LabVIEW (2009). "Signal Express: Getting Started with LabVIEW Signal Express."

122. Ladhane, K. B., and Sawant, V. A. (2016). "Effect of pile group configurations on nonlinear dynamic response." *International Journal of Geomechanics*, 16(1).

123. Li, Z., Escoffier, S., and Kotronis, P. (2016a). "Centrifuge modeling of batter pile foundations under sinusoidal dynamic excitation." *Bulletin of Earthquake Engineering*, 14(3), 673-697.

124. Li, Z., Escoffier, S., and Kotronis, P. (2016b). "Centrifuge modeling of batter pile foundations under earthquake excitation." *Soil Dynamics and Earthquake Engineering*, 88, 176-190.

125. Lopes, P., Costa, P. A., Ferraz, M., Calçada, R., and Cardoso, A. S. (2014). "Numerical modeling of vibrations induced by railway traffic in tunnels: From the source to the nearby buildings." *Soil Dynamics and Earthquake Engineering*, 61-62, 269-285.

126. Lu, S. "Design load of bored pile laterally loaded." *Proc., l0th International Conference on Soil Mechanics and Foundation Engineering*, Stockholm, Sweden.

127. Lysmer, J., and Drake, L. A. (1972). "A finite element method for seismology." *Methods in computational physics: Advances in research and applications*, B. A. Bolt, ed., Elsevier, 181-216.
128. Lysmer, J., and Kuhlemeyer, R. L. (1969). "Finite dynamic model for infinite media." *Journal of the Engineering Mechanics Division*, 95(4), 859-878.
129. Maheshwari, B. K., Truman, K. Z., Gould, P. L., and Naggar, M. H. E. (2005). "Three-dimensional nonlinear seismic analysis of single piles using finite element model: Effects of plasticity of soil." *International Journal of Geomechanics*, 5(1), 35-44.
130. Maheshwari, B. K., Truman, K. Z., Naggar, M. H. E., and Gould, P. L. (2004). "Three-dimensional finite element nonlinear dynamic analysis of pile groups for lateral transient and seismic excitations." *Canadian Geotechnical Journal*, 41(1), 118-133.
131. Mamoon, S. M., Kaynia, A. M., and Banerjee, P. K. (1990). "Frequency domain dynamic analysis of piles and pile groups." *Journal of Engineering Mechanics*, 116(10), 2237-2257.
132. Mander, J. B., Priestley, M. J. N., and Park, R. (1988). "Theoretical stress-strain model for confined concrete." *Journal of Structural Engineering*, 114(8), 1804-1826.
133. Manna, B., and Baidya, D. (2012). "The nonlinear coupled response of single and group piles under various horizontal excitations: Experimental and theoretical Study." *Geotechnical Testing Journal*, 35(6), 949-963.
134. Manna, B., and Baidya, D. K. (2009). "Vertical vibration of full-scale pile - Analytical and experimental study." *Journal of Geotechnical and Geoenvironmental Engineering*, 135(10), 1452-1461.
135. Manna, B., and Baidya, D. K. (2010a). "Dynamic nonlinear response of pile foundations under vertical vibration—Theory versus experiment." *Soil Dynamics and Earthquake Engineering*, 30(6), 456-469.
136. Manna, B., and Baidya, D. K. (2010b). "Nonlinear dynamic response of piles under horizontal excitation." *Journal of Geotechnical and Geoenvironmental Engineering*, 136(12), 1600-1609.
137. Manoliu, I., Botea, E., and Constantinescu, A. "Behavior of pile foundations submitted to lateral loads." *Proc., 9th International Conference on Soil Mechanics and Foundation Engineering*, Tokyo, Japan.
138. McVay, M., Shang, T., and Casper, R. (1996). "Centrifuge testing of fixed-head laterally loaded battered and plumb pile groups in sand." *Geotechnical Testing Journal*, 19(1), 41-50.

139. Medina, C., Padrón, L. A., Aznárez, J. J., and Maeso, O. (2015). "Influence of pile inclination angle on the dynamic properties and seismic response of piled structures." *Soil Dynamics and Earthquake Engineering*, 69, 196-206.

140. Medina, C., Padrón, L. A., Aznárez, J. J., Santana, A., and Maeso, O. (2014). "Kinematic interaction factors of deep foundations with inclined piles." *Earthquake Engineering and Structural Dynamics*, 43(13), 2035-2050.

141. Mhanna, M., Sadek, M., and Shahrour, I. (2012). "Numerical modeling of traffic-induced ground vibration." *Computers and Geotechnics*, 39, 116-123.

142. Mitchell, D., Tinawi, R., and Sexsmith, R. G. (1991). "Performance of bridges in the 1989 Loma Prieta earthquake – lessons for Canadian designers." *Canadian Journal of Civil Engineering*, 18(4), 711-734.

143. Moayedi, H., and Mosallanezhad, M. (2017). "Uplift resistance of belled and multi-belled piles in loose sand." *Measurement*, 109, 346-353.

144. Moayedi, H., and Rezaei, A. (2019). "An artificial neural network approach for under-reamed piles subjected to uplift forces in dry sand." *Neural Computing and Applications*, 31(2), 327-336.

145. Mohan, D., Jain, G. S., and Gupta, S. P. (1979). "Pile testing using raked under-reamed piles." *Ground Engineering*, (April), 47-52.

146. Mroueh, H., and Shahrour, I. (2009). "Numerical analysis of the response of battered piles to inclined pullout loads." *International Journal for Numerical and Analytical Methods in Geomechanics*, 33(10), 1277-1288.

147. Murthy, V. "Behaviour of battered piles embedded in sand subjected to lateral loads." *Proc., Symposium on Bearing Capacity of Piles*, Roorkee, India.

148. Mylonakis, G., and Gazetas, G. (1999). "Lateral vibration and internal forces of grouped piles in layered soil." *Journal of Geotechnical and Geoenvironmental Engineering*, 125(1), 16-25.

149. Naggar, M. H. E., and Bentley, K. J. (2000). "Dynamic analysis for laterally loaded piles and dynamic p-y curves." *Canadian Geotechnical Journal*, 37(6), 1166-1183.

150. Naggar, M. H. E., and Novak, M. (1994). "Non-linear model for dynamic axial pile response." *Journal of Geotechnical Engineering*, 120(2), 308-329.

151. Nakata, N., and Snieder, R. (2013). "Monitoring a building using deconvolution interferometry. II: Ambient-vibration analysis." *Bulletin of the Seismological Society of America*, 104(1), 204-213.

152. Nazir, A., and Nasr, A. (2013). "Pullout capacity of batter pile in sand." *Journal of Advanced Research*, 4(2), 147-154.

153. Nazir, R., Moayedi, H., Pratikso, A., and Mosallanezhad, M. (2015). "The uplift load capacity of an enlarged base pier embedded in dry sand." *Arabian Journal of Geosciences*, 8(9), 7285-7296.

154. Newton, C., and Snieder, R. (2012). "Estimating intrinsic attenuation of a building using deconvolution interferometry and time reversal." *Bulletin of the Seismological Society of America*, 102(5), 2200-2208.

155. Nimbalkar, S. S., Punetha, P., Basack, S., and Mirzababaei, M. (2019). "Piles subjected to torsional cyclic load: Numerical analysis." *Frontiers in Built Environment*, 5(24).

156. Niroumand, H., Kassim, K. A., Ghafooripour, A., and Nazir, R. (2012). "Uplift capacity of enlarged base piles in sand." *Electronic Journal of Geotechnical Engineering*, 17, 2721-2737.

157. Novak, M., and El Sharnouby, B. (1984). "Evaluation of dynamic experiments on pile groups." *Journal of Geotechnical and Geoenvironmental Engineering*, 110(6), 738–756.

158. Novak, M., and Grigg, R. F. (1976). "Dynamic experiments with small pile foundations." *Canadian Geotechnical Journal*, 13(4), 372-385.

159. NSW (2006). *Assessing vibration: A technical guideline*. Department of Environment and Conservation. New South Wales, Australia.

160. Okawa, K., Kamei, H., Zhang, F., and Kimura, M. "Seismic performance of group-pile foundation with inclined steel piles." *Proc., 1st Greece-Japan Workshop on Seismic Design, Observation and Retrofit of Foundations*, Athens, Greece.

161. Padrón, L. (2009). "Numerical model for the dynamic analysis of pile foundations." *Las Palmas: University of Las Palmas de Gran Canaria*.

162. Padrón, L. A., Aznárez, J. J., Maeso, O., and Saitoh, M. (2012). "Impedance functions of end-bearing inclined piles." *Soil Dynamics and Earthquake Engineering*, 38, 97-108.

163. Padrón, L. A., Aznárez, J. J., Maeso, O., and Santana, A. (2010). "Dynamic stiffness of deep foundations with inclined piles." *Earthquake Engineering and Structural Dynamics*, 39(12), 1343-1367.

164. Padrón, L. A., Suárez, A., Aznárez, J. J., and Maeso, O. (2015). "Kinematic internal forces in deep foundations with inclined piles." *Earthquake Engineering and Structural Dynamics*, 44(12), 2129-2135.

165. Peter, J. A., Lakshmanan, N., and Manoharan, P. D. (2006). "Investigations on the static behavior of self-compacting concrete under-reamed piles." *Journal of Materials in Civil Engineering*, 18(3), 408-414.

166. Petrovic, B., and Parolai, S. (2016). "Joint deconvolution of building and downhole strong-motion recordings: Evidence for the seismic wavefield being radiated back into the shallow geological layers." *Bulletin of the Seismological Society of America*, 106(4), 1720-1732.

167. Petrovic, B., Parolai, S., Pianese, G., Dikmen, S. U., Moldobekov, B., Orunbaev, S., and Paolucci, R. (2018). "Joint deconvolution of building and downhole seismic recordings: An application to three test cases." *Bulletin of Earthquake Engineering*, 16(2), 613-641.

168. Phanikanth, V., and Choudhury, D. (2013). "Single piles in cohesionless soils under lateral loads using elastic continuum approach." *Indian Geotechnical Journal*, 44(3), 225-233.

169. Phanikanth, V. S., and Choudhury, D. (2012). "Effects of lateral loads on a single pile." *Journal of The Institution of Engineers (India): Series A*, 93(3), 163-173.

170. Phanikanth, V. S., Choudhury, D., and Srinivas, K. (2013). "Response of flexible piles under lateral loads." *Indian Geotechnical Journal*, 43(1), 76-82.

171. Pianese, G., Petrovic, B., Parolai, S., and Paolucci, R. (2018). "Identification of the nonlinear seismic response of buildings by a combined Stockwell Transform and deconvolution interferometry approach." *Bulletin of Earthquake Engineering*, 16(7), 3103-3126.

172. Picozzi, M., Parolai, S., Mucciarelli, M., Milkereit, C., Bindi, D., Ditommaso, R., Vona, M., Gallipoli, M. R., and Zschau, J. (2011). "Interferometric analysis of strong ground motion for structural health monitoring: The example of the L'Aquila, Italy, Seismic sequence of 2009." *Bulletin of the Seismological Society of America*, 101(2), 635-651.

173. Pinto, P., McVay, M., Hoit, M., and Lai, P. (1997). "Centrifuge testing of plumb and battered pile groups in sand." *Transportation Research Record*, 1569(1), 8-16.

174. Poulos, H. G. (2006). "Raked piles: Virtues and drawbacks." *Journal of Geotechnical and Geoenvironmental Engineering*, 132(6), 795-803.

175. Prakash, S., and Subramanyam, G. (1965). "Behaviour of battered piles under lateral loads." *Indian Journal of Soil Mechanics and Foundation Engineering*, 4(2), 177-196.

176. Priestley, N., Singh, J., Youd, T., and Rollins, K. (1991). "Costa Rica earthquake of April 22, 1991, Reconnaissance Report." Earthquake Engineering Research Institute 59-91.

177. Qian, Y. M., Ren, J. J., and Yin, X. S. (2012). "The simulated analysis in the computer on the effect of pile and soil working together about the push-extend multi-under-reamed pile." *Applied Mechanics and Materials*, 479-481, 59-64.

178. Qian, Y. M., Zhao, D. P., and Xie, X. W. (2014). "The research on the ultimate bearing capacity of soil around the push-extend multi-under-reamed pile at sliding failure state." *Applied Mechanics and Materials*, 578-579, 232 - 235.

179. Qin, H., and Guo, W. D. (2014). "Nonlinear response of laterally loaded rigid piles in sand." *Geomechanics and Engineering, An Int'l Journal*, 7(6), 679-703.

180. Rahman, M. A., and Sengupta, S. (2017). "Uplift capacity of inclined underreamed piles subjected to vertical load." *Journal of The Institution of Engineers (India): Series A*, 98(4), 533-544.

181. Rahmani, M., and Todorovska, M. I. (2013). "1D system identification of buildings during earthquakes by seismic interferometry with waveform inversion of impulse responses - method and application to Millikan library." *Soil Dynamics and Earthquake Engineering*, 47, 157-174.

182. Rajashree, S. S., and Sitharam, T. G. (2001). "Nonlinear finite-element modeling of batter piles under lateral load." *Journal of Geotechnical and Geoenvironmental Engineering*, 127(7), 604-612.

183. Ranjan, G., Ramasamy, G., and Tyagi, R. (1980). "Lateral response of batter piles and pile bents in clay." *Indian Geotechnical Journal*, 10(2), 135-142.

184. Rathod, D., Muthukkumaran, K., and Sitharam, T. G. (2016a). "Response of laterally loaded pile in soft clay on sloping ground." *International Journal of Geotechnical Engineering*, 10(1), 10-22.

185. Rathod, D., Muthukkumaran, K., and Sitharam, T. G. (2017). "Development of non-dimension p–y Curves for laterally loaded piles in sloping ground." *Indian Geotechnical Journal*, 47(1), 47-56.

186. Rathod, D., Muthukkumaran, K., and Sitharam, T. G. (2018). "Effect of slope on p-y curves for laterally loaded piles in soft clay." *Geotechnical and Geological Engineering*, 36(3), 1509-1524.

187. Rathod, D., Muthukkumaran, K., and Sitharam, T. G. (2019). "Experimental investigation on behavior of a laterally loaded single pile located on sloping ground." *International Journal of Geomechanics*, 19(5).

188. Rathod, D., Sitharam, T. G., and Muthukkumaran, K. (2016b). "Effect of earthquake on a single pile located in sloping ground." *International Journal of Geotechnical Earthquake Engineering (IJGEE)*, 7(1), 57-72.

189. Ravazi, S. A., Fahker, A., and Mirghaderi, S. R. (2007). "An insight into the bad reputation of batter piles in seismic performance of wharves." *Proc., 4th International Conference on Earthquake Geotechnical Engineering*, Thessaloniki, Greece.

190. Real, T., Zamorano, C., Ribes, F., and Real, J. I. (2015). "Train-induced vibration prediction in tunnels using 2D and 3D FEM models in time domain." *Tunnelling and Underground Space Technology*, 49, 376-383.

191. Rezaei, M., Hamidi, A., and Farshi Homayoun Rooz, A. (2016). "Investigation of peak particle velocity variations during impact pile driving process." *Civil Engineering Infrastructures Journal*, 49(1), 59-69.

192. Rooz, A. F. H., and Hamidi, A. (2017). "Numerical analysis of factors affecting ground vibrations due to continuous impact pile driving." *International Journal of Geomechanics*, 17(12).

193. Sadek, M., and Shahrour, I. (2004). "Three-dimensional finite element analysis of the seismic behavior of inclined micropiles." *Soil Dynamics and Earthquake Engineering*, 24(6), 473-485.

194. Sadek, M., and Shahrour, I. (2006). "Influence of the head and tip connection on the seismic performance of micropiles." *Soil Dynamics and Earthquake Engineering*, 26(5), 461-468.

195. Sanayei, M., Kayiparambil P, A., Moore, J. A., and Brett, C. R. (2014). "Measurement and prediction of train-induced vibrations in a full-scale building." *Engineering Structures*, 77, 119-128.

196. Sarkar, R., Roy, N., and Serawat, A. (2018). "A three dimensional comparative study of seismic behaviour of vertical and batter pile groups." *Geotechnical and Geological Engineering*, 36(2), 763-781.

197. Schiavi, A., and Rossi, L. (2015). "Vibration perception in buildings: A survey from the historical origins to the present day." *Energy Procedia*, 78, 2-7.

198. SEAOC (1991). "Reflections on the October 17, 1989 Loma Prieta earthquake." E. E. Cole, and J. F. Meehan, eds. Sacramento, California, 174.

199. Semblat, J. F. (2011). "Modeling seismic wave propagation and amplification in 1D/2D/3D linear and nonlinear unbounded media." *International Journal of Geomechanics*, 11(6), 440-448.

200. Semblat, J.-F., and Brioist, J. J. (2000). "Efficiency of higher order finite elements for the analysis of seismic wave propagation." *Journal of Sound and Vibration*, 231(2), 460-467.

201. Sen, R., Davies, T. G., and Banerjee, P. K. (1985). "Dynamic analysis of piles and pile groups embedded in homogeneous soils." *Earthquake Engineering & Structural Dynamics*, 13(1), 53-65.

202. Shadlou, M., and Bhattacharya, S. (2014). "Dynamic stiffness of pile in a layered elastic continuum." *Géotechnique*, 64(4), 303-319.

203. Shih, J. Y., Thompson, D. J., and Zervos, A. (2016). "The effect of boundary conditions, model size and damping models in the finite element modelling of a moving load on a track/ground system." *Soil Dynamics and Earthquake Engineering*, 89, 12-27.

204. SIS (1999). *Vibration and shock - Guidance levels and measuring of vibrations in buildings originating from piling, sheet piling, excavating and packing to estimate permitted vibration levels (in Swedish)*. SS 02 52 11. Swedish Institute for Standards. Stockholm, Sweden.

205. Souri, A., Abu-Farsakh, M., and Voyiadjis, G. (2015). "Study of static lateral behavior of battered pile group foundation at I-10 Twin Span Bridge using three-dimensional finite element modeling." *Canadian Geotechnical Journal*, 53(6), 962-973.

206. Subramanian, R. M., and Boominathan, A. (2015). "Finite element studies on batter piles subjected to lateral dynamic loads." *Proc., 6th International Geotechnical Symposium on Disaster Mitigation in Special Geoenvironmental Conditions*, Chennai, India.

207. Subramanian, R. M., and Boominathan, A. (2016). "Dynamic experimental studies on lateral behaviour of batter piles in soft clay." *International Journal of Geotechnical Engineering*, 10(4), 317-327.

208. Svinkin, M. R. (2006). "Mitigation of soil movements from pile driving." *Practice Periodical on Structural Design and Construction*, 11(2), 80-85.

209. Tamura, S., Adachi, K., Sakamoto, T., Hida, T., and Hayashi, Y. (2012). "Effects of existing piles on lateral resistance of new piles." *Soils and Foundations*, 52(3), 381-392.

210. Tazoh, T., Sato, J., Jang, J., Taji, Y., Gazetas, G., and Anastaspoulos, I. (2010). "Kinematic response of batter pile foundation." *Soil-Foundation-Structure Interaction*, Taylor & Francis Group, London, 41–47.

211. Thandavamoorthy, T. S. (2004). "Piling in fine and medium sand - A case study of ground and pile vibration." *Soil Dynamics and Earthquake Engineering*, 24(4), 295-304.

212. Tombari, A., El Naggar, M. H., and Dezi, F. (2017). "Impact of ground motion duration and soil non-linearity on the seismic performance of single piles." *Soil Dynamics and Earthquake Engineering*, 100, 72-87.

213. Tschebotarioff, G. P. (1953). "The resistance to lateral loading of single piles and pile groups." *Special Publication*, 154, 38-48.

214. UNI (1991). *Criteri di misura e valutazione degli effetti delle vibrazioni sugli edifice (Criteria for the measurement of vibrations and the assessment of their effects on buildings)*. UNI 9916. Ente Nazionale Italiano di Unificazione (UNI). Milano, Italia.

215. Veeresh, C., and Rao, S. N. (1996). "Vertical pullout capacity of model batter anchor piles in marine clays." *Marine Georesources & Geotechnology*, 14(3), 205-215.

216. Wang, J., Zhou, D., Ji, T., and Wang, S. (2017). "Horizontal dynamic stiffness and interaction factors of inclined piles." *International Journal of Geomechanics*, 17(9).

217. Wen, W., and Kalkan, E. (2017). "System identification based on deconvolution and cross correlation: An application to a 20-story instrumented building in Anchorage, Alaska." *Bulletin of the Seismological Society of America*, 107(2), 718-740.

218. Werner, S. D. (1998). *Seismic guidelines for ports*, ASCE Publications, Reston, VA.

219. Wong, J. C. (2004). "Seismic behavior of micropiles." Thesis (M.S.), Washington State University.

220. Wu, Y., Yamamoto, H., and Yao, Y. (2013). "Numerical study on bearing behavior of pile considering sand particle crushing." *Geomechanics and Engineering, An Int'l Journal*, 5(3), 241-261.

221. Xia, H., Chen, J., Wei, P., Xia, C., De Roeck, G., and Degrande, G. (2009). "Experimental investigation of railway train-induced vibrations of surrounding ground and a nearby multi-story building." *Earthquake Engineering and Engineering Vibration*, 8(1), 137-148.

222. Xia, H., Zhang, N., and Cao, Y. M. (2005). "Experimental study of train-induced vibrations of environments and buildings." *Journal of Sound and Vibration*, 280(3), 1017-1029.

223. Xu, H.-F., Yue, Z., and Qian, Q.-H. (2009). "Predicting uplift resistance of deep piles with enlarged bases." *Proceedings of the Institution of Civil Engineers - Geotechnical Engineering*, 162(4), 225-238.

224. Xu, R., and Fatahi, B. (2018). "Effects of pile group configuration on the seismic response of buildings considering soil-pile-structure interaction." Springer Singapore, Singapore.

225. Yang, D. Y., Wang, K. H., Zhang, Z. Q., and Leo, C. J. (2009). "Vertical dynamic response of pile in a radially heterogeneous soil layer." *International Journal for Numerical and Analytical Methods in Geomechanics*, 33(8), 1039-1054.

226. Yang, Y. B., Liang, X., Hung, H.-H., and Wu, Y. (2017). "Comparative study of 2D and 2.5D responses of long underground tunnels to moving train loads." *Soil Dynamics and Earthquake Engineering*, 97, 86-100.

227. Yao, W.-j., and Xiao, L. (2019). "Analytical solutions of deformation of uplift belled group piles considering reinforcement effect." *KSCE Journal of Civil Engineering*, 23(3), 1007-1016.

228. Zhang, F., Okawa, K., and Kimura, M. (2008). "Centrifuge model test on dynamic behavior of group-pile foundation with inclined piles and its numerical simulation." *Frontiers of Architecture and Civil Engineering in China*, 2(3), 233-241.

229. Zhang, L., Goh, S. H., and Liu, H. (2017). "Seismic response of pile-raft-clay system subjected to a long-duration earthquake: centrifuge test and finite element analysis." *Soil Dynamics and Earthquake Engineering*, 92, 488-502.

230. Zhang, L., and Liu, H. (2017). "Seismic response of clay-pile-raft-superstructure systems subjected to far-field ground motions." *Soil Dynamics and Earthquake Engineering*, 101, 209-224.

231. Zhang, L., McVay, M., and Lai, P. (1998). "Centrifuge testing of vertically loaded battered pile groups in sand." *Geotechnical Testing Journal* 21(4), 281-288.

232. Zhang, L., McVay, M. C., and Lai, P. W. (1999). "Centrifuge modelling of laterally loaded single battered piles in sands." *Canadian Geotechnical Journal*, 36(6), 1074-1084.

233. Zhang, M., and Tao, M. (2011). "A parametric study on factors affecting ground vibrations during pile driving through finite element simulations." *GeoRisk 2011: Geotechnical Risk Assessment and Management*, C. H. Juang, K. K. Phoon, A. J. Puppala, R. A. Green, and G. A. Fenton, eds., American Society of Civil Engineers, Atlanta, Georgia, United States.

234. Zhang, M., Tao, M., Gautreau, G., and Zhang, Z. D. (2013). "Statistical approach to determining ground vibration monitoring distance during pile driving." *Practice Periodical on Structural Design and Construction*, 18(4), 196-204.

235. Zheng, C., Liu, H., and Ding, X. (2016). "Lateral dynamic response of a pipe pile in saturated soil layer." *International Journal for Numerical and Analytical Methods in Geomechanics*, 40(2), 159-184.

236. Zou, C., Wang, Y., Moore, J. A., and Sanayei, M. (2017). "Train-induced field vibration measurements of ground and over-track buildings." *Science of the Total Environment*, 575, 1339-1351.

LIST OF PUBLICATIONS

IN INTERNATIONAL JOURNALS

1. **Bharathi, M.** and Dubey, R.N. (2019), "Dynamic lateral response of under-reamed vertical and batter piles", *Construction and Building Materials*, Elsevier, 158: 910-920. (SCI Expanded; Impact factor: 4.046)
2. **Bharathi, M.,** Dubey, R.N. and Shukla, S.K. (2019), "Experimental investigation of vertical and batter pile groups subjected to dynamic loads", *Soil Dynamics and Earthquake Engineering*, Elsevier, 116: 107-119. (SCI; Impact factor: 2.578)*
3. **Bharathi, M.,** Dubey, R.N. and Shukla, S.K., "Behaviour of batter piles under machine-induced vibrations", *Soils and Foundations*, Elsevier. (Review comments received)
4. **Bharathi, M.,** Dubey, R.N. and Shukla, S.K., "Effect of vibration induced by dynamic lateral load tests on vertical and batter pile groups on the adjacent building – Experimental and finite element investigations", *International Journal of Geomechanics*, ASCE. (Under review)
5. **Bharathi, M.,** Dubey, R.N. and Shukla, S.K., "Dynamic response of under-reamed batter piles subjected to vertical vibrations". (To be submitted)
6. **Bharathi, M.,** Dubey, R.N. and Shukla, S.K., "3D finite element analysis of batter piles and pile groups". (Under preparation)

** Listed in "The most downloaded articles from Soil Dynamics and Earthquake Engineering in the last 90 days".*